

N63-19498

**ADVANCED
TECHNOLOGY
LABORATORIES**

STUDIES OF SPECIAL TOPICS IN SEALING

EDITED BY

R.C. ELWELL

REPORT NO. 63GL100

JULY 2, 1963

GENERAL  ELECTRIC

**CASCADE
ELECTRIC**

The information contained in this report has been prepared for use by the General Electric Company and its employees. No distribution should be made outside the Company except when indicated below:

GENERAL DISTRIBUTION APPROVED

TECHNICAL INFORMATION SERIES

ADVANCED
TECHNOLOGY
LABORATORIES



GENERAL ELECTRIC

AUTHOR	Editor-	SUBJECT	NO. 63GL100
R. C. Elwell		Sealing	DATE July 2, 1963
TITLE	Studies of Special Topics in Sealing		G.E. CLASS I
REPRODUCIBLE COPY FILED AT G.E. TECHNICAL DATA CENTER BLDG. 5, SCHENECTADY, N. Y.		GOVT. CLASS None	NO. PAGES 160
ADDITIONAL COPIES OF THIS REPORTS 63GL99 THROUGH 63GL102 MAY BE OBTAINED FROM THE GE TECHNICAL DATA CENTER AT A COST OF \$15.00 FOR THE FOUR VOLUME SET			
<p>This is the second volume of a report describing various technical efforts applied under contract NAS 7-102, during the period Feb. 26, 1962 to Feb. 25, 1963.</p> <p>Seven individual reports make up this volume, each covering a specific subject pertinent to the technology of fluid sealing. These are as follows, with authorship as shown:</p> <ol style="list-style-type: none">1. Gas Permeation Through Solids-Dr. H.J. Sneek2. General Seal Analysis-Dr. G.M. Rentzepis3. The Labyrinth Seal-L. H. Bernd4. Leak Detection and Measurement-Dr. J.W. Marr5. Cryogenic Sealing-Dr. R. B. Fleming6. Two Phase Phenomena in Dynamic Face Seals-L.H. Bernd7. Seal Materials-R. E. Lee, Jr.			
KEY WORDS Seals, Sealing, Permeation, Diffusion, Analysis, Labyrinth Seal, leak, leakage, leak detection, leakage measurement, cryogenics, two phase fluids, face seals, materials			

INFORMATION PREPARED FOR Missile and Space Division

TESTS MADE BY R. S. White

AUTHOR Edited by R. C. Elwell

COMPONENT Mechanical Engineering Laboratory

APPROVED G. R. Fox, Manager, Bearing Laboratory

R. C. Elwell
G. R. Fox

Table of Contents

Page

Introduction - R. C. Elwell	1
Appendix A - Gas Permeation Through Solids-H.J. Sneek	4
The Permeation Process	4
Permeation Rate Data	8
Numerical Example	11
Conclusions	12
References	13
Appendix B - General Seal Analysis - Dr. G.M. Rentzepis	14
1. Introduction	16
2. Formulation of Equations of State	17
3. Flow Between Two Vertical Concentric Cylinders	25
4. Flow Between Two Parallel Disks	32
5. Bibliography	49
Appendix C - The Labyrinth Seal - L.H. Bernd	50
References	58
Figures	59-62
Appendix D - Leak Detection and Measurement - Dr. J.W. Marr	63
1. Definitions	63
2. Conversion of Measured Leakage to Standard Leakage Rate	77
3. Leak Detection and Measurement Techniques	88
List of Symbols	100
Tables	102-105
References	106
Appendix E - Cryogenic Sealing - Dr. R.B. Fleming	107
1. Introduction	107
2. Problems Associated with Cryogenic Sealing	108
3. Present Practice	109
4. Experimental Work on Dynamic Sealing of Cryogenic Fluids	112
5. Experimental Work on Friction and Wear	114
6. Areas in Which Further Knowledge is Needed	118
7. References	120
Appendix F - Two Phase Phenomena in Dynamic Face Seals - L. H. Bernd	122
A. Conditions Causing 2 Phases in Liquids	122
B. Cavitation Trails in Seals	125
C. Cavitation	128
D. Conclusions	130
E. References	131
Tables	132-137
Figures	138-144
Appendix G - Seal Material Study - R.E. Lee, Jr.	145
Seal Material Considerations	145
State of the Art	147
Friction and Wear	149
New Concepts	150
References	152
Tables	153-160

INTRODUCTION - R. C. Elwell, Project Engineer

This is the second volume of the final report on this study of static and dynamic seals for liquid rocket engines. It contains individual reports on detailed studies of special topics in the technology of sealing.

In many cases, as discussed in the description of this program in Volume 1, we have had to devote a considerable effort to simply establish the state of the art, before proceeding to advance it. Much of the content of the reports in this volume are therefore devoted to this type of material. The subsequent Volumes 3A and 3B present extensive bibliographies, which are intended to reduce the disorder in which we found the literature on this subject, for the benefit of future investigators.

The content of the subsequent studies may be summarized as follows:

Appendix A - Gas Permeation through Solids

This is a report on the state of knowledge on the phenomena of the passage of gas through "solid" material by the permeation process. In storing gases for long periods of time, such as in some projected spacecraft, losses from this mechanism could be significant. It is concluded that more experimental data is required, for use in existing analyses.

Appendix B - General Seal Analysis

This report documents a largely-completed mathematical analysis which is intended to lay the groundwork for subsequent computations on special sealing devices. It has been necessary to start on a very fundamental level in this area, because the sealing technology suffers from a particular weakness in analytical techniques. Derivation of the basic equations for analysis of flow between concentric vertical cylinders and parallel plates is presented, using tensor notation.

Appendix C - The Labyrinth Seal

This is a survey of present knowledge and design ability on this device, which is particularly important because of its wide use in liquid rocket engine turbomachinery. It is found that design information on this type of seal is in a much better state than most other dynamic sealing devices.

Appendix D - Leak Detection and Measurement

This report is a rather extensive description of the state of the art in this area, which is directly related to sealing in that evaluation of seal effectiveness is just as important as design ability. Topics covered include types of leakage flows, conversion of flow rates to standard conditions, and leakage testing methods.

Appendix E - Cryogenic Sealing

This topic has been singled out for a special state of the art evaluation due to the wide use of cryogenic propellants in both present and future engines. It is concluded that uniqueness of sealing problems in this area is mainly due to friction and wear of dynamic seals in atmospheres of propellant gases. A description of major current activities in this field is included.

Appendix F - Two Phase Phenomena in Dynamic Face Seals

These devices are even more widely used than labyrinth seals (Appendix C) in rocket engines and are not understood to any significant extent. Most theoretical work has been concerned with the problem of fluid film load capacity in the device, to the apparent detriment of theories on the subject of the mechanism by which it seals. In this section a new theory of its function is presented, based on two phase fluid phenomena.

Appendix G - Materials Study

This report presents a discussion of some of the materials problems in

rocket engine seals and a description of the limited amount of data thus far available to apply to these problems.

There is considerable interrelation between several of the above studies. For instance, materials considerations are important to the studies on gas permeation (App. A), the labyrinth seal (App. C), cryogenic sealing (App. E), and the occurrence of the two phase phenomena in face seals (App. F). For another example, the occurrence of the two phase phenomena will ultimately be predictable through the results of the general analysis in Appendix B. Leakage measurement, of course, applies to all sealing applications.

Appendix A

GAS PERMEATION THROUGH SOLIDS - H.J. Sneek

The Permeation Process

The process whereby gases pass through sound solid membranes is described by Norton¹ as follows:

1. The gas on the high pressure side is first adsorbed and dissolved in an external surface layer on the membrane surface. Surface pretreatment is important here.

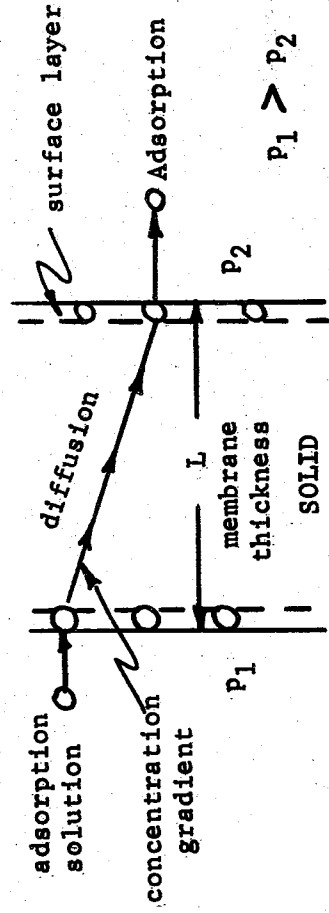


Figure 1

2. The gas then diffuses through the "solid" driven by the concentration gradient according to Fick's Law. The diffusion of the gas may be as atoms of a dissociated molecule if the membrane is metallic, or molecules if the membrane is a polymer.
3. When the gas reaches the low pressure side of the membrane, it undergoes a transition from a dissolved state to an adsorbed state and is desorbed at the surface and passes into the surroundings (where it will reassociate if the diffusion was atomic). Again surface pretreatment may be important.

The overall steady-state process described above is termed "permeation" and the speed of the permeation process is controlled by the slowest of the above steps.

A very excellent discussion of gases in metals is found in Cupp's paper (Ref. 11).

Generalities for Permeation

There are very few generalities one can make for the permeation process as a whole. Norton (Ref. 2) gives the known generalities as follows:

Gas Permeation Through

Metals

No rare gas passes through any metal (and Halogen gases to no marked degree - Ref. 11)

H₂ permeates most metals, especially Fe

O₂ permeates Ag

H₂ through Fe by corrosion, electrolysis

Permeation rates vary as $\sqrt{\text{pressure}}$

Polymers

All gases permeate all polymers

H₂O rate apt to be high

Many specificities

Permeation rates vary as pressure

Permeation Equations

The volumetric flow rate (S.T.P.) for the molecular permeation of a gas through a "solid" is described by the equation

$$Q = PA \frac{\Delta P}{L} \dots\dots\dots 1$$

- where Q = volumetric flow rate at STP
- A = area normal to the flow
- Δp = pressure drop along the flow path
- L = length of the flow path
- P = permeation rate

This equation can be derived from Fick's Law of diffusion

$$Q = - DA \frac{\partial c}{\partial x} \dots\dots\dots 2$$

where D = diffusion coefficient $\frac{\text{cm}^2}{\text{sec}}$

$\frac{\partial c}{\partial x}$ = concentration gradient

if the solubility is small. The concentration for very small solubility is related to the pressure through Henry's Law

$$c = Sp \dots\dots\dots 3$$

where S = solubility

$$-\frac{\partial c}{\partial x} = -S \frac{\partial p}{\partial x} = S \frac{\Delta p}{L}$$

Under this condition the diffusion coefficient is, in general constant so that equation 2 may be written for a membrane of uniform thickness as

$$Q = DSA \frac{\Delta p}{L} \dots\dots\dots 4$$

where Δp = pressure drop across the membrane.

If the permeation rate is defined as

$$P = DS \dots\dots\dots 5$$

equation 4 becomes equation 1.

It should be noted that equation 1 is strictly applicable only if the diffusion is molecular in nature, as in polymers. Some exceptions to Henry's Law have however been noted for rubber by Jost (Ref. 3). If the diffusion process is atomic in nature, as with diatomic gases permeating through metals, Equation 1 is not strictly applicable. Dushman (Ref. 4) indicates that when the diffusion is atomic

$$Q \propto (\sqrt{P_1} - \sqrt{P_2}) \dots\dots\dots 6$$

The permeation rate (P) used in Equation 1 is exponentially temperature dependent according to the relation (Ref. 5)

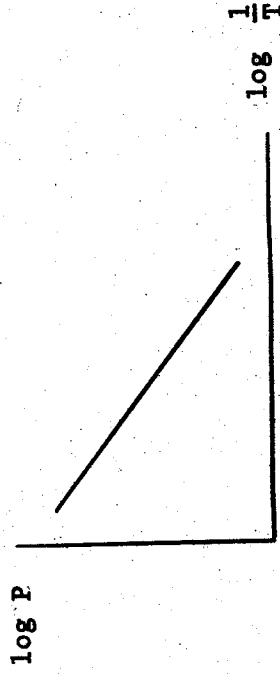


Fig. 2

$$P = P_0 e^{-\frac{E}{JRT}} \dots\dots\dots 7$$

where

- P_0 = constant, independent of temperature variation
 E = activation energy of permeation
 j = dissociation number (2 for diatomic gases permeating metals)
 R = 1.986 cal/K°
 T = degrees Kelvin

This equation is particularly useful for extrapolating permeation rates to higher or lower temperatures.

Permeation Rates and their Application to Calculations

The calculation of leakage rates due to permeation hinges on the experimental determination of the permeation rates, (P) as defined by Equation 1. For polymers, experimental permeation rates can be extrapolated to different temperatures using Equation 7 and then applied directly in Equation 1.

The problem is not quite so straight-forward for metals where relation 6 applies rather than equation 1. One finds that the literature contains permeation rates for metals as defined by equation 1. These rates are still exponentially temperature dependent as given by equation 7 but they are correct only for the specific pressure difference given in their units (eg; 1 torr or 1 mm Hg, 1 cm of Hg, 1 atmosphere). If the experimental values were determined when P_2 was very nearly equal to zero, and the case to be calculated also has P_2 very nearly equal to zero, then pressure extrapolations can be made using the simplified proportion

$$\frac{Q_{\text{actual}}}{Q_{\text{experimental}}} = \sqrt{\frac{P_1 \text{ actual}}{P_1 \text{ experimental}}} \dots\dots\dots 8$$

Otherwise extrapolations must be made according to Equation 6. Equation 8 is particularly useful when comparing, roughly, the results of different experimenters (Ref. 4).

Experimental Values of the Permeation Rate

Considerable care must be exercised when collecting permeation rate data from the literature for the following reasons:

- 1) Some of it is in error (as pointed out by Dayton, Ref. 5) - particularly that given by Jost (Ref. 3) and Barrer (Ref. 6).
- 2) The temperature must be noted because of the exponential dependence.
- 3) At least four different sets of units have been used for the permeation rates. They are

$$a) \quad \frac{\text{cm}^3 - \text{mm}}{\text{sec} - \text{cm}^2 - \text{torr}}$$

$$b) \quad \frac{\text{cm}^3 - \text{cm}}{\text{sec} - \text{cm}^2 - \text{atm}}$$

$$c) \quad \frac{\text{cm}^3 - \text{mm}}{\text{sec} - \text{cm}^2 - \text{atm}}$$

$$d) \quad \frac{\text{cm}^3 - \text{mm}}{\text{sec} - \text{cm}^2 - \text{cm Hg}}$$

This complicates the comparison of permeation rates of gases through metals for the reasons given above.

- 4) There are many specificities with regard to the membrane material (especially polymers) or pretreatment of materials (metals). This complicates the comparison of permeations for the same apparent material-gas combination.

Permeation Rate Data

The following represents the consensus of data gathered from the references already cited as well as References 7 and 8. (It is worth noting here that when searching German language literature the key word, permeation, is translated as "Gasdruchlässigkeit"). All data is for approximately 25°C.

P

$$\frac{\text{cm}^3 - \text{mm}}{\text{sec} - \text{cm}^3 - \text{atm}}$$

P

$$\frac{\text{cm}^3 - \text{mm}}{\text{sec} - \text{cm}^3 - \text{torr}}$$

H₂

5 - 15 (10⁻⁹)

3 (10⁻¹⁰) (low carbon)

1 (10⁻¹²) (27% chrome)

1.4 (10⁻¹⁰)

N₂ 4.2 (10⁻¹⁹) 1.5 (10⁻²⁰)

Al

P
 $\frac{\text{cm}^3 - \text{mm}}{\text{sec} - \text{cm}^2 - \text{atm}}$

H₂ 3.1 (10⁻²²)

Natural Rubber

P
 $\frac{\text{cm}^3 - \text{mm}}{\text{sec} - \text{cm}^2 - \text{atm}}$

H₂ 1.5 - 4.0 (10⁻⁶)
O₂ 1.8 (10⁻⁶)
N₂ 1.0 (10⁻⁶)
He 3.0 (10⁻⁶)

Neoprene

P
 $\frac{\text{cm}^3 - \text{mm}}{\text{sec} - \text{cm}^2 - \text{atm}}$

H₂ 1.0 (10⁻⁷)
O₂ 0.3 (10⁻⁷)
N₂ 0.1 (10⁻⁷)
He 0.6 (10⁻⁷)

The following permeation rate data for air was obtained from references 9 and 10.

	Permeation rate P in $\frac{\text{cm}^3}{\text{sec-cm}^2\text{-atm}}$ at Temperature		
	75°F	176°F	350°F
Butyl Rubber	0.02 (10^{-6})	0.32 (10^{-6})	6.1 (10^{-6})
Silicone Rubber	22.0 (10^{-6})	45 (10^{-6})	112 (10^{-6})
Kel-F	-----	0.8 (10^{-6})	-----

Remarks

While the data above appears skimpy, it represents the result of gleaning many different sources and careful comparison of the data for consistency.

The only gases cited in the literature surveyed were H₂, O₂, N₂, Xe, Ar, He and Air. None of the exotic gases or vapors, particularly fluorine compounds, were encountered in the references. Cupp (ref. 11) indicates that the halogen gases do not permeate metals to any marked degree; and if this is true, then they might be lumped in with the rare gas generalization.

The only metals encountered were Fe, (composition of alloying elements sometimes specified), Cu, Ni, Ag, Au, Al. Here wide variations on permeability are encountered due to differences in composition, surface condition, heat treatment, etc. Private conversations with F.J. Norton at the General Electric Research Laboratory brought out the fact that hydrogen permeates metals at the highest rate of any of the gases. Hydrogen data can therefore be used to predict the upper limit of leakage loss for any metal in question.

A considerable amount of data is available for polymers. Some of the more common types have been chosen to indicate the order of magnitude of permeation rate and to indicate that the losses can be great if the polymers are not chosen properly (see Numerical Example). In a current article by Frank (Ref. 12), he indicates that recent work on polymers has taken two directions:

1. Development of new polymers of low permeability (Mylar, Saran (Ref. 1), polyvinyl alcohol).
2. Treatment of polymers already available to decrease their permeability (impregnation with fillers, metal coating the surface)

Numerical Example

In order to get a "feel" for the flow losses attributable to permeation, consider the following example:

A gasket 0.1" thick 0.1" wide and 5" nominal diameter with a 1 atmosphere pressure difference across it.

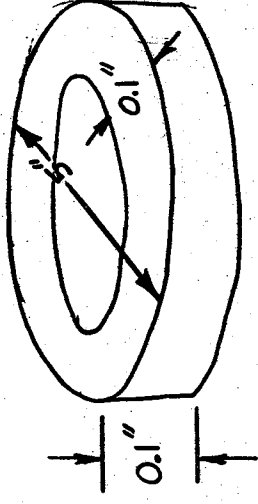


Fig. 3

$$A = 5(2.54) \pi (0.1)(2.54) = 10.13 \text{ cm}^2$$

$$L = 0.254 \text{ cm} = 2.54 \text{ mm}$$

$$\Delta p = 1 \text{ atm.}$$

Equation 1 becomes

$$Q = PA \frac{\Delta p}{L} = \frac{10.13}{2.54} P = 3.99 P$$

For a natural rubber gasket at 25°C

	P $\frac{\text{cm}^3 - \text{mm}}{\text{sec} - \text{cm}^2} - \text{atm}$	Q $\frac{\text{cm}^3}{\text{sec}}$	ρ $\frac{\text{lbs.}}{\text{cm}^3}$	Loss $\frac{\text{lbs.}}{\text{year}}$
H ₂	4.0 (10 ⁻⁶)	15.96 (10 ⁻⁶)	1.83 (10 ⁻⁷)	92.0 (10 ⁻⁶)
O ₂	1.8 (10 ⁻⁶)	7.18 (10 ⁻⁶)	29.2 (10 ⁻⁷)	661.0 (10 ⁻⁶)
N ₂	1.0 (10 ⁻⁶)	3.99 (10 ⁻⁶)	25.5 (10 ⁻⁷)	321.0 (10 ⁻⁶)
He	3.0 (10 ⁻⁶)	11.97 (10 ⁻⁶)	3.65 (10 ⁻⁷)	137.7 (10 ⁻⁶)

For a Neoprene gasket at 25°C

	P	Q	e	Loss $\frac{\text{lbs.}}{\text{year}}$
H ₂	10 (10 ⁻⁶)	3.99 (10 ⁻⁶)	1.83 (10 ⁻⁷)	2.30 (10 ⁻⁶)
O ₂	0.3 (10 ⁻⁶)	1.2 (10 ⁻⁶)	29.2 (10 ⁻⁷)	110.0 (10 ⁻⁶)
N ₂	0.1 (10 ⁻⁶)	0.399 (10 ⁻⁶)	25.5 (10 ⁻⁷)	32.1 (10 ⁻⁶)
He	0.6 (10 ⁻⁶)	2.4 (10 ⁻⁶)	3.65 (10 ⁻⁷)	27.6 (10 ⁻⁶)

By way of comparison, a 9-10 foot long steel pipe of the same diameter and thickness would lose Hydrogen at a rate comparable to those given above.

Conclusions

In conventional engineering practice, gas losses of the order shown above would of course be of no practical concern. When these figures are multiplied by perhaps 100, to allow for the presence of many such sealing devices in a spacecraft, however, the order of magnitude begins to have significance. This is particularly true of vehicles for very long missions, where launch weight will be critical and a minimum amount of fuel will be carried. In such vehicles, the phenomena must be examined for its effect.

To carry out such calculations in the future, more data, carefully obtained, will be necessary. For the long run, a better understanding of the permeation process is still required in order to be able to predict the performance of untested combinations of materials and fluids.

References for Permeation Data and Theory

1. Norton, F. J. "Permeation of Gases Through Solids," J. of Applied Physics, Vol. 28, p. 28-34 (1957)
2. Norton, F. J. "Gas Permeation through the Vacuum Envelope," G.E. Research Lab Report No. 61-RL-2874C Nov. 1961
3. Jost, W. "Diffusion" 1951 Academic Press.
4. Dushman, S. "Scientific Foundations of Vacuum Technique" Wiley and Son
5. Dayton, B.B. "Relations Between Size of a Vacuum Chamber, Outgassing Rate, and Required Pumping Speed," Vacuum Symposium Transactions, 1959.
6. Barrer, R.M. "Diffusion in and through Solids," Cambridge University Press
7. Espe, W. "Werkstoffkunde der Hochvakuum Technik", Deutscher Verlag der Wissenschaften
8. von Ardenne, M. "Tabellen der Elektronenphysik. Ionenphysik und Ultramikroskopie, Band II, Deutscher Verlag der Wissenschaften
9. Hayes, Smith, Smith, Kitchen "Development of High Temperature Resistant Rubber Compounds" WADC Technical Report 56-331 - February 1958
10. Islinger, J.S. "Research and Development of Design Concepts for Sealing Applications in Aerospace Vehicle Cabins" February 1962
Armour Research Foundation ASO Technical Report 61-696.

References for Discussion and Bibliography

11. Cupp, C.R. "Gases in Metals," Progress in Metal Physics Vol. 4, 1953
Pergamon Press.
12. Frank, C.F. "Gases in Solids," International Science and Technology, No. 9, Sept. 1962.

Appendix B

GENERAL SEAL ANALYSIS - Dr. G. M. Rentzepis

The task undertaken in this part of the program is to analyze the basic phenomena of seals and sealing mechanisms and recognize the character of each fundamental problem essential to understanding the behavior of seals, both static and dynamic in nature.

Subsequently, each fundamental problem is systematically approached to determine the qualitative and quantitative effects of physical properties of fluids or materials involved, the boundary, as well as the forces under which the system is subjected. Should this ambitious objective be accomplished, a systematic theory on seals will be available and, furthermore, capable of providing the basic guidance to the engineer and designer for a large class of seal applications.

It is with this in mind that the purpose of this section of the program is not to deal with the analysis of complicated operating seals, for the time being, but with carefully chosen simpler models where the fundamental nature of the mechanisms are not buried under cumbersome details of design and mathematics.

For example, the general problem of dynamic seals is essentially a problem of thin fluid films in which the predominant objective is the knowledge and control of flow in one primary direction. In order to achieve this goal, it is necessary to describe the behavior of the fluid under the imposed restricted flow and determine the conditions under which this flow can be realized. Consider again the thin fluid film of a dynamic seal and an essential question that may arise: is the fluid film a continuous medium

throughout the range of operating velocities or are we faced with a discontinuous fluid? If so, should this change of the flow to many-phased flow be avoided or is it beneficial to the purpose of the goal? Thus, the basic approach of this section shall be characterized by the following:

- i) The description of the flow of the problem under consideration.
- ii) The behavior of the fluid under the above flow, the imposed forces, and subjected to prescribed conditions.
- iii) The stability of such a velocity and "stress" field in view of physical limitations of the fluid and its boundary.

1. INTRODUCTION

This report deals with the formulation of an approach to the question of the behavior of the fluid under some particular flow. The explanation of various phenomena observed in thin fluid flows can be obtained by various methods and several mathematical representations. The predominant ones are (i) non-linear representation of the rheological equations or (ii) linear models valid only in infinitesimal neighborhood, otherwise called linear-in-the-small. The disadvantage of the first is the mathematical difficulties involved with non-linear equations. The latter needs further work to transform the behavior in-the-small to expressions in-the-whole where the equations of motion, continuity, etc. are usually given. Having chosen the second approach, we proceed in reviewing and developing the laws of transformation for tensors from a deformable coordinate system to a fixed in space one in Section 2. The case of second order tensors is given for covariant, contravariant and mixed components, and their time derivatives that appear in the rheological equations. Section 3 deals with the simple problem of two concentric cylinders. The stress field for the covariant and contravariant cases are reported. Section 4 presents the same information for the case of two parallel disks.

2. THE FORMULATION OF THE EQUATIONS OF STATE

The general problem of flow under consideration can be formulated in two stages. First, it is necessary to express the physical properties of the fluid by means of a set of rheological equations; second, to predict the behavior of the fluid as a whole, for a prescribed type of motion under the action of force and subject to certain conditions.

In this attempt for a formulation of a general approach to a seal theory, the fluid is characterized by the following assumptions:

1) The rheological equations are linear in-the-small.^{1*}

2) The rheological properties of an element of the continuum and, therefore, the rheological equations of state-in-the-small are independent of the state of the neighboring elements.

3) The rheological equations of state-in-the-small are independent of the motion of the element as a whole in space.

In formulating the equations of state in-the-small under the above assumptions, it is convenient to use a convected frame of reference rather than a fixed one.

a. The Rheological Equations of State in a Convected Coordinate System

Let ξ^i , ($i=1,2,3$), be a convected^{2,3} coordinate system such that ξ^i = constant defines a coordinate surface embedded in the moving medium and continuously deforming with it. A coordinate system of this type is the most convenient way in term of which to express the rheological equations of a fluid satisfying the conditions stated above, since in this system a fluid element can be assumed to behave according to some suitable linear integro-differential type of equations of state.

In the first attempt for a general approach to a seal theory the model is assumed to be of the following form⁴

(*) Superscript numbers refer to Bibliography at the end of this report.

$$\left(1 + \lambda_1 \frac{d}{dt} + \lambda_2 \frac{d^2}{dt^2} + \dots\right) \tau_{ij} = 2\eta_0 \left(1 + \tau_1 \frac{d}{dt} + \tau_2 \frac{d^2}{dt^2} + \dots\right) \epsilon_{ij} \quad (2-1)$$

and for the first examples to be worked out the simpler model^{2,5}

$$\left(1 + \lambda \frac{d}{dt}\right) \tau_{ij} = 2\eta_0 \left(1 + \tau \frac{d}{dt}\right) \epsilon_{ij} \quad (2-2)$$

shall be employed. $\bar{\tau}_{ij}$ are components of the stress tensor, ϵ_{ij} components of the strain rate tensor, λ , τ , η are constants of the fluid, and

$$\bar{\tau}_{ij} = \tau_{ij} - P g_{ij} \quad (2-3)$$

P is the pressure scalar associated with dilatation g_{ij} in the metric tensor, it should be pointed out that the general approach is not limited to models (2-1) or (2-2). These models are employed because of their simplicity and seem to be capable of representing a large class of fluids. The rheological equations are assumed to be valid in-the-small, hence in the convected coordinate system and the operations indicated in the above models, differentiation with respect to time, are valid in a convected frame of reference, in the sense that they preserve the tensor order of the equations of state, since differentiation over time takes place at the same material point. Therefore, tensor calculations in a convected system may be made as if the point under consideration was fixed in space.

b. Transformation of the Rheological Equations to a Fixed Coordinate System.

The equations of motion and continuity as well as the boundary and initial conditions are usually expressed in terms of quantities associated

with a fixed frame of reference. Therefore, it will be necessary to transform the rheological equations of state from the convected system to a fixed one. Observing that the models (2-1) and (2-2) contain tensor components and their time derivatives, the laws of transformation of tensors and the concept of differentiation in convected coordinates must be reviewed. Let x^j , ($j=1,2,3$) be a fixed coordinate system and ξ^i , ($i=1,2,3$) a convected one associated with a particular flow problem. Then

$$x^j = x^j(\xi, t) \quad ; \quad \xi^i = \xi^i(x, t) \quad (2-4)$$

These equations completely define the motion of the fluid due to the definition of the ξ^i . Let $\sigma_{i_1 \dots i_n}^{m_1 \dots m_n}(\xi, t)$ be any tensor associated with some point in the convected system. Then $\sigma_{i_1 \dots i_n}^{m_1 \dots m_n}(\xi, t)$ can be transformed to the x^j -system by means of the usual laws^{6,7}

$$\sigma_{i_1 \dots i_n}^{m_1 \dots m_n}(\xi, t) = \left(\frac{\partial x^{k_1}}{\partial \xi^{i_1}} \right) \dots \left(\frac{\partial \xi^{m_1}}{\partial x^{p_1}} \right) \left(\frac{\partial \xi^{m_2}}{\partial x^{p_2}} \right) \dots \left(\frac{\partial \xi^{m_n}}{\partial x^{p_n}} \right) \sigma_{k_1 \dots k_n}^{p_1 \dots p_n}(x, t) \quad (2-5)$$

where $S_{k_1 \dots k_n}^{p_1 \dots p_n}(x, t)$ are the tensor components in the fixed coordinates. In our particular case the absolute second order tensors transform as follows:

$$\sigma_{ij} = \left(\frac{\partial x^k}{\partial \xi^i} \right) \left(\frac{\partial x^m}{\partial \xi^j} \right) S_{km} \quad (2-6)$$

$$\sigma^{ij} = \left(\frac{\partial \xi^i}{\partial x^k} \right) \left(\frac{\partial \xi^j}{\partial x^m} \right) S^{km} \quad (2-7)$$

$$\sigma^i_j = \left(\frac{\partial \xi^i}{\partial x^k} \right) \left(\frac{\partial x^m}{\partial \xi^j} \right) S^k_m \quad (2-8)$$

The transformation laws for the convected time derivatives of tensors can be obtained in the following manner:

$$\begin{aligned} \frac{D}{Dt} \sigma_{ij} &= \left(\frac{\partial x^e}{\partial \xi^i} \right) \left(\frac{\partial x^m}{\partial \xi^j} \right) \frac{D}{Dt} s_{em} + \frac{D}{Dt} \left[\left(\frac{\partial x^e}{\partial \xi^i} \right) \left(\frac{\partial x^m}{\partial \xi^j} \right) \right] s_{em} \\ &= \left(\frac{\partial x^e}{\partial \xi^i} \right) \left(\frac{\partial x^m}{\partial \xi^j} \right) \left[\frac{\partial}{\partial t} s_{em} + v^r \frac{\partial}{\partial x^r} s_{em} \right] + \\ &\quad + \frac{\partial v^e}{\partial \xi^i} \frac{\partial x^m}{\partial \xi^j} s_{em} + \frac{\partial x^e}{\partial \xi^i} \frac{\partial v^m}{\partial \xi^j} s_{em} \end{aligned} \quad (2-9)$$

Since

$$\frac{D}{Dt} s_{em} = \frac{\partial}{\partial t} s_{em} + v^r \frac{\partial}{\partial x^r} s_{em} \quad (2-10)$$

and

$$\frac{D}{Dt} x^r = v^r \quad (2-11)$$

$$\frac{D}{Dt} \left(\frac{\partial x^e}{\partial \xi^i} \right) = \frac{\partial}{\partial \xi^i} \frac{D}{Dt} x^e = \frac{\partial v^e}{\partial \xi^i} \quad (2-12)$$

Now let $\xi^i = \text{constant}$ coincide with $x^i = \text{constant}$ at some time $t = t_0$, then,

$$\frac{\partial x^e}{\partial \xi^i} = \delta^e_i, \quad \sigma_{ij} = s_{ij} \quad (2-13)$$

and

$$\frac{D}{Dt} \sigma_{ij} = \frac{\partial}{\partial t} s_{ij} + v^r \frac{\partial}{\partial x^r} s_{ij} + \frac{\partial v^c}{\partial x^r} s_{ij} + \frac{\partial v^m}{\partial x^l} s_{im} \quad (2-14)$$

Recalling that the covariant derivative is given as

$$s_{ij,q} = \frac{\partial}{\partial x^q} s_{ij} - s_{hi} \Gamma_{jq}^h - s_{jh} \Gamma_{iq}^h \quad (2-15)$$

and the Γ_{ij}^k are the Christoffel symbols defined by

$$\Gamma_{ij}^k = \frac{g^{hk}}{2} \left(\frac{\partial}{\partial x^i} g_{jk} + \frac{\partial}{\partial x^j} g_{ik} - \frac{\partial}{\partial x^k} g_{ij} \right) \quad (2-16)$$

we obtain from (2-15)

$$\frac{\partial}{\partial x^q} s_{ij} = s_{ij,q} + s_{hj} \Gamma_{iq}^h + s_{ih} \Gamma_{jq}^h \quad (2-17)$$

Similarly we have

$$v_{,q}^r = \frac{\partial v^r}{\partial x^q} + v^r \Gamma_{pq}^r \quad (2-18)$$

Substituting eqs. (2-17) and (2-18) into (2-14) we obtain

$$\begin{aligned} \frac{D}{Dt} \sigma_{ij} = & \frac{\partial}{\partial t} s_{ij} + v^r (s_{ij,r} + s_{hj} \Gamma_{ir}^h + s_{ih} \Gamma_{rj}^h) + \\ & + (v_{,i}^s - v^r \Gamma_{ri}^s) s_{sj} + (v_{,j}^m - v^r \Gamma_{rj}^m) s_{im} \end{aligned} \quad (2-19)$$

rearrangement of terms yields

$$\begin{aligned} \frac{D}{Dt} \sigma_{ij} = & \frac{\partial}{\partial t} s_{ij} + v^r s_{ij,r} + v_i^c s_{ej} + v_{,ij}^m s_{im} + \\ & + v^r (s_{rj} \Gamma_{ir}^t + s_{it} \Gamma_{rj}^t - s_{ej} \Gamma_{ri}^c - s_{im} \Gamma_{ir}^m) \end{aligned} \quad (2-20)$$

and upon simplification of the above equation we have

$$\frac{D}{Dt} \sigma_{ij} = \frac{\partial}{\partial t} s_{ij} + v^r s_{ij,r} + v_i^c s_{ej} + v_{,ij}^m s_{im} \quad (2-21)$$

Introducing the definition of vorticity and strain-rate

$$\omega_{ik} = \frac{1}{2} (v_{k,i} - v_{i,k}) \quad (2-22)$$

$$\epsilon_{ik} = \frac{1}{2} (v_{k,i} + v_{i,k}) \quad (2-23)$$

the time derivative (2-21) can be written in the following form

$$\frac{D}{Dt} \sigma_{ij} = \frac{\partial}{\partial t} s_{ij} + v^r s_{ij,r} + (\omega_i^c + \epsilon_i^c) s_{ej} + (\omega_j^m + \epsilon_j^m) s_{im} \quad (2-24)$$

Using the same method the time derivative for contravariant tensors can be found to be

$$\frac{D}{Dt} \sigma^{ij} = \frac{\partial}{\partial t} s^{ij} + v^r s^{ij}_{,r} - (\omega_i^c + \epsilon_i^c) s^{ej} - (\omega_j^m + \epsilon_j^m) s^{im} \quad (2-25)$$

and for mixed tensors

$$\frac{D}{Dt} \sigma_i^j = \frac{\partial}{\partial t} s_i^j + v^r s_{i,r}^j + (\omega_i^c + \epsilon_i^c) s_{ej} - (\omega_j^m + \epsilon_j^m) s_{im} \quad (2-26)$$

We shall introduce the symbol $\frac{D}{Dt}$ to mean the transformation of $\frac{D}{dt}$ from the convected coordinates $\{i\}$ to the fixed ones $\{j\}$, thus for the covariant case

$$\frac{D}{Dt} S_{ij} = \left(\frac{\partial \xi^c}{\partial X^i} \right) \left(\frac{\partial \xi^m}{\partial X^j} \right) \frac{D}{Dt} \sigma_{cm} \quad (2-27)$$

Similarly for the contravariant and mixed tensors. It should be remarked here, that while the convected coordinates, embedded in the moving continuum are the most convenient to derive the transformation of the rheological equations to a fixed frame of reference they are not necessarily the easiest to work with or to define. In most practical cases the convected system is a set of rigid coordinates, which are often called material coordinates, rotating and translating with the moving fluid, but not deforming with it. The time derivatives in such a frame of reference will be

$$\left(\frac{D}{Dt} \sigma_{ij} \right)_{\text{rigid}} = \frac{D}{Dt} s_{ij} + v^r s_{i,r} + w_i^c s_{c,j} + w_j^m s_{i,m} \quad (2-28)$$

and

$$\left(\frac{D}{Dt} \sigma_{ij} \right)_{\text{convected}} = \left(\frac{D}{Dt} \sigma_{ij} \right)_{\text{rigid}} + \epsilon_i^c s_{c,j} + \epsilon_j^m s_{i,m} \quad (2-29)$$

Similarly for the contravariant and mixed tensors. Thus if a rigid convected system is used then the time derivatives should be corrected as indicated above.

Now using the results obtained above the equations of state assumed to be of the form (2-1) or (2-2) in the convected coordinate system may be expressed in terms of a fixed coordinate frame. Thus models (2-1) and (2-2) become:

$$(1 + \lambda_1 \frac{\partial}{\partial t} + \lambda_2 \frac{\partial^2}{\partial t^2} + \dots) t_{ij} = 2\gamma_0 (1 + \tau_1 \frac{\partial}{\partial t} + \tau_2 \frac{\partial^2}{\partial t^2} + \dots) e_{ij} \quad (2-30)$$

and

$$(1 + \lambda \frac{\partial}{\partial t}) t_{ij} = 2\gamma_0 (1 + \tau \frac{\partial}{\partial t}) e_{ij} \quad (2-31)$$

and similarly for their contravariant and mixed counterparts. Here t_{ij} and e_{ij} are the stress and strain rate components in the fixed system. In the rest of this work only model (2-2) and thus (2-31) will be used. The application of the more general model (2-1) will be reported in a future work.

3. THE FLOW BETWEEN TWO VERTICAL CONCENTRIC CYLINDERS

The steady state flow between two upright coaxial cylinders is considered here. Let the inner and outer cylinders be of radius r_1 , r_2 , rotating with angular velocity w_1 , w_2 , respectively.

Let x_1 , x_2 , x_3 be a cartesian frame of reference with the x_3 -axis along the common axis of the cylinders. Also, introduce a cylindrical coordinate system (r, θ, z) such that

$$x_1 = r \cos \theta, \quad x_2 = r \sin \theta, \quad x_3 = z \quad (3-1)$$

The velocity field in cartesian coordinates is

$$v^i = [-x_2 w(r), x_1 w(r), 0] \quad (3-2)$$

and in cylindrical coordinates

$$v^i = [0, r w(r), 0] \quad (3-3)$$

where $w(r)$ is the angular velocity.

The vorticity (w_{ij}) and the strain rate components are found, by use of equations (2-22) and (2-23), to be, in cartesian coordinates

$$\begin{aligned} w_{11} = w_{22} = w_{33} = w_{21} = w_{32} = 0 \\ w_{12} = -w_{21} = w + \frac{1}{2} r w_r \end{aligned} \quad (3-4)$$

and

$$\begin{aligned} \epsilon_{11} = -\frac{x_1 x_2}{r} w_r, \quad \epsilon_{33} = 0 \\ \epsilon_{22} = \frac{x_1 x_2}{r} w_r, \quad \epsilon_{31} = 0 \\ \epsilon_{12} = \frac{x_1^2 - x_2^2}{2r} w_r, \quad \epsilon_{32} = 0 \end{aligned} \quad (3-5)$$

Transforming to cylindrical coordinates we obtain for the vorticity components

$$\begin{aligned} \omega_{rr} = \omega_{\theta\theta} = \omega_{zz} = \omega_{r\theta} = \omega_{rz} = \omega_{z\theta} = 0 \\ \omega_{r\theta} = -\omega_{\theta r} = \omega + \frac{1}{2} r \omega_r \end{aligned} \quad (3-6)$$

and for the strain-rate field

$$e_{rr} = e_{\theta\theta} = e_{zz} = e_{r\theta} = e_{rz} = e_{z\theta} = 0 \quad (3-7)$$

$$e_{r\theta} = \frac{1}{2} r \omega_r$$

where

$$\omega_r = \frac{d}{dr} \omega$$

The associated stress fields⁸ are assumed in the cylindrical frame of reference and taking into account the axi-symmetric nature of the problem.

$$t_{ij} = \begin{bmatrix} t_{rr} & t_{r\theta} & 0 \\ t_{\theta r} & t_{\theta\theta} & 0 \\ 0 & 0 & t_{zz} \end{bmatrix} \quad (3-8)$$

and therefore, in cartesian coordinates

$$\begin{aligned} r^2 \tau_{11} &= x_1^2 t_{rr} + x_2^2 t_{\theta\theta} - 2x_1 x_2 t_{r\theta} \\ r^2 \tau_{22} &= x_2^2 t_{rr} + x_1^2 t_{\theta\theta} + 2x_1 x_2 t_{r\theta} \\ \tau_{33} &= t_{zz} \\ r^2 \tau_{12} &= x_1 x_2 (t_{rr} - t_{\theta\theta}) + (x_1^2 - x_2^2) t_{r\theta} \\ \tau_{23} = \tau_{31} &= 0 \end{aligned} \quad (3-9)$$

The convected time derivatives, computed by means of eqs. (2-24) and (2-27) are tabulated below, first for the covariant components of strain rates

$$\begin{aligned} \frac{\partial}{\partial t} e_{rr} &= (rv_r)^2 \\ \frac{\partial}{\partial t} e_{\theta\theta} &= \frac{\partial}{\partial t} e_{zz} = 0 \\ \frac{\partial}{\partial t} e_{r\theta} &= \frac{\partial}{\partial t} e_{\theta z} = \frac{\partial}{\partial t} e_{zr} = 0 \end{aligned} \quad (3-10)$$

and stress field

$$\begin{aligned} \frac{\partial}{\partial t} t_{rr} &= rv_r t_{r\theta} \\ \frac{\partial}{\partial t} t_{r\theta} &= rv_r t_{\theta\theta} \\ \frac{\partial}{\partial t} (t_{\theta\theta}, t_{zz}, t_{z\theta}, t_{zr}) &= 0 \end{aligned} \quad (3-11)$$

and for the contravariant components

$$\begin{aligned} \frac{\partial}{\partial t} e^{rr} &= \frac{\partial}{\partial t} e^{zz} = 0 \\ \frac{\partial}{\partial t} e^{\theta\theta} &= -(rv_r)^2 \\ \frac{\partial}{\partial t} e^{r\theta} &= \frac{\partial}{\partial t} e^{\theta z} = \frac{\partial}{\partial t} e^{zr} = 0 \end{aligned} \quad (3-12)$$

and

$$\begin{aligned} \frac{\partial}{\partial t} t^{\theta\theta} &= -2rv_r t^{r\theta} \\ \frac{\partial}{\partial t} t^{r\theta} &= -rv_r t^{rr} \\ \frac{\partial}{\partial t} t^{rr} &= \frac{\partial}{\partial t} t^{zz} = \frac{\partial}{\partial t} t^{zr} = \frac{\partial}{\partial t} t^{r\theta} = 0 \end{aligned} \quad (3-13)$$

The rheological equations may now be obtained by use of eqs. (3-8) through (3-13) and the model $(1 + \lambda \frac{\partial}{\partial t}) t_{ij} = 2\eta (1 + \tau \frac{\partial}{\partial t}) e_{ij}$ in its covariant form. Thus

$$t_{rr} + 2\lambda (r w_r) t_{r\theta} = 2\eta \tau (r w_r)^2$$

$$t_{r\theta} = \eta (r w_r) \quad (3-14)$$

$$t_{\theta\theta} = t_{z z} = t_{z r} = t_{z \theta} = 0$$

Serving for the non-zero components of the stress tensor t_{ij} we obtain

$$t_{rr} = 2\eta (\tau - \lambda) (r w_r)^2$$

$$t_{r\theta} = \eta (r w_r) \quad (3-15)$$

and the rest of the components are zero.

Using the contravariant model

$$(1 + \lambda \frac{\partial}{\partial t}) t^{ij} = 2\eta (1 + \tau \frac{\partial}{\partial t}) e^{ij}$$

and the results reported in eqs. (3-8) through (3-13) the rheological equations are

$$t^{\theta\theta} - 2\lambda (r w_r) t^{r\theta} = -2\eta \tau (r w_r)^2$$

$$t^{r\theta} = \eta (r w_r) \quad (3-16)$$

$$t^{rr} = t^{zz} = t^{zr} = t^{z\theta} = 0$$

and upon simplification we obtain the expressions for the stress field

$$t^{\theta\theta} = -2\eta (\tau - \lambda) (r w_r)^2$$

$$t^{r\theta} = \eta (r w_r) \quad (3-17)$$

The equations of motion

$$\Gamma_{ij,i} + \rho F_j = \rho \dot{v}_j \quad (3-18)$$

in cylindrical coordinates for the case of axial symmetry yield

$$\frac{\partial}{\partial r} [t_{rr} - p(r,z)] + \frac{1}{r} [t_{rr} - t_{\theta\theta}] = -\rho r \omega^2 \quad (3-19)$$

$$\frac{\partial}{\partial r} t_{r\theta} + \frac{2}{r} t_{r\theta} = 0$$

$$\frac{\partial}{\partial z} p(r,z) = -Rg$$

$$\Gamma_{ij} = t_{ij} - p(r,z) \delta_{ij} \quad (3-20)$$

where

and $p(r,z)$ is the pressure scalar and g the gravitational acceleration.

The boundary conditions for this flow problem are

$$\omega(r_1) = \omega_1, \quad \omega(r_2) = \omega_2 \quad (3-21)$$

Solving simultaneously eqs. (3-15) and (3-19) and by taking advantage of the second equation of eqs. (3-19) we obtain

$$t_{r\theta} = C_1 r^{-2} \quad (3-22)$$

$$t_{rr} = 2 \left(\frac{T-\lambda}{r} \right) C_1^2 r^{-4} \quad (3-23)$$

and

$$r \omega_r = \frac{C_1}{r} r^{-2} \quad (3-24)$$

$$\omega(r) = C_2 - \frac{C_1}{2r} r^{-2} \quad (3-25)$$

Using the boundary conditions (3-21) to evaluate C_1 , C_2 we have

$$C_1 = 2\eta (w_2 - w_1) \frac{r_1^2 r_2^2}{r_2^2 - r_1^2} \quad (3-26)$$

$$C_2 = \frac{w_2 r_2^2 - w_1 r_1^2}{r_2^2 - r_1^2} \quad (3-27)$$

Substituting eqs. (3-22) and (3-23) in the equations of motion, (3-19) we obtain the stress field for the covariant case

$$\begin{aligned} \bar{t}_{rr} &= t_{rr} - p(r,t) \\ \bar{t}_{\theta\theta} &= -p(r,t) \quad ; \quad \bar{t}_{\theta z} = 0 \\ \bar{t}_{z\theta} &= -p(r,t) \quad ; \quad \bar{t}_{zr} = 0 \\ \bar{t}_{r\theta} &= C_1 r^{-2} \end{aligned} \quad (3-28)$$

$$p(r,t) = \frac{3}{2}\eta(\tau-\lambda) C_1 r^{-4} + \rho \left[\frac{1}{2} C_1^2 r^{-2} - \frac{C_1^2}{8\eta^2} r^{-2} - \frac{C_2}{\eta} \ln r - g\tau \right] + C_3$$

where C_3 is a constant.

Similarly solving simultaneously eqs. (3-17) and (3-19) we obtain the stress field for the contravariant case. Thus

$$\begin{aligned} t^{\theta\theta} &= -2(\tau-\lambda) \frac{C_1^2}{\eta} r^{-4} \\ t^{r\theta} &= C_1 r^{-2} \\ t^{rr} &= t^{zz} = t^{zr} = t^{z\theta} = 0 \end{aligned} \quad (3-29)$$

and

$$\bar{t}^{rr} = -p(r, z) \quad ; \quad \bar{t}^{\theta\theta} = t^{\theta\theta} - p(r, z)$$

$$\bar{t}^{zz} = -p(r, z) \quad ; \quad \bar{t}^{r\theta} = 0, r^{-2} \quad (3-30)$$

$$p(r, z) = -\frac{1}{2}(\tau - \lambda)r^{-4} + \rho \left[\frac{1}{2}c_1^2 r^2 - \frac{c_1^2}{8\eta^2} r^{-2} - \frac{c_1 c_2}{2} \ln r - q_2 \right] + C_3$$

The stress fields, (3-28) and (3-30) give a complete description of the behavior of the fluid under the assumed flow. Furthermore, important questions, such as under what conditions such a flow can be sustained and under what pressure can be considered intelligently. Also, by the nature of the behavior of fluid under the conditions described in this flow problem, one can decide on the type of model that should be used in analyzing a particular seal problem.

4. THE FLOW BETWEEN TWO PARALLEL DISKS

The steady state flow between two coaxial parallel circular plates is considered here. Let the radii of both disks be r_0 , and the distance between the disks be z_0 . The two disks are rotating with angular velocities ω_1 , ω_2 respectively.

Let x_1, x_2, x_3 be a cartesian coordinate system, the x_3 - axis being along the common axis. Also, introduce a cylindrical frame of reference (r, θ, z) such that

$$x_1 = r \cos \theta, \quad x_2 = r \sin \theta, \quad x_3 = z \quad (4-1)$$

The velocity is

$$v^j = [-X_2 \omega(r, z), X_1 \omega(r, z), 0] \quad (4-2)$$

in cartesian coordinates, and

$$v^j = [0, r \omega(r, z), 0] \quad (4-3)$$

in cylindrical coordinates.

Recalling that the vorticity and strain-rate tensors are given in terms of the velocity vector by

$$\omega_{ij} = \frac{1}{2} (v_{ji} - v_{ij}) \quad ; \quad \epsilon_{ij} = \frac{1}{2} (v_{ji} + v_{ij}) \quad (4-4)$$

they are found to be in cartesian coordinates

$$\begin{aligned} \omega_{11} = \omega_{22} = \omega_{33} = 0 \quad ; \quad \omega_{13} &= \frac{x_2}{2} \omega_z \\ \omega_{12} = \omega + \frac{1}{2} r \omega_r \quad ; \quad \omega_{23} &= -\frac{x_1}{2} \omega_z \end{aligned} \quad (4-5)$$

and

$$\begin{aligned} \epsilon_{11} &= -\frac{x_1 x_2}{r} w_r & ; & \quad \epsilon_{12} = \frac{x_1^2 - x_2^2}{2r} w_r \\ \epsilon_{22} &= \frac{x_1 x_2}{r} w_r & ; & \quad \epsilon_{23} = \frac{x_1}{2} w_2 \\ \epsilon_{31} &= 0 & ; & \quad \epsilon_{13} = -\frac{x_2}{2} w_2 \end{aligned} \quad (4-6)$$

By transformation to cylindrical coordinates

$$\begin{aligned} w_{rr} = w_{\theta\theta} = w_{zz} = w_{zr} = 0 & \quad (4-7) \\ w_{r\theta} = w + \frac{1}{2} r w_r & ; \quad w_{z\theta} = \frac{1}{2} r w_2 \end{aligned}$$

and

$$\begin{aligned} e_{rr} = e_{\theta\theta} = e_{zz} = e_{zr} = 0 & \quad (4-8) \\ e_{r\theta} = \frac{1}{2} r w_r + w & ; \quad w_{z\theta} = \frac{1}{2} r w_2 \\ w_r = \frac{\partial}{\partial r} w & ; \quad w_z = \frac{\partial}{\partial z} w \end{aligned}$$

where

The associated stress fields, assumed in the cylindrical reference system to be

$$t_{ij} = \begin{bmatrix} t_{rr} & t_{r\theta} & t_{rz} \\ t_{\theta r} & t_{\theta\theta} & t_{\theta z} \\ t_{zr} & t_{z\theta} & t_{zz} \end{bmatrix} \quad (4-9)$$

and, therefore, in cartesian coordinates

$$r^2 T_{11} = X_1^2 t_{rr} + X_2^2 t_{\theta\theta} - 2X_1 X_2 t_{r\theta}$$

$$r^2 T_{22} = X_2^2 t_{rr} + X_1^2 t_{\theta\theta} + 2X_1 X_2 t_{r\theta}$$

$$T_{33} = t_{zz}$$

(4-10)

$$r^2 T_{12} = X_1 X_2 (t_{rr} - t_{\theta\theta}) + (X_1^2 - X_2^2) t_{r\theta}$$

$$r^2 T_{13} = X_1 t_{rz} - X_2 t_{\theta z}$$

$$r^2 T_{23} = X_2 t_{rz} + X_1 t_{\theta z}$$

The convected time derivatives, computed by means shown in Section 2 are tabulated below

$$\frac{d}{dt} e_{rr} = (r w_r)^2 ; \quad \frac{d}{dt} e_{r\theta} = 0$$

$$\frac{d}{dt} e_{\theta\theta} = 0 ; \quad \frac{d}{dt} e_{\theta z} = 0$$

(4-11)

$$\frac{d}{dt} e_{zz} = (r w_z)^2 ; \quad \frac{d}{dt} e_{rz} = r^2 w_r w_z$$

and for the associate stress field

$$\frac{d}{dt} t_{rr} = 2r w_r t_{r\theta} ; \quad \frac{d}{dt} t_{r\theta} = r w_r t_{\theta\theta}$$

$$\frac{d}{dt} t_{\theta\theta} = 0 ; \quad \frac{d}{dt} t_{\theta z} = r w_z t_{\theta\theta}$$

(4-12)

$$\frac{d}{dt} t_{zz} = 2r w_z t_{\theta z} ; \quad \frac{d}{dt} t_{zr} = r w_r t_{\theta z} - r w_z t_{r\theta}$$

The rheological equations of state are obtained by means of

$$\left(1 + \lambda \frac{\partial}{\partial t}\right) t_{ij} = 2\eta \left(1 + \tau \frac{\partial}{\partial t}\right) e_{ij}$$

in cartesian rotating coordinates for the covariant model.

$$t_{rr} + 2\lambda r w_r t_{r\theta} = 2\eta \tau (r w_r)^2$$

$$t_{z z} + 2\lambda r w_z t_{\theta z} = 2\eta \tau (r w_z)^2$$

$$t_{r\theta} + \lambda r w_r t_{\theta\theta} = \eta (r w_r)$$

$$t_{\theta z} + \lambda r w_z t_{\theta\theta} = \eta (r w_z)$$

$$t_{rz} + \lambda r w_r t_{\theta z} - \lambda r w_z t_{r\theta} = 2\eta \tau (r w_r)(r w_z)$$

$$t_{\theta\theta} = 0$$

by simplifying and solving for t_{ij} 's

$$t_{r\theta} = \eta (r w_r)$$

$$t_{z\theta} = \eta (r w_z)$$

$$t_{rz} = 2\eta \tau (r w_r)(r w_z)$$

$$t_{rr} = 2\eta \tau (r w_r)^2$$

$$t_{\theta\theta} = 0$$

$$t_{zz} = 2\eta \tau (r w_z)^2$$

(4-13)

(4-14)

The equations of motion

$$\bar{t}_{ij,j} + \rho \bar{F}_j = \rho \dot{v}_i \quad (4-15)$$

expressed in cylindrical coordinates yield

$$\begin{aligned} \frac{\partial}{\partial r} \bar{t}_{rr} + \frac{1}{r} \frac{\partial}{\partial \theta} \bar{t}_{r\theta} + \frac{\partial}{\partial z} \bar{t}_{rz} + \frac{1}{r} \bar{t}_{r\theta} + \frac{1}{r} (\bar{t}_{rr} - \bar{t}_{\theta\theta}) &= -\rho r \omega^2 \\ \frac{\partial}{\partial r} \bar{t}_{r\theta} + \frac{1}{r} \frac{\partial}{\partial \theta} \bar{t}_{r\theta} + \frac{\partial}{\partial z} \bar{t}_{r\theta} + \frac{2}{r} \bar{t}_{r\theta} &= 0 \\ \frac{\partial}{\partial r} \bar{t}_{rz} + \frac{1}{r} \frac{\partial}{\partial \theta} \bar{t}_{\theta z} + \frac{\partial}{\partial z} \bar{t}_{rz} + \frac{1}{r} \bar{t}_{rz} &= \rho g \end{aligned} \quad (4-16)$$

Since $\bar{t}_{ij} = t_{ij} - p \delta_{ij}$ and assuming rotational symmetry, thus $t_{ij} \neq t_{ij}(\theta)$ and $p \neq p(\theta)$ the equations of motion become

$$\begin{aligned} \frac{\partial}{\partial r} t_{rr} + \frac{\partial}{\partial z} t_{rz} + \frac{1}{r} (t_{rr} - t_{\theta\theta}) &= \frac{\partial}{\partial r} p - \rho r \omega^2 \\ \frac{\partial}{\partial r} t_{r\theta} + \frac{\partial}{\partial z} t_{\theta z} + \frac{2}{r} t_{r\theta} &= 0 \\ \frac{\partial}{\partial r} t_{rz} + \frac{\partial}{\partial z} t_{rz} + \frac{1}{r} t_{rz} &= \frac{\partial}{\partial z} p + \rho g \end{aligned} \quad (4-17)$$

The equation of continuity

$$\bar{r} + \rho v_{i,i} = 0 \quad (4-18)$$

is identically satisfied by the velocity field, eq. (4-2) or (4-3).

Solving simultaneously eqs. (4-14) and (4-17) one can obtain explicitly the velocity field $w(r, z)$, the pressure $p(r, z)$ and the stress field t_{ij} . In attempting to solve this system substitute the first two equations of eqs. (4-14) into the second equation of eqs. (4-17), thus obtaining

$$\nu \frac{\partial}{\partial r} (rw_r) + \frac{2\nu}{r} (rw_r) + \nu \frac{\partial}{\partial z} (rw_z) = 0$$

or after some manipulations

$$\frac{\partial^2}{\partial r^2} w + \frac{3}{r} \frac{\partial}{\partial r} w + \frac{\partial^2}{\partial z^2} w = 0 \quad (4-19)$$

Let now

$$w(r, z) = \frac{R(r)}{r} \cdot Z(z) \quad (4-20)$$

and eq. (4-19) yields the system

$$Z'' - \lambda^2 Z = 0 \quad (4-21)$$

$$R'' + \frac{1}{r} R' + \left(\lambda^2 - \frac{1}{r^2}\right) R = 0 \quad (4-22)$$

Therefore

$$Z(z) = C_1 e^{\lambda z} + C_2 e^{-\lambda z} \quad (4-23)$$

and

$$R(r) = A_1 J_{\lambda}(r) + A_2 Y_{\lambda}(r) \quad (4-24)$$

and the velocity field given by

$$w(r,t) = \frac{1}{r} \left\{ C_1 e^{\lambda r} + C_2 e^{-\lambda r} \right\} \cdot \left\{ A_1 J_1(\lambda r) + A_2 Y_1(\lambda r) \right\} \quad (4-25)$$

where $J_1(\lambda r)$, $Y_1(\lambda r)$ are Bessel functions of the first and second kind respectively, λ is a constant. $Y_1(\lambda r)$ has to be rejected in this problem because it is unbounded at $r=0$, and $w(r,t)$ becomes:

$$w(r,t) = (B_1 e^{\lambda r} + B_2 e^{-\lambda r}) \frac{J_1(\lambda r)}{r} \quad (4-26)$$

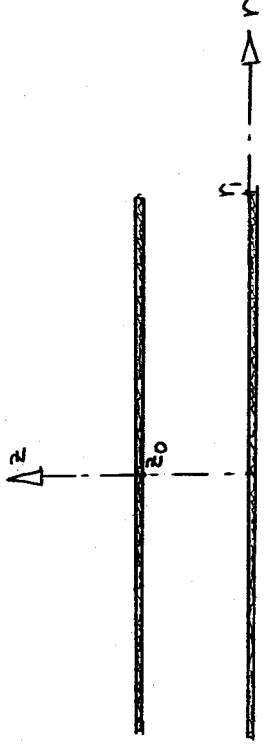
The determination of the constants B_1, B_2 and λ depends on the boundary conditions imposed on the problem.

The Boundary Value Problem:

The following two sets of boundary conditions are considered in this

section:

(I)



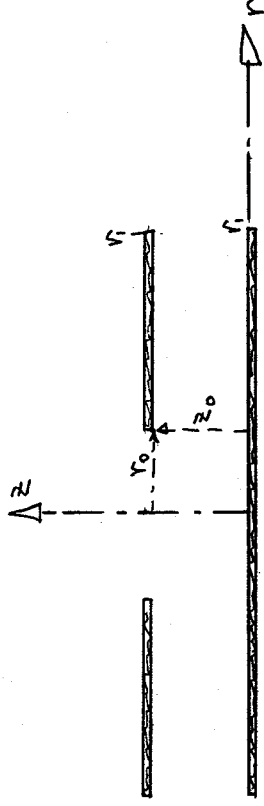
$$w(r, 0) = w_1$$

$$(\nabla r) r \in [0, r_1]$$

$$w(r, z_0) = w_2$$

$$(\nabla r) r \in [0, r_1] \quad (4-27)$$

(II)



$$w(r, 0) = w_1$$

$$(\nabla r) r \in [0, r_1]$$

$$w(r, z_0) = w_2$$

$$(\nabla r) r \in [r_0, r_1] \quad (4-28)$$

The solution to the equation of motion is repeated here for convenience.

$$w(r, z) = \left(\beta_1 e^{\lambda z} + \beta_2 e^{-\lambda z} \right) \frac{J_1(\lambda r)}{r} \quad (4-26)$$

Case (1): The boundary conditions (4-27) yield

$$(B_1 + B_2) \frac{J_1(\lambda r)}{r} = w_1$$

$$(B_1 e^{\lambda z_0} + B_2 e^{-\lambda z_0}) \frac{J_1(\lambda r)}{r} = w_2$$

or

$$B_1 = \frac{\Omega e^{-\lambda z_0} - 1}{1 - \Omega e^{\lambda z_0}} B_2 \quad (4-29)$$

where

$$\Omega = \frac{w_1}{w_2} \quad (4-30)$$

Thus by use of eq (4-29) eq (4-26) becomes

$$w(r, z) = \frac{2B}{\Omega e^{\lambda z_0} - 1} \left[\sinh \lambda z + \Omega \sinh \lambda (z_0 - z) \right] \frac{J_1(\lambda r)}{r} \quad (4-31)$$

and the boundary conditions (4-27) reduce to

$$\left(\frac{2\Omega \sinh \lambda z_0}{\Omega e^{\lambda z_0} - 1} B \right) \frac{J_1(\lambda r)}{r} = w_1 \quad (4-32)$$

$$\left(\frac{2 \sinh \lambda z_0}{\Omega e^{\lambda z_0} - 1} B \right) \frac{J_1(\lambda r)}{r} = w_2$$

which are identical. Now define

$$A = \frac{2 \sinh \lambda z_0}{\Omega e^{\lambda z_0} - 1} B \quad (4-33)$$

and conditions (4-23) can be replaced by

$$A J_1(\lambda r) = w_2 r \quad (4-34)$$

or by means of Fourier-Bessel series

$$w_2 r = f(r) = \sum_{j=0}^{\infty} a_j J_1(\lambda_j r) \quad (4-35)$$

or

$$f(r) = \sum_{j=0}^{\infty} \frac{J_1(\lambda_j r)}{N_{1j}} \int_0^{r_1} \bar{r} J_1(\lambda_j \bar{r}) f(\bar{r}) d\bar{r} \quad (4-36)$$

where

$$N_{1j} = \int_0^{r_1} r J_1^2(\lambda_j r) dr = \frac{r_1^2}{2} [J_2(\lambda_j r_1)]^2 \quad (4-37)$$

Thus for $f(r) = w_2 r$

$$a_j = \frac{2 w_2}{J_2(\lambda_j r_1)} \quad (4-38)$$

where

$$\lambda_j = \frac{r_j}{r_1} \quad (4-39)$$

and $J_1(r_j) = 0$; $r_j = \{\text{set of zeros of } J_1(r)\}$ (4-40)

and λ_j are set in ascending order, i.e. $\lambda_0 < \lambda_1 < \lambda_2$ etc. Substituting (4-38) into (4-26) and in view of (4-29) and (4-33) the solution for the angular velocity field subjected to boundary conditions (i) yields

$$w(r, z) = 2 w_2 \sum_{j=0}^{\infty} \left\{ \frac{\sinh \lambda_j z + \cosh \lambda_j (z_0 - z)}{\sinh \lambda_j z_0} \right\} \left\{ \frac{J_1(\lambda_j r)}{r J_2(\lambda_j r_1)} \right\} \quad (4-41)$$

Returning to eqs (4-3) and (4-16)

$$\left(\frac{\partial}{\partial r} + \frac{Q}{r} \right) (r w_r) = - \frac{\partial}{\partial z} (r w_z) \quad (4-42)$$

$$\left(\frac{\partial}{\partial r} - \frac{1}{r} \right) (r w_z) = \frac{\partial}{\partial z} (r w_r)$$

By elimination of $(r w_r)$ and $(r w_z)$ the following equations are obtained

$$\left(\frac{\partial^2}{\partial r^2} + \frac{1}{r} \frac{\partial}{\partial r} - \frac{4}{r^2} + \frac{\partial^2}{\partial z^2} \right) (rw_r) = 0 \quad (4-43)$$

$$\left(\frac{\partial^2}{\partial r^2} + \frac{1}{r} \frac{\partial}{\partial r} - \frac{1}{r^2} + \frac{\partial^2}{\partial z^2} \right) (rw_z) = 0 \quad (4-44)$$

whose solution yields:

$$(rw_r)_i = (A_{1i} e^{\lambda_i z} + A_{2i} e^{-\lambda_i z}) J_2(\lambda_i r) \quad (4-45)$$

$$(rw_z)_j = (B_{1j} e^{\lambda_j z} + B_{2j} e^{-\lambda_j z}) J_1(\lambda_j r) \quad (4-46)$$

which are in complete agreement with eq. (4-26) and (4-41) since

$$\frac{d}{dr} \left(\frac{J_1(\lambda_1 r)}{r} \right) = -\frac{\lambda_1}{r} J_2(\lambda_1 r)$$

and

$$\frac{d}{dz} \left\{ \sinh \lambda_i z + \mathcal{Q} \sinh \lambda_i (z_0 - z) \right\} = \frac{\lambda_i (1 + \mathcal{Q} e^{-\lambda_i z_0})}{2 \sinh \lambda_i z_0} e^{\lambda_i z} + \frac{\lambda_i (1 - \mathcal{Q} e^{\lambda_i z_0})}{2 \sinh \lambda_i z_0} e^{-\lambda_i z}$$

thus the solution (4-41) is compatible to the assumed velocity field.

Before leaving this case two particular solutions are given:

a. $w_1 = 0, w_2 \neq 0$, then

$$w(r, z) = 2w_2 \sum_{j=0}^{\infty} \left(\frac{\sinh \lambda_j z}{\sinh \lambda_j z_0} \right) \left(\frac{J_1(\lambda_j r)}{r J_2(\lambda_j r)} \right) \quad (4-47)$$

b. This implies that the solution to eq. (4-19) becomes:

$$w(r, z) = (A_1 r^{-2} + A_2) (C_1 z + C_2) \quad (4-48)$$

which yields, for boundary conditions (i)

$$w(r, z) = \left(\frac{w_2 - w_1}{z_0} \right) z + w_1 \quad (4-49)$$

In the future this solution shall be referred to as the "elementary-solution."

Case (ii). The boundary conditions (4-28) imposed on eq. (4-26) yield:

$$w(r, 0) = (B_1 + B_2) \frac{J_1(\lambda r)}{r} = w_1$$

$$w(r, z_0) = (B_1 e^{\lambda z_0} + B_2 e^{-\lambda z_0}) \frac{J_1(\lambda r)}{r} = w_2 \quad \text{for } r \in [r_0, r_1]$$

In the region $[r_0, r_1]$ it can be shown that

$$B_1 = \frac{\varphi e^{-\lambda z_0} - 1}{1 - \varphi e^{\lambda z_0}} B_2$$

where φ is defined by (4-30).

Substituting the above into eq. (4-26) and after some manipulations one can obtain

$$w(r, z) = \frac{2B}{\varphi e^{\lambda z_0} - 1} \left[\sinh \lambda z + \varphi \sinh(\lambda(z_0 - z)) \right] \frac{J_1(\lambda r)}{r} \quad (4-50)$$

and the boundary conditions (4-28) reduce to

$$\left(\frac{2 \sinh \lambda z_0}{\varphi e^{\lambda z_0} - 1} B \right) \frac{J_1(\lambda r)}{r} = w_2 \quad (4-51)$$

or

$$A \frac{J_1(\lambda r)}{r} = w_2 \quad (4-52)$$

Now let $\rho = r - r_0$ with $\rho \in [0, r_1 - r_0 = \delta r]$

Thus, the Fourier-Bessel expansion for this problem gives

$$\sum_k a_k J_1[\lambda_k(\rho + r_0)] = w_2(\rho + r_0) \quad (4-53)$$

where

$$a_k = \frac{1}{N_{1k}} \int_0^{\delta r} (\rho + r_0) J_1[\lambda_k(\rho + r_0)] [w_2(\rho + r_0)] d\rho$$

$$N_{1k} = \frac{(\delta r)^2}{2} [J_2(\lambda_k \delta r)]^2$$

or

$$a_k = \frac{2w_2}{J_2(\lambda_k r_0)} \quad (4-54)$$

where

$$\lambda_k = \frac{r_k}{\delta r} \quad ; \quad \text{and} \quad J_1(r_k) = 0 \quad (4-55)$$

hence

$$w_2 r = \sum_{k=0}^{\infty} \frac{2w_2}{J_2(\lambda_k \delta r)} J_1(\lambda_k r) \quad (4-56)$$

In view of the expansion (4-56) and eqs. (4-51) and (4-50) the solution to the boundary value problem (ii) becomes:

$$w(r, z) = 2w_2 \sum_k \left\{ \frac{\sinh \lambda_k z + Q \sinh \lambda_k (z_0 - z)}{\sinh \lambda_k z_0} \right\} \frac{J_1(\lambda_k r)}{r J_2(\lambda_k \delta r)} \quad (4-57)$$

It is apparent that eqs. (4-42) are satisfied by (4-57). For the particular cases where

a. $w_1 = 0$, $w_2 \neq 0$ the expression (4-57) yields

$$w(r, z) = 2w_2 \sum_k \left(\frac{\sinh \lambda_k z}{\sinh \lambda_k z_0} \right) \cdot \frac{J_1(\lambda_k r)}{r J_2(\lambda_k \delta r)} \quad (4-58)$$

b. $\lambda = 0$ reduces the solution of eq(14-19) to

$$w(r, z) = (A_1 r^2 + A_2) (C_1 z + C_2) \quad (4-59)$$

and for the boundary conditions (ii), one obtains

$$w(r, z) = \left(\frac{w_2 - w_1}{z_0} \right) z + w_1 \quad (4-60)$$

where $w(r, z_0) = w_2$ for $r \in [0, r_0]$ or, if $w(r, z_0) \neq w_2$ in $[0, r_0]$ then there exists no solution for $\lambda = 0$.

The contravariant model:

$$\left(1 + \lambda \frac{\partial}{\partial t}\right) \dot{t}^{ij} = 2\gamma \left(1 + \tau \frac{\partial}{\partial t}\right) e^{ij} \quad (4-61)$$

Again using the velocity field

$$v^j = \left[-X_2 w(r, z), X_1 w(r, z), 0 \right]$$

in cartesian coordinates, and

$$v^j = \left[0, r w(r, z), 0 \right]$$

in cylindrical coordinates, the vorticity and strain-rate tensor components are computed and tabulated below

$$\begin{aligned} \omega^{11} = \omega^{22} = \omega^{33} &= 0 & ; & & \omega^{13} &= \frac{X_2}{2} \omega_z \\ \omega^{12} &= \omega + \frac{1}{2} r \omega_r & ; & & \omega^{23} &= -\frac{X_1}{2} \omega_z \end{aligned} \quad (4-62)$$

and

$$\begin{aligned} \epsilon^{11} &= -\frac{X_1 X_2}{r} \omega_r & ; & & \epsilon^{12} &= \frac{X_1^2 - X_2^2}{2r} \omega_r \\ \epsilon^{22} &= \frac{X_1 X_2}{r} \omega_r & ; & & \epsilon^{23} &= \frac{X_1}{2} \omega_z \\ \epsilon^{33} &= 0 & ; & & \epsilon^{31} &= -\frac{X_2}{2} \omega_z \end{aligned} \quad (4-63)$$

and their counterparts in cylindrical coordinates computed by the usual means are

$$\begin{aligned} \omega^{rr} = \omega^{\theta\theta} = \omega^{zz} &= \omega^{zr} = 0 \\ \omega^{r\theta} &= \omega + \frac{1}{2} r \omega_r & ; & & \omega^{\theta z} &= -\frac{1}{2} r \omega_z \end{aligned} \quad (4-64)$$

and

$$\begin{aligned} \epsilon^{rr} = \epsilon^{\theta\theta} = \epsilon^{zz} &= \epsilon^{zr} = 0 \\ \epsilon^{r\theta} &= \frac{1}{2} r \omega_r & ; & & \epsilon^{\theta z} &= \frac{1}{2} r \omega_z \end{aligned} \quad (4-65)$$

As in the covariant case, let the associated stress field be

$$t^{ij} = \begin{bmatrix} t^{rr} & t^{r\theta} & t^{rz} \\ t^{\theta r} & t^{\theta\theta} & t^{\theta z} \\ t^{zr} & t^{z\theta} & t^{zz} \end{bmatrix} \quad (4-66)$$

in cylindrical coordinates, thus by transformation to cartesian frame of reference, the stress components are

$$\begin{aligned}
 r^2 T^{11} &= X_1^2 t^{rr} + X_2^2 t^{\theta\theta} - 2X_1 X_2 t^{r\theta} & ; & & r T^{13} &= X_1 t^{r2} - X_2 t^{\theta2} \\
 r^2 T^{22} &= X_1^2 t^{rr} + X_2^2 t^{\theta\theta} + 2X_1 X_2 t^{r\theta} & ; & & r T^{23} &= X_1 t^{r2} + X_2 t^{\theta2} \\
 r^2 T^{12} &= X_1 X_2 (t^{rr} - t^{\theta\theta}) + (X_1^2 - X_2^2) t^{r\theta} & ; & & T^{33} &= t^{z2}
 \end{aligned}
 \tag{4-67}$$

The other terms needed before the rheological equations are determined are the convected time derivatives of the strain-rate tensor and its associated stress tensor. They are obtained by means of eqs. (2-25) and (2-27). The results are listed below:

$$\begin{aligned}
 \frac{\partial}{\partial t} e^{rr} &= 0 & ; & & \frac{\partial}{\partial t} e^{r\theta} &= 0 \\
 \frac{\partial}{\partial t} e^{\theta\theta} &= -(r\omega_r)^2 & ; & & \frac{\partial}{\partial t} e^{\theta z} &= 0 \\
 \frac{\partial}{\partial t} e^{z\theta} &= (r\omega_r)^2 & ; & & \frac{\partial}{\partial t} e^{zz} &= r^2 \omega_r \omega_z
 \end{aligned}
 \tag{4-68}$$

for the strain-rate components, and

$$\begin{aligned}
 \frac{\partial}{\partial t} t^{rr} &= 0 & ; & & \frac{\partial}{\partial t} t^{r\theta} &= -r\omega_r t^{r\theta} \\
 \frac{\partial}{\partial t} t^{\theta\theta} &= -2r\omega_r t^{r\theta} & ; & & \frac{\partial}{\partial t} t^{\theta z} &= -r\omega_z t^{r\theta} \\
 \frac{\partial}{\partial t} t^{z\theta} &= -2r\omega_r t^{\theta z} & ; & & \frac{\partial}{\partial t} t^{zz} &= r\omega_z t^{r\theta} - r\omega_r t^{\theta z}
 \end{aligned}
 \tag{4-69}$$

By means of the above tables and eq (4-61) one can obtain the equations of state for the assumed model, in rotating cylindrical coordinates:

$$\begin{aligned}
 t^{rr} &= 0 \\
 t^{\theta\theta} - 2r\omega_r t^{r\theta} &= -2r^2 \tau (r\omega_r)^2
 \end{aligned}$$

$$t^{z\theta} - 2\lambda r w_z t^{\theta z} = 2\eta \tau (r w_z)^2$$

$$t^{r\theta} - \lambda r w_r t^{r\theta} = \eta (r w_r)$$

(4-70)

$$t^{\theta z} - \lambda r w_z t^{r\theta} = \eta (r w_z)$$

$$t^{zr} + \lambda (r w_z) t^{r\theta} - \lambda (r w_r) t^{\theta z} = 2\eta \tau (r w_r) (r w_z)$$

solving for the t^{ij} 's, the stress components are

$$t^{rr} = 0$$

$$t^{\theta\theta} = 2\eta (\lambda - \tau) (r w_r)^2$$

$$t^{z\theta} = 2\eta (\lambda + \tau) (r w_z)^2$$

(4-71)

$$t^{r\theta} = \eta (r w_r)$$

$$t^{\theta z} = \eta (r w_z)$$

$$t^{zr} = 2\eta \tau (r w_r) (r w_z)$$

The equations of motion

$$\bar{T}^{\dot{w}}_{,j} + \rho F^{\dot{w}} = \rho \dot{v}^i$$

given in cylindrical coordinates, and keeping in mind the assumption of rotational symmetry in the tensor and force fields yield

$$\frac{\partial}{\partial r} t^{rr} + \frac{\partial}{\partial z} t^{zr} + \frac{1}{r} (t^{rr} - t^{\theta\theta}) = \frac{\partial}{\partial r} p - \rho r \dot{w}^z$$

(4-72)

$$\frac{\partial}{\partial r} t^{r\theta} + \frac{\partial}{\partial z} t^{\theta z} + \frac{2}{r} t^{r\theta} = 0$$

$$\frac{\partial}{\partial r} t^{rz} + \frac{\partial}{\partial z} t^{zr} + \frac{1}{r} t^{rz} = \frac{\partial}{\partial z} p + \rho g$$

The second of equations (4-72) in view of (4-71) can be written as follows

$$\eta \frac{\partial}{\partial r} (r w_r) + \eta \frac{\partial}{\partial z} (r w_z) + \frac{2\eta}{r} (r w_\theta) = 0 \quad (4-73)$$

which after some operations becomes

$$\left(\frac{\partial^2}{\partial r^2} + \frac{3}{r} \frac{\partial}{\partial r} + \frac{\partial^2}{\partial z^2} \right) w = 0 \quad (4-74)$$

which is identical to eq. (4-19).

Thus the solutions obtained for the angular velocity of the covariant model are also solution for the velocity field of the contravariant model. The stress fields however will be different as can be seen from (4-71).

5. BIBLIOGRAPHY

1. C. Eckart, "the Thermodynamics of Irreversible Processes. IV. The Theory of Elasticity and Anelasticity", *Physical Reviews*, 73, 1948, pp. 373.
2. J. G. Oldroyd, "The Motion of an Elasto-Viscous Liquid Contained Between Coaxial Cylinders, I", *Quarterly Journal of Mechanics and Applied Mathematics*, 4, 1951, pp. 271.
3. L. I. Sedov, "Different Definitions of the Rate of Change of a Tensor", *Soviet Journal of Applied Mathematics and Mechanics*, (PMM), Vol. 24, No. 3, 1960, pp. 579.
4. G. M. Rentzepis, "On a Formulation of the Rheological Equations of State of Visco-Elastic Media" (to be published, Royal Society of London).
5. H. Frolick, R. Sack, "Theory of Rheological Properties of Dispersions", *Proceedings of Royal Society of London*, 185, 1946, pp. 415.
6. L. P. Eisenhart, "Riemannian Geometry", Princeton University Press, Princeton, 1949.
7. H. Jeffreys, "Cartesian Tensors", Cambridge University Press, Cambridge, England, 1952.
8. A. E. H. Love, "The Mathematical Theory of Elasticity", Dover Publications, New York, 1944.



Appendix C

The Labyrinth Seal - L. H. Bernd

The purpose of this article is to assess the state of present knowledge of labyrinth seals. A labyrinth seal is widely used to minimize gas leakage along a rotating shaft as in Figure 1. It basically consists of a series of restrictions placed in the leakage flow path. Labyrinth seals are used where it is not feasible to permit direct contact between sealing members, and as a consequence have a relatively high rate of leakage compared to a "contact" type of seal. "Zero" leakage therefore can only be obtained by establishing auxiliary flow circuits to remove the leakage as in Figure 1d. Labyrinth seals are particularly suited to sealing gases, and in many instances are the only type of seal that can be used.

The available knowledge about labyrinth seals is rated "fair" to "good" in accordance with our definition of the state of knowledge in each field. Three references of major importance, (1), (2), (3), in the English language serve to cover the art of labyrinth sealing. When dealing with fluids and seal configurations for which test data is available, knowledge is rated as "Good" (25% design accuracy). When dealing with different configurations, or using fluids that deviate considerably from ideal properties, the knowledge is rated as fair or poor, and testing becomes necessary in the design.

The labyrinth seal functions by:

- a) Restricting the cross-sectional area of the leakage flow path. Thus the clearance between seal and shaft that forms the flow path is made as small as possible. The minimum clearance possible is limited by shaft deflections, the variations in fluid film thickness in the bearings supporting the shaft, unequal thermal expansions, etc.
- b) Taking advantage of the large specific volume of a gas. For a given pressure drop across a seal, the less dense the fluid, the

lower the resultant mass flow rate. This is one of the reasons that a labyrinth seal that is quite effective in sealing a fluid in its gaseous state may be quite useless to seal the same fluid in its liquid state.

c) Creating a turbulent flow path with as much internal friction as possible in the fluid, thereby making for an inefficient flow process to produce low leakage. This is the direct opposite of conventional flow through nozzles and pipes, where it is desired to make for as little friction as possible.

High turbulence and frictional losses are produced in the seal by expanding the gas as it passes through the orifices formed by successive restrictions, thereby converting the energy of the gas into kinetic energy, then attempting as space and geometry permits to dissipate the kinetic energy into heat by changing the direction of flow between successive restrictions. Several labyrinth seals that do this are illustrated in Figure 1b and 1c. The sources of the energy that must be dissipated in this way are: (1) the pressure drop acting across the seal to cause the fluid to flow, (2) the energy stored in the gas because it is initially under pressure, and (3) the energy the fluid may initially possess because of its temperature. The sum of the energy thus contained in the gas as a consequence of its pressure and temperature state is termed the enthalpy of the gas. Item (2) is large for gases, but negligible for liquids because a liquid is relatively incompressible. This fact is of prime importance in determining the basic actions within a labyrinth seal and makes it a device suited primarily to gas properties rather than liquid properties.

Many have investigated labyrinth seals. The approach is largely experimental because of the difficulty of analysis. The University of Tennessee (

has recently made a literature survey of labyrinth sealing, noting the basic analytical approach used by each investigator. There are two starting points: i.e., considering the seal as a nozzle, or as turbulent pipe flow. Neither approach is exact; the actual process lies somewhere in between. The analysis must also take into account the varying properties of the gas because of the large change in pressure and density of the gas as it passes through the seal. Hence the simple basic equations of the above processes must be modified; and the useability of the modification (if simple) depends upon the conditions of use. Equations requiring successive trial and error solutions often result. Graphical solutions are also used.

In addition, much of the existent test data has been obtained using steam. Historically, labyrinth seals were developed for steam turbines. Hence, ideally, further corrections should be made for the deviation of steam from the perfect gas laws when applying this data to other gases. Deviations from the perfect gas laws become insignificant at low pressures. Simple, elemental gases, such as O_2 , N_2 , etc., do not deviate significantly except at very high pressures; higher molecular weight gases such as CO_2 , SO_2 , H_2O , freons, etc. show significant deviations at moderate pressures, such as may be encountered in rocket engines.

It is therefore not surprising to find that Zabriskie and Sternlicht (2) who have briefly investigated labyrinth sealing literature, note errors of as much as 200% in estimating leakage. Their contribution has been to treat the labyrinth as a rough pipe, replotting data from different sources on a comparable basis employing the Reynolds number, thereby enabling them to select material they believed most useful, to achieve according to their estimation, a probable accuracy in estimating leakage of 20%, using a fairly rapid computational procedure. They lament the lack of adequate flow information for

many cases.

Reference (3) although not recent, is recommended because it enables one to rapidly obtain an appreciation of the variables affecting labyrinth seals. Extracts from this reference are given in this article.

It is worthwhile to consider the elementary forms of the equations that can be used to treat flow through a labyrinth. This will give a qualitative appreciation of the significant variables that affect labyrinth sealing to help point out the knowledge needed for seal design.

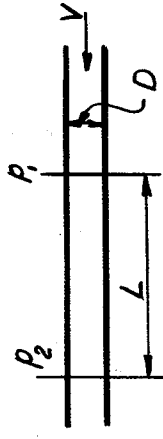
First, considering an incompressible fluid (a liquid rather than a gas), and using nozzle and turbulent pipe flow relations side by side:

$$\Delta p = p_1 - p_2 = \frac{\Delta p}{\rho}$$

Pipe Flow



- f = Friction factor
- ρ = Density
- V = Velocity
- A = Area
- Q = Mass flow rate
- L = Pipe Length



$$V = \sqrt{2gH} \quad (1)$$

$$H = f \left(\frac{L}{D} \right) \left(\frac{V^2}{2g} \right)$$

(11)

$$V = \sqrt{\frac{H D}{f L} 2g}$$

$$Q = V \cdot A \cdot \rho = A \rho \sqrt{2gH}$$

$$Q = V \cdot A \cdot \rho = A \rho \sqrt{\frac{H D}{f L} 2g}$$

But the fluid head $H = \frac{4p}{\rho}$

Also $A = \frac{\pi D^2}{4}$

Substituting:

$$Q = A (\rho)^{.5} (4p)^{.5} (2g)^{.5} \quad (2)$$

$$Q = A^{.25} (\rho)^{.5} (4p)^{.5} (2g)^{.5} \left[\frac{4}{f L} \right]^{.5} \left[\frac{4}{\pi} \right]^{.25}$$

For a concentric annulus of clearance h , the flow area = $A = h \pi d$, where

d = diameter of the annulus:

$$Q \propto h \quad (3)$$

$$Q \propto h^{1.25} \quad (13)$$

Flow Area

Putting the equations in the above form shows that the flow cross-sectional area A of the flow path is the most important variable affecting the leakage rate. Hence a major effort is made in constructing a seal to reduce the clearance between shaft and seal.

In fact, clearances may be used that are so small that occasional contact may take place between seal and shaft. The seal may be made of a soft material, and the shaft then run in to wear away the edges of the seal restrictions. On the other hand, the seal edges may be of hard materials, and carbon used as the material capable of wearing. In some constructions (Fig. 2), the metal in contact with the edges of the seal is made of a light honeycomb structure so that controlled damage will result. The use of honeycomb introduces the disadvantage that additional leakage takes place through the honeycomb spaces that provide additional flow channels across the edges of the seal.

If sufficient deflection of the shaft occurs to make the annulus forming the leakage path appreciably eccentric, increased leakage will result. For turbulent pipe flow in a circular annulus, the maximum increase in flow (upon contact) is 30%. (4) Flow rate vs. eccentricity is plotted in Fig. 4. Thus it is desirable to decrease both clearance and eccentricity. "Floating" constructions are sometimes used to permit clearances tighter than the total variation in shaft position that occurs as a turbine operates.

The effective flow area at a restriction, depending upon geometry and flow conditions, may also be reduced in a manner analogous to the vena contracta of a constant-cross section nozzle (Fig. 3a) to produce as much as 30% variation

in flow. To correct for this contraction in a nozzle, the coefficient of discharge C_d , is introduced into the nozzle formula:

$$Q = C_d \sqrt{2gH} \quad (4)$$

Depending upon upstream flow conditions, C_d , for a constant cross-section nozzle or a square edged orifice is in the order of .6 to 1.0. Comparable variations in flow are found for labyrinth seals (Fig. 5a).

Gas Density

Equations (2) and (12) also illustrate the desirability of using a low density gas to reduce the mass flow Q . In each equation:

$$Q \propto \sqrt{P} \quad (5)$$

Thus a gas at a low pressure (approaching a vacuum) can have a low mass flow rate even though it may actually have a fairly high flow velocity expressed as volume/time. Hence it is desirable to expand a gas to as low a pressure as possible before allowing the gas to emerge from the seal.

Viscosity

The conclusion reached in the previous paragraph remains essentially true even when considering the reduction in viscosity that occurs as the pressure on a gas is reduced to make the gas less dense. Viscosity is also reduced by a decrease in temperature. Both flow processes being considered for illustration are relatively independent of viscosity. For a nozzle, viscosity variations are usually taken into account by plotting the coefficient of discharge versus Reynolds number. This information is available in the literature. The friction factor f also takes into account viscosity variations for turbulent flow, but does not change greatly. To illustrate the order of magnitude of the effect of viscosity, test data on turbulent pipe flow yields the following experimental relations:

$\Delta P \propto \frac{.15 \text{ to } .25}{M}$ $M = \text{viscosity}$
 $\propto \frac{1.15 \text{ to } 1.25}{D}$
 $\propto V^{2.0}$ (For rough pipes)

Nevertheless, estimating leakage for a gas radically different in viscosity than the gas used to obtain test data may require consideration of the viscosity, particularly for cryogenic gases.

Labyrinth Geometry

With suitable approximations, Egli (3) is able to obtain a simple form of equation that applies to steam through a series of labyrinth restrictions that is similar to the basic nozzle equation $Q = A \sqrt{2g p_1 \rho_1}$:

$$Q = \alpha \phi \gamma A \sqrt{g p_1 \rho_1} \quad (6)$$

α , ϕ , γ , are introduced as variables to correct the flow. Using test data, Egli plots these variables as given in Fig. 5.

α is a contraction factor taking into account vena contracta effects
 ϕ is a function of P_1/P_2 , and the number of stages
 γ = Carryover correction factor - to take into account the amount of energy not dissipated in successive stages

Thus, by means of Egli's plottings, one can readily see that increasing the number of stages brings diminishing returns in reducing leakage. In this way one is able to select the optimum point when balancing cost and bulk against leakage.

To illustrate the order of magnitude of the leakage in a labyrinth seal, let us use Egli's data on steam (Fig. 5). Assume a 3" diameter (d) concentric annulus with a .003" clearance (h) for the flow restriction; 12 stages of throttling; an initial pressure of 100 psia at saturation conditions, a

final pressure of 0.1 psia.

$$Q = \alpha \phi \gamma A \sqrt{g \rho \rho_1}$$

Q = Leakage flow in pounds per second

$$A = \text{Leakage area in ft}^2 = \frac{\pi d h}{144} = \frac{\pi \cdot 3 \cdot 0.003}{144} = 0.000196$$

$$\frac{\rho_2}{\rho_1} = \text{Pressure ratio} = \frac{0.1}{100} = 0.001$$

$$\rho_1 = \text{Initial pressure} = 100 \times 144 = 14400 \text{ lb/ft}^2$$

$$\rho = \text{Initial density} = \frac{1}{\text{Specific Volume}} = \frac{1}{4.4} \frac{\text{lb}}{\text{ft}^3}$$

$$\alpha = \text{Contraction factor} = 0.68$$

$$\phi = 0.275$$

$$\gamma = 2.2 \text{ for } \frac{h}{s} = 0.1$$

$$g = 32.2 \text{ ft/sec}^2$$

$$Q = 0.68 \times 0.275 \times 2.2 \times 0.000196 \sqrt{32.2 \frac{1}{4.4} \times 14400} = 0.00826 \text{ lbs/sec.}$$
$$\times 3600 = \underline{29.7 \text{ lbs./hour}}$$

However, suppose, as for a space application, that it is necessary to decrease both leakage and bulk. Then it would be desirable to apply data such as Egli's to smaller seals, using a Reynolds number plotting. Sternlicht and Zabriskie have made such plottings (2).

In general, the following information should be known to design a labyrinth seal. A deficiency in any one aspect may vitiate the accuracy of leakage estimation.

1. The net flow area at successive restrictions
2. Flow geometry vs. flow effects vs. Reynolds number; and viscosity and density to compute the Reynolds number
3. The thermodynamic properties of the gas; i.e. specific volume, enthalpy, entropy, vs. temperature and pressure
4. Adequate graphic or mathematical procedures to represent the

leakage flow process; appropriate awareness when sonic velocity is reached, or of 2-phase flow conditions where liquid and gas co-exist.

In addition, if very small clearances are used, the ability of the materials to withstand rubbing is very important.

References:

1. Arnold and Stair, The Labyrinth Seal--Theory and Design, The University of Tennessee, Department of Mechanical Engineering, March 1962.
2. Sternlicht and Zabriskie, Labyrinth Seal Leakage Analysis, Gen. Elec. Report 57GL279, Sept. 26, '57, Gen. Engineering Laboratory, Schenectady, New York.
3. Zabriskie and Sternlicht, Labyrinth-Seal Leakage Analysis, Trans. ASME, Vol. 81, Series D, 3, pp. 332-340.
3. Egli, The Leakage of Steam Through Labyrinth Seals, ASME Transactions, Vol. 57, 1935, p. 115-122.
4. Tao and Donovan, Through Flow in Concentric and Eccentric Annuli of Fine Clearance With and Without Relative Motion of the Boundaries, Trans. ASME, Vol. 77, 1955, p. 1291.

Low Pressure

High Pressure

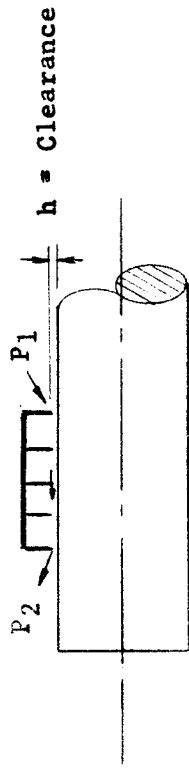


Fig. 1a.

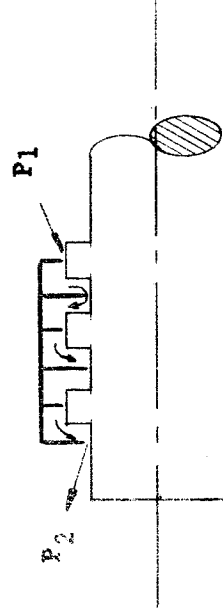


Fig. 1b.

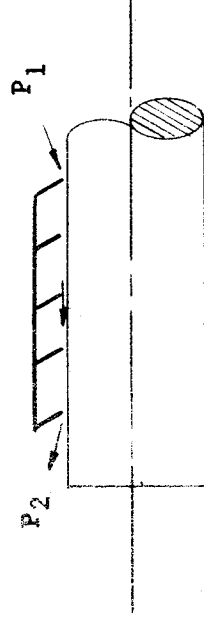


Fig. 1c.

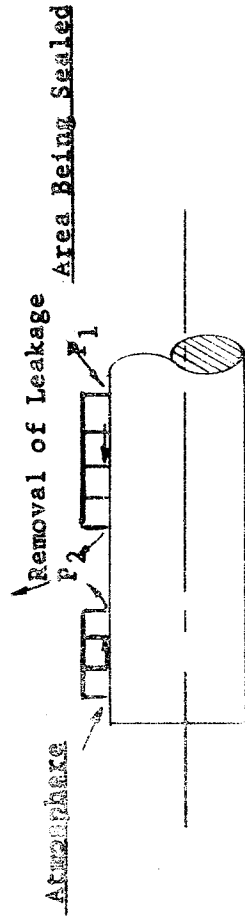


Fig. 1d.

Pressure Drop = $\Delta p = P_1 - P_2$

Initial Pressure = P_1

Final Pressure = P_2

Pressure Ratio = $\frac{P_2}{P_1}$

Clearance Between Seal and Shaft = h

Figure 1. Labyrinth Seal

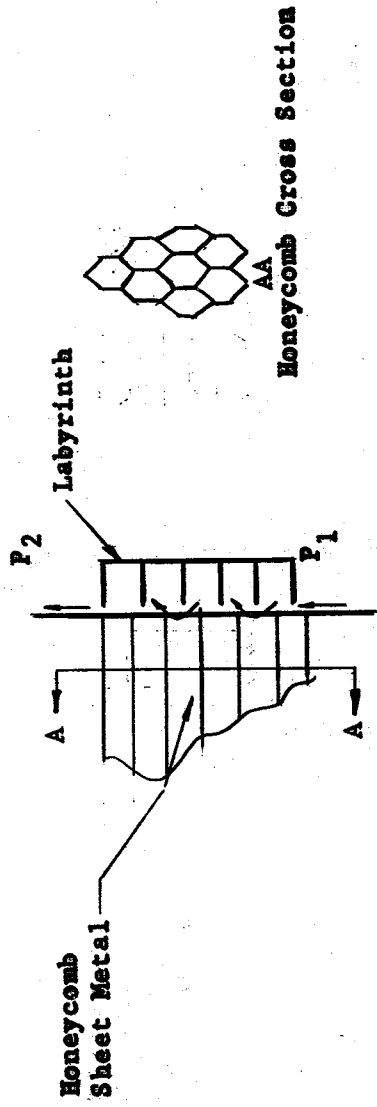


Figure 2. Honeycomb wearing surface in Labyrinth Seal

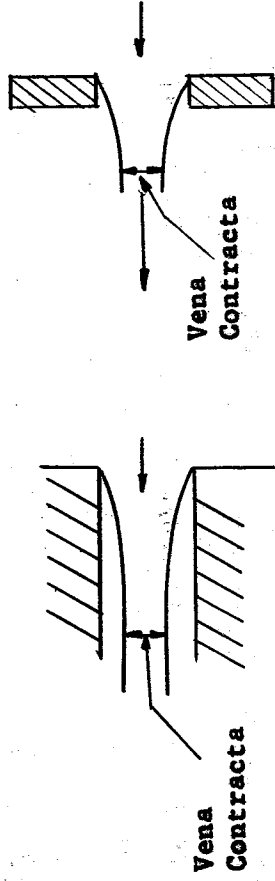


Figure 3a. Nozzle and Orifice

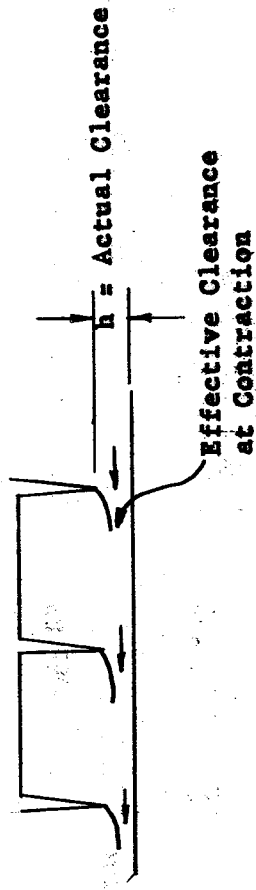


Figure 3b. Seal

Figure 3. Flow Contraction Effects

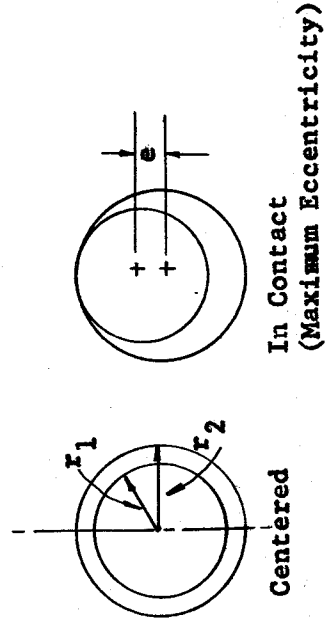
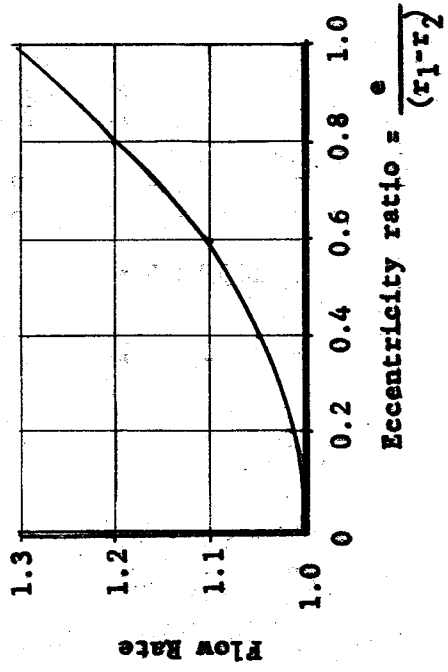


Figure 4. Flow Rate vs. Eccentricity - Turbulent Flow in Annulus

Reference (4)

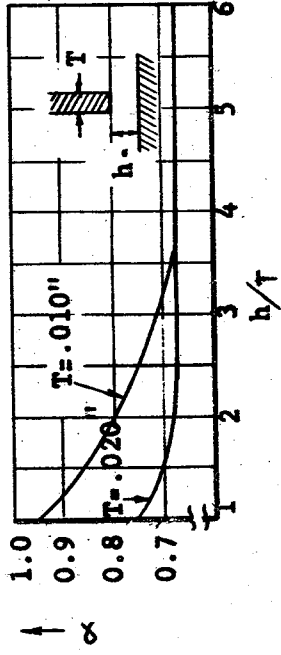


Figure 5a.

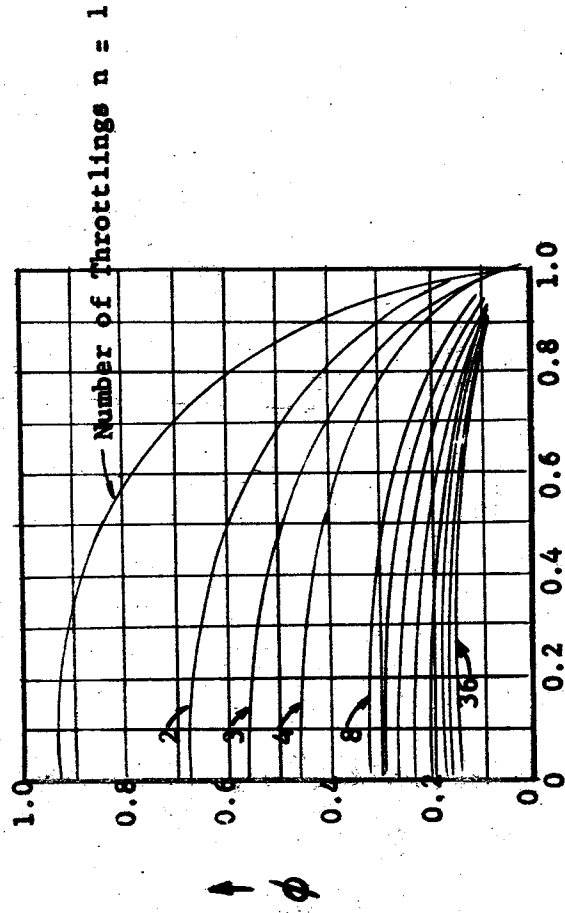


Figure 5b.

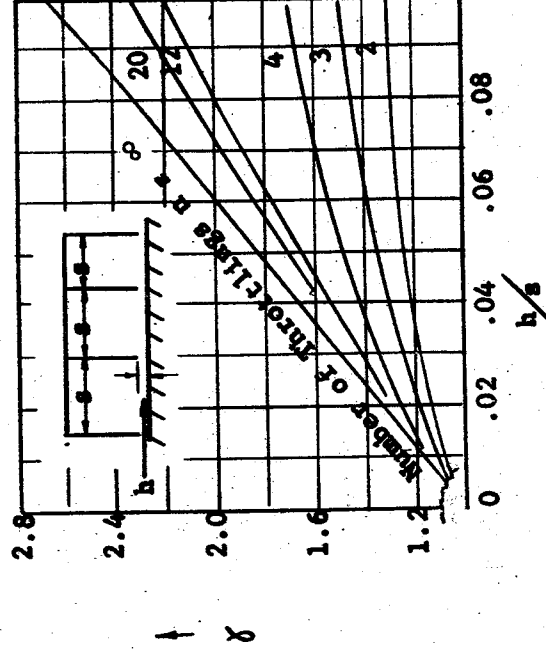


Figure 5c.

Appendix D

LEAK DETECTION AND MEASUREMENT - Dr. J. W. Marr

A closely associated problem to sealing technology is that of locating and measuring leakage, since this information is necessary to evaluate the effectiveness of any seal. In this Appendix, the significant terms used in this field are defined and illustrated. Discussions are also presented on major flow phenomena, and special problems such as clogging. Typical instrumentation for leak detection is described.

1. Definitions

The literature in the field of leak detection is cluttered with different nomenclature and sets of units. Important nomenclature is defined as follows:

a. Leak

In vacuum technology, a hole or porosity in the wall of an enclosure capable of passing gas from one side of the wall to the other under pressure or concentration differential existing across the wall(Ref.1).

A leak is not usually indicated by certain dimensions. Rather, it represents a physical hole of a certain length and width. However, since a leak is not intentionally manufactured into an item, its dimensions are generally unknown. In leak detection the dimension used to describe the leak is the leak rate.

b. Leak or Leakage Rate

The leak or leakage rate is defined as the rate of flow through a leak with gas at a specified high pressure (usually atmospheric pressure) on the inlet side and gas at a pressure on the exit side

which is low enough to have little effect on the leakage rate. The units of leak rate are:

$$\frac{\text{Pressure x Volume}}{\text{Time}}$$

This is occasionally referred to as mass flow. At a constant temperature, this unit is proportional to the mass flow rate. In describing a leak, the nature of the leaking gas and its temperature are usually known, so that using the formula:

$$PV = \frac{g}{M} RT \quad *$$

Eq. 1

where P = Pressure

V = Volume of Cylinder

g = Mass of the Gas

M = Molecular Weight

R = Gas Constant

T = Absolute Temperature

The actual leakage mass may be determined by:

$$g = \frac{PVM}{RT} \quad \text{Eq. 2}$$

c. Units

In scientific work on leaks, mass flow is usually expressed in Torr x liters/sec or atm x cc/sec at 25°C. In engineering work a wide variety of units for leakage are used. The justification for this diversity of units is the relative ease with which this variety of units can be adapted to individual engineering problems. For example,

* - A Torr is the suggested international standard to replace the English term millimeters of mercury. A Torr is defined as 1/760 of a standard atmosphere and differs by only one part in seven million from the International Standard millimeter of mercury.

* - A list of symbols appears at the end of this Appendix.

an operator has a gas cylinder with a pressure gauge calibrated in lb/sq in. If this operator reads the gauge daily, it is convenient for him to express the leakage as:

$$\frac{\text{pressure difference} \times \text{cylinder volume}}{\text{time increment}} \left(\frac{\text{psi} \times \text{ft}^3}{\text{day}} \right)$$

Because of the variety of these units, conversion factors have been included in Table 1 (at end of this Appendix).

Leakage rate discussions are further complicated by the use of units of mass instead of pressure x volume/time units. Equation 2 can be used for conversion in this case.

d. Modes of Flow

The leakage of fluid occurs by a variety of flow mechanisms: permeation, molecular flow, laminar flow, transition flow, turbulent flow and choked flow. These, as well as the circumstances leading to this flow, will be described in this section.

Although the flow characteristics of a leak may be expressed in many ways, the most common is in terms of conductance of the leak. Conductance is defined by:

$$C = \frac{Q}{P_2 - P_1}$$

Eq. 3

where C = Conductance

Q = Mass Flow

$P_2 - P_1$ = The Pressure Drop Across the Leak

Conductance has the dimensions of volume/unit time and may be thought of as the volume of gas that enters the leak/second. Conductance is the flow rate-pressure x volume/unit time divided by pressure drop.

The net conductance of a channel (C) is given by the following equation:

$$\frac{1}{C} = \frac{1}{C_1} + \frac{1}{C_2} + \frac{1}{C_3} + \dots + \frac{1}{C_n} \quad \text{Eq. 4}$$

where C_1, C_2, C_3 , etc., are the conductances of various lengths of the channel in series. The above equation shows that a constriction with an unusually low conductance will cause a very large constriction factor in the flow of liquid. Conductances and their influence on flow are discussed in the following subsections.

1. Permeation

Permeation is passage of a fluid into, through, and out of a solid barrier having no holes large enough to permit more than a small fraction of the molecules to pass through any one hole. The process always involves diffusion through a solid and may involve other phenomena such as adsorption, dissociation, migration and desorption.

The general formula for permeation is:

$$Q = K_p A \frac{\Delta P}{l} \quad \text{Eq. 5}$$

where Q = Rate of Flow

K_p = Permeation Rate Constant

A = Area Normal to Flow

ΔP = Pressure Drop Along the Flow Path

l = Length of Flow Path

Permeation was described as a separate subject in Appendix A.

ii. Molecular Flow

Molecular flow is defined as flow through a duct under conditions such that the mean free path is greater than the largest dimension of a transverse section of the duct. (Ref.1) In such a flow, each atom moves independently by random movement from a volume of high to one of low concentration. The mean free path is the average distance that a molecule travels between successive collisions with the other molecules of an ensemble. The mean free path λ is:

$$\lambda = \frac{1}{\sqrt{2}n\sigma^2} \quad \text{Eq. 6}$$

where n = Number of molecules in a unit volume

σ = Molecular diameter

$$\text{If } n = \frac{gA^0}{MV} \quad \text{Eq. 7}$$

where g = Mass of the gas

A^0 = Avogadro's number; i.e. number of molecules per mole

M = Molecular weight of the gas

V = Volume

and replacing V from Equation 1 the value in Equation 7

we obtain:

$$\lambda = \frac{RT}{\sqrt{2}\pi PA^0 \sigma^2} \quad \text{Eq. 8}$$

Equation 8 shows that at constant pressure, the mean free path is proportional to temperature. However, if the amount of gas in a volume is kept constant, the mean free path is independent of temperature (Equation 6).

The magnitude of molecular diameters and mean free paths are shown in Table 2 (at the end of this Appendix). As a convenient calculation guide, the mean free path of air at room temperature is:

$$\lambda_{\text{air}} = \frac{5 \times 10^{-3}}{P} \text{ centimeters} \quad \text{Eq. 9}$$

when P is expressed in Torr.

The original mathematical derivations of molecular flow are attributed to Knudsen (Ref.2). The rate of flow in a long pipe is:

$$Q = \frac{\sqrt{2\pi}}{6} \sqrt{\frac{RT}{M}} \frac{d^3}{l} (P_2 - P_1) \quad \text{Eq. 10}$$

where d = The diameter of the pipe

l = The length of the pipe

P₂ and P₁ = The pressures at the two ends

For this formula to apply, the pipe must be of a circular cross-section. For pipes and ducts of a non-circular cross-section the conductance is less than for pipes of circular cross-section and equal area. Equation 10 applies only if the pipe is much longer than its diameter. Any difficulty experienced by a molecule in entering the pipe must be negligibly small compared to the difficulty in traversing its length. If difficulty is experienced in entering the pipe, the kinetic theory shows that the rate of free molecular escape of gas from the container into a small aperture of area A is:

$$Q = \frac{1}{\sqrt{2\pi}} \sqrt{\frac{RT}{M}} A (P_2 - P_1) \quad \text{Eq. 11}$$

In the case of an aperture, using the formula given above the opening does not have to be circular.

In molecular flow, the conductance of lines and apertures is independent of pressure. Calculations may be made of the effect of turns, apertures, and change in pipe diameter to calculate the overall flow in a leak. Formulas are available in the literature (Refs.3 and 4) on the effect of structure on the leakage rate.

iii. Laminar Flow

The laminar flow of a fluid in a pipe is defined as a condition when the velocity distribution of the fluid in the cross-section of the pipe is parabolic. Laminar flow is one of the two classes of viscous flow, the other class being turbulent flow. Because turbulent flow is rarely encountered in leaks, the term viscous flow is sometimes incorrectly used to describe laminar flow in leak detection work.

The most familiar viscous flow equation is one developed by Poiseuille (Ref. 5) for the flow through a straight tube of a circular cross-section.

$$Q = \frac{\pi}{8} \left(\frac{d}{2}\right)^4 \frac{P_a}{\eta l} (P_2 - P_1) \quad \text{Eq. 12}$$

where η = The viscosity of the gas

P_a = The arithmetic mean between P_2 and P_1

In the range where that equation is applicable, it has been substantially verified experimentally. The viscous conductance of the tube by definition of Equation 3 is:

$$C = \frac{\pi}{8} \left(\frac{d}{2}\right)^4 \frac{P_a}{\eta l} \quad \text{Eq. 13}$$

Laminar flow takes place when the Reynolds' number of flow is lower than a defined critical value. The Reynolds' number is a unitless quantity which defines the flow conditions and is given by:

$$N_{Re} = \frac{d_0 F}{\eta} \quad \text{Eq. 14}$$

where N_{Re} = The Reynolds' number

ρ = The fluid density

η = The absolute viscosity

F = The average flow velocity across a plane in the tube

By substituting the ideal gas equation in the above formula we obtain the expression for the Reynolds' number of a gas as:

$$N_{Re} = \frac{Q}{d} \left(\frac{4M}{\pi \eta RT} \right) \quad \text{Eq. 15}$$

The critical value of Reynolds' number has been shown to be dependent upon the entrance conditions, roughness of the walls of a tube, and shape of the flow path. In general for smooth tubes, with well rounded entrances, the critical value is about 1,200. For flow corrections due to turns, constrictions, and surface roughness refer to Ref. 6 and 7.

The kinetic theory states that the viscosity of a gas is given by the relationship (Ref. 8):

$$\eta = \frac{m \bar{F}}{3 \sqrt{2} \pi \sigma^2} \quad \text{Eq. 16}$$

where \bar{F} = Average velocity of the individual molecules

m = Their mass

σ = Their diameter

The average velocity of a molecule is:

$$\bar{V} = \left(\frac{8RT}{\pi M} \right)^{1/2} \quad \text{Eq. 17}$$

the mass of the individual molecules is:

$$m = \frac{M}{A_0} \quad \text{Eq. 18}$$

Substituting Equation 17 and 18 in Equation 16 we obtain:

$$\eta = \frac{2(MRT)^{1/2}}{3\pi^{3/2} A_0^2} \quad \text{Eq. 19}$$

It may be seen from the above equation that the viscosity of a gas is independent of pressure and is proportional to the square root of temperature.

iv. Transition Flow

The transition from laminar flow to molecular flow is gradual. The mathematical treatment of this region is extremely difficult. However, a treatment of this region is necessary because a leak from a volume to a vacuum necessarily involves a transition from laminar to molecular flow. Equation 10 shows that the conductivity of a passage in molecular flow is proportional to the cube of the passage diameter and independent of pressure. Conversely Equation 13 shows that the conductivity of the same passage in laminar flow is proportional to the fourth power of the diameter of passage and proportional to the pressure. In viscous flow the mixture of gases travels at a rate inversely proportional to the viscosity of this mixture and no separation of gases takes place. However, in molecular flow the rate of flow of the individual gases present

in a gas mixture is inversely proportional to the square root of their individual masses. Therefore a certain amount of separation takes place through a leak.

Knudsen (Ref. 2) derived a semiempirical formula for the flow of gases through long tubes in the transition region.

This formula is:

$$C = \left[\frac{\pi}{8} \left(\frac{d}{2} \right)^4 \frac{P_a}{\eta l} \right] + \left[\frac{1}{6} \sqrt{\frac{2\pi RT}{M}} \frac{d^3}{l} \right] \left[\frac{1 + \frac{M}{RT} \frac{dp}{da}}{1 + 1.24 \sqrt{\frac{M}{RT} \frac{dp}{da}}} \right] \quad \text{Eq. 20}$$

The formula is valid providing that

1. the flow is not turbulent in any part of the pipe.
2. the pressure difference between the ends is not so great that the mechanism of flow (i.e. viscous or molecular) changes along the pipe.

Although the first of these conditions is usually satisfied in the leak, the second generally is not; that is the transition from viscous to molecular flow does take place. The above equation at low pressures becomes an equation of molecular flow; whereas at high pressure this equation reduces to one of strictly laminar flow.

Knudsen used the above equation to represent his experimental data. The equation which has the effect of molecular flow added to the effect of laminar flow is not an actual representation of the flow mechanism taking place in the leak. For that reason the restriction, that the pressure difference between the two ends is not large, is necessary,

i.e., change of flow mode does not take place. An addition of the two effects is not a true representation since the same amount of fluid which travels part of the pipe as laminar flow will eventually travel via the molecular flow mode. Other authors have (Refs. 9, 10) attempted to derive equations to represent this phenomenon of transition from one type of flow to another, however, none of them have been successful. One satisfactory method (Ref. 11) is to calculate viscous flow through one section of the tube, molecular flow through another, and approximate the in between region.

v. Turbulent Flow

Above a critical value of the Reynolds' number (about 2100 in the case of circular pipe flow) flow becomes unstable resulting in innumerable eddies or vortices in the flow. Any particle in turbulent flow follows a very erratic path, whereas in laminar flow the particle follows a straight line.

The laws for turbulent flow are quite different from the laws for laminar flow. The equation relating mass flow rate (Q) in units of pressure x volume/time may be written:

$$Q = \pi d^{5/2} \left[\frac{RT(P_2^2 - P_1^2)}{8fM\ell} \right]^{1/2} \quad \text{Eq. 21}$$

where f, the friction factor, is defined on p. 125 of Ref. 7. The friction factor depends on roughness of the channel walls, and can be considered a constant in fully developed turbulent flow.

Turbulent flow, because it requires relatively high velocity, probably occurs only in rather large leaks.

vi. Choked Flow

Choked flow, or sonic flow as it is sometimes called, occurs under certain conditions of geometry and pressure. Assume there exists a passage in the form of an orifice or a venturi, and assume that the pressure upstream is kept constant. If the pressure downstream is gradually lowered, the velocity through the throat or orifice will increase until it reaches the speed of sound through the fluid. The downstream pressure at the time the orifice velocity reaches the speed of sound is called the critical pressure. If the downstream pressure is lowered below this critical pressure, no further increase in orifice velocity can occur, with the consequence that the mass flow rate has reached its maximum. This condition is known as "choked" or "sonic" flow.

Choked flow can occur under the following two conditions:

(1) the flow passage must be in the form of an orifice or venturi, in which only negligible frictional losses occur upstream of the orifice or throat of the venturi; (2) the ratio of downstream to upstream pressure must be below a certain "critical" value, which is

$$r_c = \left(\frac{2}{\gamma+1} \right)^{\frac{\gamma}{\gamma-1}}$$

Eq. 22

The velocity of sound through a gas can be written:

$$F_c = \sqrt{\frac{2\gamma}{\gamma+1} \frac{RT_1}{M}}$$

Eq. 23

where F_c = Velocity of sound

T_1 = Absolute temperature upstream of the orifice
where the velocity is low

$$\gamma = C_p / C_v$$

Eq. 24

where C_p = Heat capacity at constant pressure

C_v = Heat capacity at constant volume

The mass flow rate under a choked flow conditions is:

$$Q = \frac{\pi d^2 P_1}{4} \sqrt{\frac{2\gamma}{\gamma+1} \frac{RT_1}{M}}$$

Eq. 25

where d = Orifice diameter

P_1 = Upstream pressure

For an ideal monatomic gas, the value of γ is 1.67. For polyatomic molecules, the heat energy supplied is used for increasing not only the kinetic energy of translation, but also the kinetic energy of rotation and vibration. Since the same amount of extra energy is required at both constant pressure and constant volume, γ decreases with molecular complexity. Characteristic values of γ are shown in Table 3 (at the end of this Appendix). Additional values may be calculated (Ref. 12) or obtained from other references (Ref. 13).

vii. Distinction Between Modes of Flow

In the above subsections, the equations have been presented for the various possible modes of flow that can be encountered in a leak. The following rules may be used to predict the mode most likely to occur. In distinguishing between laminar and molecular flow the size of the passage and the mean free path are the two important parameters. The distinction may be specified by a dimensionless parameter called the Knudsen number. The Knudsen number is defined as the ratio of the mean free path of the molecule to a characteristic dimension of the channel through which the gas is flowing.

$$N_K = \frac{\lambda}{d} \quad \text{Eq. 26}$$

where N_K = Knudsen number

λ = Mean free path

d = Channel diameter

The type of flow encountered in the various Knudsen number ranges is shown in Equation 27.

$$\frac{\lambda}{d} < 0.01 \text{ laminar flow}$$

$$\frac{\lambda}{d} > 1.00 \text{ molecular flow}$$

$$0.01 < \frac{\lambda}{d} < 1.00 \text{ transition flow}$$

Eq. 27

Flow in the viscous region is determined by the Reynolds' number which was described both in Equation 15 (the following) and in subsection iii.

$$N_{Re} = \frac{d_o F}{\eta} \frac{Q}{d} \left(\frac{4M}{\pi \eta R T} \right) \quad \text{Eq. 15}$$

The distinction between laminar and turbulent flow is shown in Equation 28.

$N_{Re} > 2100$	Turbulent flow
$N_{Re} < 1200$	Viscous flow
$1200 < N_{Re} < 2100$	Either turbulent or viscous depending on duct conditions

In choked flow, the flow takes place when the pressure ratio between outlet and inlet reaches a certain minimum value. This of course is dependent on other characteristics such as aperture dimension, etc. The formula for the critical pressure ratio is defined by Equation 29.

$$r = \frac{P_2}{P_1} \quad \text{Eq. 29}$$

The critical ratio, the ratio below which choked flow takes place is:

$$r_c = \left(\frac{2}{\gamma + 1} \right)^{\frac{\gamma}{\gamma - 1}} \quad \text{Eq. 22}$$

Choked flow cannot take place when P_1 is so low that molecular flow exists.

2. Conversion of Measured Leakage to Standard Leakage Rate

Converting leakage measured on a detector to the amount of leakage anticipated when the container is filled with working fluid is a difficult problem. The problem consists of three general categories. The inability to obtain a mathematical correlation between the measured leakage and the anticipated one, the inability to obtain a good standard leak and the difficulty experienced due to clogging. These problems will be discussed individually in the following subsections.

a. Mathematical Correlation of Leak Test Results

In the preceding section entitled 'Modes of Flow' the mathematical equations describing the various types of fluid flow were presented. If the physical dimensions of the leak were known, it would be easy to calculate the anticipated leakage rate during working conditions from the leakage rate measured on a detector. A leak is not usually built into a system. For this reason its dimensions are rarely known. Even if all the dimensions were known, the flow mode still has to be ascertained. To define the flow mode the geometry of a leak has to be known. However, this is usually not the case. Another approach to this problem is to assume the leak dimensions and flow mode remain constant. Therefore, the flow rate will be dependent upon pressure. In Equation 30 the dependence of flow rate on pressure is shown in four different modes of flow:

$$\text{Molecular } Q \propto \frac{P}{\sqrt{M}} \quad \text{Eq. 30a}$$

$$\text{Laminar } Q \propto \frac{P^2}{\eta} \quad \text{Eq. 30b}$$

$$\text{Turbulent } Q \propto \frac{P}{\sqrt{M}} \quad \text{Eq. 30c}$$

$$\text{Choked } Q \propto \frac{P \sqrt{\frac{\gamma}{\gamma+1}}}{\sqrt{M}} \quad \text{Eq. 30d}$$

Also placed in the above equations are the physical constants of the fluids which affect the above flow properties. When using the above equations the flow mode in a leak may change during a change of pressure or constants of the gas.

Working with a variety of leaks of different sizes and under different conditions, some of the above equations may readily be eliminated. For example, if the leak rate is small, it is relatively easy to assume that no turbulent flow will take place. If the leak is one going from high pressure to a slightly lower pressure, but not a vacuum, it is likely that molecular flow is not the flow mechanism. In the above case, the flow may be of either a choked or laminar flow nature and therefore conversion to a second flow pressure is relatively easy. However, in this particular case conversion to a different gas is not as easy since this leaves the choice of converting as a function of either heat capacity differences, which might be negligibly small (Equation 30d), or viscosity ratios which conceivably could be large (Equation 30b).

Another example - convert one leakage rate flowing into a vacuum to an anticipated rate of a different pressure into the same vacuum. Calculations described in (Ref. 10), show that if the leak is of relatively small size (10^{-5} atm cc/sec or less) the molecular flow will play a major role in such a leak. However should the leak be relatively large (10^{-3} atm cc/sec or greater) the leakage will be predominately of laminar nature. If one can accurately predict the type of flow which will predominate in the leak, one could therefore make accurate conversions to a different set of conditions. Unfortunately the state-of-the-art is such that these predictions are usually not possible.

An attempt to derive a general method for leak conversion is described in the paper by Santeler and Moller (Ref. 14). These authors use the viscous and molecular flow equations to develop a graphical method of leakage conversion. The above approach was tested on gaskets recently being used in the Advanced Technology Laboratories. The Laboratory is currently performing the work on another NASA Contract (NAS 8-4012) in an attempt to develop zero leakage fluid connectors for liquid rocket propellant transmission lines. On this contract a large number of gaskets are subjected to a gradually increasing helium pressure and the leakage rate very carefully measured with a modified helium leak detector. In this way, leakage rate at a variety of pressures is measured. The results of these experiments were compared with predictions made by the graphs developed by Santeler and Moller. It was found that in approximately half the experiments the leakages predicted were correct. The results which were in error, were so by as much as one order of magnitude, both positive and negative. No definite conclusions have been reached as to the reasons for these large errors.

b. Limitations of Standard Leaks

One of the difficulties encountered in leak detection calibration techniques is the difficulty of obtaining a proper leak standard. It is possible to purchase from a number of vacuum equipment manufacturers a calibrated leak. These leaks are calibrated to an outflow of a particular gas at a particular working pressure. In such a leak, an operator using a leak detector is able to calibrate his

instrument, to determine the magnitude of an unknown leakage. Unfortunately most of these leaks are calibrated for only one gas at one pressure difference. Since the flow mode is unknown a good mathematical relationship is not available for its behavior at another pressure or gas without performing actual tests. For example, the Vacuum Laboratory produces a calibrated leak by collapsing a metal capillary tube. This type of calibrated leak may be made to a leakage rate as small as 10^{-7} atm cc/sec. Although smaller leaks have been manufactured by this technique they are extremely difficult to produce, and even more difficult to keep from clogging (discussion of clogging is in the next section). If this leak is calibrated with a couple of gases at several different pressures, it might be possible to determine if the flow exhibited is of viscous, choked, or molecular nature. Therefore, it would be possible to determine the mathematical relationships to extrapolate to a different set of pressure differences. If it can be determined that the flow mode is the same in both the existing leaks and in the standard leak, then the standard leak may be placed in the operating conditions to determine the anticipated leakage rate without extensive mathematical calculations.

If a calibrated leak is required with a leakage rate smaller than 10^{-7} atm cc/sec, the leak has to be manufactured in a different manner. Small leaks are made from a sintered glass plug, or sometimes by utilizing the principle of permeation. The mechanism of flow in such a leak will be different from the flow in the long crack or seal face. Therefore, a calibrated leak of this small leak rate can only be used to calibrate instruments.

c. Computation of Theoretical Leak Size

In an attempt to determine the order of magnitude of the physical size of leaks, Knudsen's semiempirical equation was used by R. Loeving and A. Guthrie (Ref. 15) for the flow of gas through a capillary in the transition region. The conductance, as shown in Equation 20 is:

$$C = \left[\frac{\pi}{8} \left(\frac{d}{2} \right)^4 \frac{P}{\eta \ell} \right] + \left[\frac{1}{6} \sqrt{\frac{2\pi RT}{M}} \frac{d^3}{\ell} \right] \left[\frac{\frac{M}{RT} \frac{a}{\eta}}{1 + 1.24 \sqrt{\frac{M}{RT} \frac{a}{\eta}}} \right] \frac{dP}{\eta} \quad \text{Eq. 20}$$

This equation may be rewritten in the form:

$$C = \frac{1}{\Delta \ell} \left[aP + b \frac{1 + iP}{1 + hP} \right] \quad \text{Eq. 31}$$

where $\Delta \ell$ is the length of the short segment in which the average pressure is P and the pressure drop is ΔP . The flow through such a segment is based on Equation 3:

$$Q = \left(aP + b \frac{1 + iP}{1 + hP} \right) \frac{\Delta P}{\Delta \ell} \quad \text{Eq. 32}$$

Integrating Equation 32 over the length of the capillary:

$$Q = \frac{1}{\ell} \int_{P_2}^{P_1} \left(aP + b \frac{1 + iP}{1 + hP} \right) dP = \quad \text{Eq. 33}$$

$$= \frac{1}{\ell} \left[\frac{a}{2} P^2 + \frac{b iP}{h} + \frac{b(h-i)}{h^2} \ln |1 + hP| \right]_{P_2}^{P_1}$$

where $a = \frac{\pi}{8\eta} \left(\frac{d}{2} \right)^4$

$b = \frac{1}{6} \sqrt{\frac{2\pi RT}{M}} d^3$

$j = \sqrt{\frac{M}{RT}} \frac{d}{\eta}$

$h = 1.24 \sqrt{\frac{M}{RT}} \frac{d}{\eta}$

Flow Q is a constant in a steady state condition.

This is an elegant use of Knudsen's equation for transition flow. In the differential, change in flow mode does not take place, thus following one of the important rules of Knudsen's derivation. However, a change of flow mode takes place between the entrance and the exit of the tube, but this is a result of integrating the equation. The results of these calculations for air are shown on Table 4. (at the end of this Appendix).

The calculations to obtain Table 4 assumed that the pressure inside the hypothetical cylindrical leak dropped to a low value P_2 which is negligible as compared to the atmospheric pressure. Inside the leak the velocity of the gas will rise from some small value at the inlet to a maximum value not greater than the velocity of sound under the prevailing temperature and pressure conditions. According to kinetic theory the velocity of sound in any gas is:

$$F_c = \sqrt{\gamma \frac{P}{\rho}} \quad \text{Eq. 34}$$

where γ = Ratio of heat capacities

P = Pressure

ρ = density

Then if isothermal expansion is assumed, it follows from the isothermal equation of state:

$$P = \rho \frac{RT}{M} \quad \text{Eq. 35}$$

$$F_c = \sqrt{\gamma \frac{RT}{M}} \quad \text{Eq. 36}^*$$

* Equation 36 differs from Equation 22 because the temperature in the latter is an upstream temperature prior to adiabatic expansion. In Equation 36 the gas temperature is expressed at the same point as the velocity.

the velocity of sound in a gas at constant temperature is constant. These minimum pressures in the leak were calculated and given in column P₂ in Table 4. The implication of the pressure calculations is that the flow reaches a sonic velocity. Therefore a choked flow mode situation exists somewhere in the leak, unless the pressure P₂ is so low that the flow is molecular. Calculations cannot be made in this manner for tube diameters larger than 10⁻² centimeters because at this point the Reynolds' number is high enough to produce turbulent flow.

It may be seen from Equation 17 that the difference between flow of air and flow of other gases is dependent on their molecular weight and viscosities. The upper and lower limits of flow corrections for other gases applicable to the calculations are presented in Table 4 (at end of this Appendix).

These calculations were entered by Loevinger and Guthrie, as a general guide and not as ultimate figures. Of course in an actual leak the holes are neither circular in diameter or of a constant diameter. However we may obtain a certain insight as to the properties of the leak from the numbers in Table 4.

d. The Special Problem of Clogging

The Vacuum Laboratory of General Electric's Advanced Technology Laboratories perform a service of leak checking equipment for the General Electric Schenectady Plants. Certain properties of leaks are commonly observed in the performance of this service. The leak

testing is generally done with a helium mass spectrometer leak detector having sensitivities of approximately 10^{-10} atm cc/sec.

A phenomenon frequently observed is that if a container to be tested for leaks has at any time after manufacture been in contact with a liquid, no leaks small in size (i.e. 10^{-7} atm cc/sec or smaller) will be found. The explanation for this is that the small leaks are clogged with liquid due to its surface tension. If water has entered a capillary tube, the pressure necessary to force it out of the tube is given by the following equation (Ref. 16):

$$P = \frac{4\phi}{d} \quad \text{Eq. 37}$$

where ϕ = surface tension of the liquid
usually expressed in dynes per centimeter

d = tube diameter in centimeters *

P = pressure expressed in dynes/cm²

Referring back to Table 4, a leak with a diameter of 1×10^{-4} centimeters will have a leakage rate for helium of approximately 1.3×10^{-6} atm/sec. If water, with a surface tension of 72 dynes/cm, enters such a leak, the pressure required to force it out is approximately 2.8 atmospheres. Since the pressure differential during leak testing is only 1 atmosphere, this leak is essentially clogged by the use of water. In actual conditions clogging is more likely to take place than in the above example. Most leaks are neither circular or regular in diameter. They usually contain constrictions and occasionally consist of slits. The rate of flow in a leak is

* One atmosphere is equal to 1.063759×10^6 dynes/cm²

approximately proportional to the leak cross-sections. If clogging were to take place, the pressure required to remove a liquid is inversely proportional to the smallest dimension in the cross-section. Therefore, clogging of an orifice or of a slit is more likely to take place than may be assumed from the above example. If the leak in the above example were in fact a slit with the ratio of width to height of 10 to 1, the pressure necessary to remove water from such a slit would be approximately 28 atmospheres. Leakage would be of the same order of magnitude as mentioned in the above example.

Unfortunately, such clogging is not of a permanent nature. If the temperature of the container were to be raised, the surface tension of the liquid decreases and quite possibly the liquid inside the leak evaporates. Because of this phenomenon, the Vacuum Laboratory does not test with soap solution or liquid on parts which are then going to be subjected to a baking procedure. The opening up of these clogged leaks is an extremely slow process, since the evaporation will take place at a rate similar to the leakage rate.

It is generally observed that leakage much smaller than 10^{-8} atm cc/sec are rarely seen. Such leakages are in the range of detectability, but are a rare phenomenon when found. When found the equipment on which they were located was new and had never been in contact with a liquid. These leaks have to be carefully treated or they will clog during normal handling. From Table 4 it may be

seen that a leak 10^{-8} atm cc/sec has a diameter in the order of 10^{-5} centimeters. To place this number in dimensions of atomic size, its diameter is about 1,000 Angstrom units.* Molecules of contaminants, for example oil either from the hand or machine, are in the order of 100 Angstroms in length. Should these molecules be adsorbed in the leak, they would reduce the size of the hole and therefore reduce the leak rate to a point of apparent clogging. It should be noticed that according to the equation for molecular flow (Equation 10) the flow mode which should predominate in this range, the leakage rate is proportional to the cube of the leak diameter.

* One centimeter is equal to 10^8 Angstrom units

3. Leak Detection and Measurement Techniques

a. Application of Instruments

In the next section some of the more common methods of leak detection are listed. It is extremely difficult to make general rules as to the situations in which the above leak detection methods are to be applied. Part of the art of leak detection consists of a person's ability to select the best leak detection method for a certain application.

Occasionally, equipment already installed on the apparatus may be profitably used for leak detection. For example, a space simulator requires leak detection, and part of the simulator's instrumentation is a partial pressure analyzer, i.e., a small mass spectrometer which measures the residual pressure of gases remaining in the system, this analyzer could be used as a leak detector. The partial pressures of various residual gases in the system would show whether the leakage consists of air entering the system, of water from one of the plumbing lines, one of various cryogenic fluids from the cooling baffles, or oil from the pumps. If air leakage is the case, the partial pressure analyzer could be used as a standard helium leak detector.

A short summary follows of various leak detection situations illustrating the most applicable methods to be used in certain cases. Leak detection instruments, like most instruments, should only be used within their design range. Instruments used to detect leakage rates smaller than they have been designed for, will cause leakages to be masked by the noise of the instrument, making the job very tedious. In addition, some instrument manufacturers are optimistic about the

sensitivity of their instruments. Conversely, the use of an instrument on leaks larger than its designed range will cause the purchase of an instrument much more expensive than necessary. In this case, helium and halogen leak detectors will be slow in their leak detection procedure due to accidental poisoning or overflowing with excessive tracer gas.

i. Vacuum systems with leakages as small as 10^{-4} atm cc/sec.

1. Pressure rise in the system with isolation of various areas.
2. Tracer gas using thermocouple, Pirani, or ionization gauge.

ii. Vacuum system with leakage as small as 10^{-6} atm cc/sec.

1. Halogen leak detector with vacuum attachment.
2. Hydrogen leak detector.
3. Oxygen leak detector.
4. Argon leak detector.
5. Helium leak detector.

iii. Vacuum system with leakages as small as 10^{-10} atm cc/sec.

1. Helium leak detector.
2. Argon leak detector (only if volume of vacuum system is small).

iv. Systems which cannot be evacuated

1. Bubble testing - Small system: immersion
- Large system: soap solution
2. Halogen leak detector.
3. Helium leak detector with probe.
4. Observation of pressure drop in system.
5. Small system - pressurize and observe weight change.

6. Small system - pressurize and place in vacuum system.

- a) Test by pump-down time
- b) Halogen leak detector
- c) Helium leak detector
- d) Argon leak detector

v. Many small sealed components

- 1. Radioactive tracer leak test.
- 2. Pressurize with helium or Freon* and place in vacuum system with helium or halogen leak detector. Sensitivity of this method is 10^{-6} times less than the radioactive gas method.
- 3. Fluorescent dye. The sensitivity of this method is 10^{-6} times less than a halogen or helium leak detector.

b. Instrumentation for Leak Detection and Measurement

Leak detection and measurement instrumentation are quite varied. Some of their methods will be described in this section. Additional information on leak testing may be found in Chapter 5, Ref. 4 and Ref. 15. Four different methods of leak detection are categorized and explained:

- i. Physical observation of leakage.
- ii. Difference in pressure due to leakage.
- iii. Change in gauge readings due to the effect of tracer gas.
- iv. Detection of the tracer gas.

i. Physical Observation of Leakage

- 1. Sonic Detectors - Leak detectors are available to physically detect the sound made by the outflow of a gas, presumably

*Trademark of DuPont

choked flow. Manufacturers stated sensitivity of these instruments is approximately 10^{-1} atm. cc/sec.

2. Fluorescent dyes.- A penetrating fluorescent dye solution is made which may be painted onto a weld and then wiped away. This dye will penetrate into any cracks and fissures. The material that is not wiped away is observed due to fluorescence, under ultraviolet light. This method of leak detection will display flaws in machining and joining. No quantitative estimates can be made as to the leak size which can be detected by this method.
3. Bubble Testing by Soap Solution - A container to be tested is pressurized and painted with a soap solution. Any leak can be seen by the growth of bubbles. The efficiency of this method depends upon: the observation abilities of the operator, the ability to completely wet the tested area, the surface tension of the soap solution, and the complexity of the part. It has been estimated that under proper conditions the sensitivity of this method is 10^{-4} atm cc/sec.
4. Bubble Testing by Immersion - A pressurized vessel may be immersed in a liquid; the bubbles rising to the surface will indicate a leak. This method is dependent on the pressure capability of the vessel, surface tension of the liquid and the size of the testing area. This method is obviously not suitable to large vessels. However, modifications can be made to cover one area by a liquid. This technique is simpler than soap solution testing because the observation abilities

of the operator are not as important. The sensitivity of this method is about 10^{-5} atm. cc/sec.

5. Halide Torch Leak Detector - The halide leak detector consists of a propane gas torch with a copper plate in the flame and a rubber tube supplying the flame with air. The system to be tested is pressurized with Freon gas and the end of the rubber tube which supplies air to the flame is passed over the suspected area. A leak is detected when the flame turns bright green, since a piece of copper in a flame containing halogen atoms gives off a characteristic green flame. This equipment is often used by household refrigerator repairmen because the refrigerant (Freon) acts as the tracer gas and the equipment is inexpensive. The sensitivity of this method is reported to be approximately 10^{-5} atm. cc/sec.

ii. Difference in pressure due to leakage

1. Pressure drop in the container - A container may be pressurized with a gauge attached to it which will show the pressure drop. This essentially is a method of measuring the leakage rate. The sensitivity of this method is defined by the equation:

$$Q = \frac{V \Delta P}{\theta} \quad \text{Equation 38}$$

where Q = leakage rate sensitivity

V = container volume

ΔP = pressure differences, which may be measured

θ = time increment between readings

The ultimate sensitivity of this method is controlled not only by the length of the time increment and the sensitivity of the

gauge, but also because temperature changes in the environment will produce independent pressure changes.

2. Pressure increase in vacuum system - A container can be placed in a vacuum system; the leakage rate can be determined by the pressure increase. Equation 38 may be used to calculate the sensitivity of this method providing the proper correction for outgassing and leakage within the vacuum system is made.

3. Ultimate pressure obtained in the vacuum system - If the container or leak is placed in the vacuum system and pumped through an orifice of known dimensions, the ultimate pressure obtained in such a system is:

$$Q = P_u S \quad \text{Equation 39}$$

where Q = measured leakage

S = pumping speed of the system

P_u = ultimate pressure obtained.

The sensitivity of this method of leak detection is dependent on the magnitude of outgassing and the pumping speed of the vacuum system as compared with the leakage rate.

4. Argon leak detector - One commercially sold detector uses the pressure rise in a vacuum system to detect leaks. The leak detector consists of a vacuum system which uses a getter pump. This type of pumping is efficient for all but the inert gases. Argon or helium is therefore used as a tracer gas. When argon enters the vacuum system through the leak, the pump is not capable of gettering it efficiently and the pressure in the

system rises. The sensitivity of this type of pressure rise method is reported to be extremely high, 10^{-9} atm. cc/sec. The major disadvantage of this method of leak testing is that it is not readily applicable to large volume systems, because of the large amount of argon needed to be pumped from the air in the system.

3. Change in pressure gauge readings due to the effect of tracer gas
Because a large number of leak detection methods involve the use of three types of vacuum gauges, it is convenient at this time to describe the three types of gauges involved.

Pirani Gauge - the heat conductivity of a gas is proportional to the pressure over a large range. The Pirani gauge consists of wire with electrical currents flowing through it. The resistance of this wire is dependent on its temperature. By the use of a Wheatstone bridge arrangement, using a sealed wire as a reference, the pressure of the system may be measured.

Thermocouple Gauge - This gauge uses the same principle for its measurement as the Pirani gage; i.e., the heat conductivity of a gas. In the thermocouple gauge the current passing through the wire remains constant and the temperature of the wire is measured by the thermocouple welded to it.

Ionization Gauge - An ionization gauge is a triode where an electrical current is passed between a cathode and the plate. The electrons passing from the cathode to the plate encounter residual gas molecules in their path.

The electrons striking these molecules ionize them and the current produced by these ions is measured as grid current. This current is dependent on the number of atoms encountered in the electron stream, and therefore is proportional to the pressure in the system.

1. Leak Testing with Pressure Gauges - If the system containing one of the pressure gauges described above is evacuated, leaks may be detected by using a tracer gas and observing the pressure. When the tracer gas enters the vacuum system, the composition of the gas within the system will change. Thus, the thermal conductance measured by the gauge will change. This pressure change may be interpreted as a tracer gas entering the leak and its location. There are many tracer gases which can be used in this technique. If a thermocouple or a Pirani gauge is used for pressure measurement, hydrogen or helium with their high heat conductivity would indicate a large rise in pressure when these gases enter the system. This indicated increase in pressure would be due to a two-fold effect; the actual rise in pressure because of increase in leakage rate with the tracer gas and the indicated increase due to their higher heat conductivity. Alternatively, acetone or alcohol could be used as the tracer fluid, in this case being painted on the suspected area with a brush. A decrease in pressure would be observed, due to possible clogging of the leak with the liquid. This would produce a pressure drop and an indicated decrease due to the lower heat conductivity of the tracer which enters.

With the use of an ionization gauge, the ionization efficiency in the tracer gas should be different from that of the air.

Further discussions of these methods are cited in the references in the section b.

2. Hydrogen Sensitive Leak Detector - A hydrogen sensitive leak detector consists of an ionization gauge connected to the vacuum system by a heated paladium diaphragm. Hydrogen, which is used as the tracer gas, permeates through the hot paladium to the ion gauge. The advantage of this system is that it is relatively insensitive to pressure changes. This detector has a reported sensitivity of about 10^{-8} atm. cc/sec.
3. Electron Emission Leak Detector - The electron emission from a tungsten or oxide coated filament decreases greatly upon contact with oxygen. This phenomenon, (Ref. 17), has been applied to leak detection. The sensitivity of this method, using oxygen as a tracer gas, is reported to be approximately 10^{-8} atm cc/sec.
4. The Halogen Leak Detector - Early investigations of thermionic emission showed that platinum, even in air, at red heat emits positive ions. This emission at any given anode temperature of positive ions in air is increased very markedly when vapors of compounds containing a halogen strike the electrode surface. This observation forms the basis of the halogen leak detector. Leak detectors using this principle are marketed by several companies. Two types of models exist. One type consists of a detector head mounted in the vacuum system and the halogen gas,

usually Freon, used as a tracer outside the vacuum system. A second type consists of a small gas pump probe; the system to be leak tested is pressurized with halogen-containing gas. The gas pump probe contains the detection apparatus. The sensitivity of this method of leak detection is approximately 10^{-6} atm. cc/sec. Special units are claimed to be as sensitive as 10^{-9} atm. cc/sec.

iii. Detection of the Tracer Gas

1. Helium Leak Detector - A very sensitive method for detection of leaks is the use of a mass spectrometer and helium as the tracer gas. The mass spectrometer is attached to the vacuum system and a probe of helium gas is passed around the suspected leak area. The mass spectrometer is set directly on the helium mass peak. Detection and measurement consists of observation of the intensity of the ion current. Helium is chosen as the tracer gas for the following reasons:

1. Low value of M - the rate of effusion through the leak is greater than for any other gas except hydrogen.
2. Helium occurs in the atmosphere only to the extent of one part per 200,000 parts of air.
3. There is no possibility that an ion, due to any other gas will give an indication that can be mistaken for helium.

Several companies manufacture commercial leak detection equipment using this principle. The sensitivity of most of these units is 10^{-10} atm. cc/sec. One company manufactures a helium leak detector which operates on a pressure build-up by getter-ion

pumping prior to detection of the peak. The sensitivity of this instrument is claimed to be 10^{-14} atm. cc/sec. Because the vacuum equipment in this apparatus is similar to the equipment in the argon leak detector previously described, (subsection b-4), this instrument could be used as a binary leak detector. For gross leaks the pressure build-up using an argon probe would be used. After all the large leaks were detected, helium gas could be used to hunt for the small leaks.

2. Helium Probe Method

Another method of using the helium leak detector is pressurizing the suspected area with helium and using a vacuum probe to collect air from outside the suspected leak area and pass it into the vacuum system containing the mass spectrometer. This method has a sensitivity of about 10^{-6} atm. cc/sec.

3. Leak Detection by Radioactivity - One nondestructive method of

leak testing hermetically sealed components is by using a radioactive gas. This type of leak detecting equipment is commercially available. The basic principle involves the detection of radioactive Krypton 85, which has been allowed to diffuse into the leaking components. The components to be tested are placed in an activating tank and sealed. Air in the tank is evacuated and diluted. Krypton 85 is pumped into the tank to a pressure up to 7 atmospheres. The radioactive gas diffuses into the existing leaks in the component. After a prescribed soaking period, the Krypton is pumped out and returned to storage for reuse. Air is circulated over the components to remove any residual Krypton 85 from the external surface. - The components are then removed

from the activating tank and tested with a scintillation counter. Under favorable conditions, leakage rates in the order of 10^{-12} atm. cc/sec can be measured.

LIST OF SYMBOLS - APPENDIX D

- A = Area of passage normal to flow.
- A^0 = Avogadro's number, number of molecules per mole.
- $a = \frac{\pi}{8\eta} \left(\frac{d}{2}\right)^4$
- $b = \frac{1}{6} \sqrt{\frac{2\pi RT}{M}} d^3$
- C = Conductance of a passage.
- C_1 = Conductance of a portion of a passage.
- C_2 = Conductance of a portion of a passage.
- C_3 = Conductance of a portion of a passage.
- C_n = Conductance of a portion of a passage.
- C_p = Heat capacity at constant pressure.
- C_r = Heat capacity at constant volume.
- d = Diameter of flow path
- F = Velocity of fluid.
- F_c = Speed of sound.
- \bar{F} = Average speed of individual molecules.
- f = Friction factor.
- g = Mass
- $h = 1.24 \sqrt{\frac{M}{RT}} \frac{d}{\eta}$
- $j = \sqrt{\frac{M}{RT}} \frac{d}{\eta}$
- K_p = Permeation rate constant.
- l = Length of passage.
- Δl = Increment of length of passage.
- M = Molecular weight.

m = Mass of individual molecules.
 N_k = Knudsen's number.
 N_{Re} = Reynolds' number.
n = Number of molecules in a unit volume.
P = Pressure.
 ΔP = Pressure drop.
 P_a = Average pressure.
 P_u = Ultimate pressure obtained in system.
 P_1 = Pressure at point upstream in system.
 P_2 = Pressure at point downstream in system.
Q = Mass flow.
R = Gas constant.
 $r = P_2/P_1$
 r_c = Critical pressure ratio. Ratio below which choked flow takes place.
S = Pumping speed.
T = Absolute temperature.
 T_1 = Absolute temperature upstream of the orifice.
V = Volume
 α = Proportional to
 $\gamma = C_p/C_v$
 η = Absolute viscosity.
 θ = Time increment.
 λ = Mean free path.
 ρ = Density.
 σ = Molecular diameter.
 ϕ = Surface tension.

TABLE 2

MEAN FREE PATHS AND MOLECULAR DIAMETERS FOR VARIOUS MOLECULES

<u>Molecule</u>	<u>Mean Free Path</u> <u>cm x 10⁻³ at 1 Torr and 25°C</u>	<u>Molecular Diameter</u> <u>cm x 10⁻⁸</u>
H ₂	9.31	2.75
He	14.72	2.18
Ne	10.45	2.60
A	5.31	3.67
O ₂	5.40	3.64
CO ₂	3.34	4.65
H ₂ O	3.37	4.68
benzene	1.34	7.65
methane	4.15	4.19
ethane	2.53	5.37
propane	1.82	6.32
n-butane	1.46	7.06
n-pentane	1.19	7.82
n-hexane	1.03	8.42

TABLE 3

MOLAR HEAT CAPACITY OF GASES
(in calories per mole at 25°C and 1 atm)

Gas	C_p	C_v	$C_p/C_v = \gamma$
A	4.97	2.98	1.67
He	4.97	2.98	1.67
H ₂	6.90	4.91	1.41
O ₂	7.05	5.05	1.40
N ₂	6.94	4.95	1.40
CO ₂	8.96	6.92	1.29
NH ₃	8.63	6.57	1.31
ethane	12.71	10.65	1.19
propane	-	-	1.13

TABLE 4

FLOW CHARACTERISTICS OF CIRCULAR CAPILLARY LEAKS (REF. 15)

d, cm	Air		Other Gases, Q/Q _{air}					
	Q, Torr x liters/sec*	P ₂ , Torr	He	CO ₂	H ₂	CH ₄	Ne	
lower limit			7.7	0.53	6.9	1.07	2.45	$= \left(\frac{\eta}{\eta_{\text{air}}} \right) \left(\frac{M_{\text{air}}}{M} \right)^{1/2}$
1 x 10 ⁻⁶	9.9 x 10 ⁻¹⁴	3.7 x 10 ⁻³	7.3	0.55				
3 x 10 ⁻⁶	1.0 x 10 ⁻¹²	4.1 x 10 ⁻³	6.8	0.59				
1 x 10 ⁻⁵	1.7 x 10 ⁻¹¹	6.3 x 10 ⁻³	5.3	0.68				
3 x 10 ⁻⁵	3.2 x 10 ⁻¹⁰	1.3 x 10 ⁻²	3.8	0.78				
1 x 10 ⁻⁴	1.4 x 10 ⁻⁸	5.5 x 10 ⁻²	2.3	0.94				
3 x 10 ⁻⁴	6.4 x 10 ⁻⁷	0.26	1.6	1.1				
1 x 10 ⁻³	6.0 x 10 ⁻⁵	2.2	1.2	1.20				
3 x 10 ⁻³	4.5 x 10 ⁻³	18	1.0	1.22				
1 x 10 ⁻²	0.47	170	0.93	1.24				$\frac{\eta_{\text{air}}}{\eta}$
upper limit			0.93	1.24	2.07	1.67	0.58	

* Q is for a leak of one centimeter length. For a leak of any other size, the length of the leak in centimeters is divided by Q.

TABLE 1

LEAKAGE CONVERSION FACTORS

micron x cc	1	1.0x10 ³	5.2x10 ⁴	7.6x10 ⁵	16	1.6x10 ⁴	8.5x10 ⁵	1.2x10 ⁷	29	2.9x10 ⁴	1.5x10 ⁶	2.2x10 ⁷	1.0x10 ³	1.0x10 ⁶	5.2x10 ⁷	7.6x10 ⁸	2.8x10 ⁴	2.8x10 ⁷	1.5x10 ⁹	2.1x10 ¹⁰
torr x cc	1.0x10 ⁻³	1	52	7.6x10 ²	1.6x10 ⁻²	16	8.5x10 ²	1.2x10 ⁴	2.9x10 ⁻²	29	1.5x10 ³	2.2x10 ⁴	1.0	1.0x10 ³	5.2x10 ⁴	7.6x10 ⁵	28	2.8x10 ⁴	1.5x10 ⁶	2.1x10 ⁷
psi x cc	1.9x10 ⁻⁵	1.9x10 ⁻²	1	15	3.1x10 ⁻⁴	0.31	16	2.4x10 ²	5.6x10 ⁻⁴	0.56	29	4.4x10 ²	1.9x10 ⁻²	19	1.0x10 ³	1.5x10 ⁴	0.53	5.3x10 ²	2.8x10 ⁴	4.1x10 ⁵
atm x cc	1.3x10 ⁻⁶	1.3x10 ⁻³	6.8x10 ⁻²	1	2.1x10 ⁻⁵	2.1x10 ⁻²	0.11	16	3.8x10 ⁻⁵	3.8x10 ⁻²	0.20	29	1.3x10 ⁻³	1.3	68	1.0x10 ³	3.6x10 ⁻²	36	1.9x10 ³	2.8x10 ⁴
micron x in ³	6.1x10 ⁻²	61	3.2x10 ³	4.6x10 ⁴	1	1.0x10 ³	5.2x10 ⁴	7.6x10 ⁵	1.8	1.0x10 ³	9.4x10 ⁴	1.4x10 ⁶	61	6.1x10 ⁴	3.2x10 ⁶	4.6x10 ⁷	1.7x10 ³	1.7x10 ⁶	8.8x10 ⁷	1.3x10 ⁹
torr x in ³	6.1x10 ⁻⁵	6.1x10 ⁻²	3.2	46	1.0x10 ⁻³	1	52	7.6x10 ²	1.8x10 ⁻³	1.8	96	1.4x10 ³	6.1x10 ⁻²	61	3.2x10 ³	4.6x10 ⁴	1.7	1.7x10 ³	8.8x10 ⁴	1.3x10 ⁶
psi x in ³	1.2x10 ⁻⁶	1.2x10 ⁻³	6.1x10 ⁻²	0.89	1.9x10 ⁻⁵	1.9x10 ⁻²	1	15	3.4x10 ⁻⁵	3.4x10 ⁻²	1.8	26	1.2x10 ⁻³	1.2	61	8.9x10 ²	3.2x10 ⁻²	32	1.7x10 ³	2.5x10 ⁴
atm x in ³	7.9x10 ⁻⁸	7.9x10 ⁻⁵	4.1x10 ⁻³	6.1x10 ⁻²	1.3x10 ⁻⁶	1.3x10 ⁻³	6.8x10 ⁻²	1	2.3x10 ⁻⁶	2.3x10 ⁻³	0.12	1.8	7.9x10 ⁻⁵	7.9x10 ⁻²	4.1	61	2.2x10 ⁻³	2.2	1.2x10 ²	1.7x10 ³
micron x fl.oz.	3.4x10 ⁻²	34	1.7x10 ³	2.6x10 ⁴	0.55	5.5x10 ²	2.9x10 ⁴	4.2x10 ⁵	1	1.0x10 ³	5.2x10 ⁴	7.6x10 ⁵	34	3.4x10 ⁴	1.8x10 ⁵	2.6x10 ⁷	9.6x10 ²	9.6x10 ⁵	4.9x10 ⁷	7.3x10 ⁸
torr x fl.oz.	3.4x10 ⁻⁵	3.4x10 ⁻²	1.7	26	5.5x10 ⁻⁴	0.55	29	4.2x10 ²	1.0x10 ⁻³	1	52	7.6x10 ²	3.4x10 ⁻²	34	1.8x10 ³	2.6x10 ⁴	0.96	9.6x10 ²	4.9x10 ⁴	7.3x10 ⁵
psi x fl.oz.	6.4x10 ⁻⁷	6.4x10 ⁻⁴	3.4x10 ⁻²	0.49	1.0x10 ⁻⁵	1.0x10 ⁻²	0.55	8.1	1.9x10 ⁻⁵	1.9x10 ⁻²	1	14.7	6.4x10 ⁻⁴	0.64	34	4.9x10 ²	1.8x10 ⁻²	18	9.6x10 ²	1.4x10 ⁴
atm x fl.oz.	4.4x10 ⁻⁸	4.4x10 ⁻⁵	2.3x10 ⁻³	3.4x10 ⁻²	7.2x10 ⁻⁷	7.2x10 ⁻⁴	3.7x10 ⁻²	0.55	1.3x10 ⁻⁶	1.3x10 ⁻³	6.8x10 ⁻²	1	4.4x10 ⁻⁵	4.4x10 ⁻²	0.23	34	1.2x10 ⁻³	1.2	65	9.6x10 ²
micron x liters	1.0x10 ⁻³	1.0	52	7.6x10 ²	1.6x10 ⁻²	16	8.3x10 ²	1.2x10 ⁴	2.9x10 ⁻²	29	1.5x10 ³	2.2x10 ⁴	1	1.0x10 ³	5.2x10 ⁴	7.6x10 ⁵	28	2.8x10 ⁴	1.5x10 ⁶	2.2x10 ⁷
torr x liters	1.0x10 ⁻⁶	1.0x10 ⁻³	5.2x10 ⁻²	0.76	1.6x10 ⁻⁵	1.6x10 ⁻²	0.83	12	2.9x10 ⁻⁵	2.9x10 ⁻²	1.5	22	1.0x10 ⁻³	1	52	7.6x10 ²	2.8x10 ⁻²	28	1.5x10 ³	2.2x10 ⁴
psi x liters	1.9x10 ⁻⁸	1.9x10 ⁻⁵	1.0x10 ⁻³	0.15	3.0x10 ⁻⁷	3.0x10 ⁻⁴	1.6x10 ⁻²	0.24	5.5x10 ⁻⁷	5.5x10 ⁻⁴	2.9x10 ⁻²	0.43	1.9x10 ⁻⁵	1.9x10 ⁻²	1	14.7	5.5x10 ⁻⁴	0.55	28	4.3x10 ²
atm x liters	1.3x10 ⁻⁹	1.3x10 ⁻⁶	6.8x10 ⁻⁵	1.0x10 ⁻³	2.1x10 ⁻⁸	2.1x10 ⁻⁵	1.1x10 ⁻³	1.6x10 ⁻²	3.8x10 ⁻⁸	3.8x10 ⁻⁵	1.9x10 ⁻³	2.9x10 ⁻²	1.3x10 ⁻⁶	1.3x10 ⁻³	6.8x10 ⁻²	1	3.8x10 ⁻⁵	3.8x10 ⁻²	1.9	28
micron x ft ³	3.5x10 ⁻⁵	3.5x10 ⁻²	1.8	27	5.8x10 ⁻⁴	0.58	30	4.4x10 ²	1.0x10 ⁻³	1.04	54	7.9x10 ²	3.5x10 ⁻²	35	1.8x10 ³	2.7x10 ⁴	1	1.0x10 ³	5.2x10 ⁴	7.6x10 ⁵
torr x ft ³	3.5x10 ⁻⁸	3.5x10 ⁻⁵	1.8x10 ⁻³	2.7x10 ⁻²	5.8x10 ⁻⁷	5.8x10 ⁻⁴	3.0x10 ⁻³	0.44	1.0x10 ⁻⁶	1.0x10 ⁻³	5.4x10 ⁻²	0.79	3.5x10 ⁻⁵	3.5x10 ⁻²	1.8	27	1.0x10 ⁻³	1	52	7.6x10 ²
psi x ft ³	6.7x10 ⁻¹⁰	6.7x10 ⁻⁷	3.5x10 ⁻⁵	5.1x10 ⁻⁴	1.1x10 ⁻⁸	1.1x10 ⁻⁵	5.8x10 ⁻⁴	9.9x10 ⁻³	1.9x10 ⁻⁸	1.9x10 ⁻⁵	1.0x10 ⁻³	1.5x10 ⁻²	6.7x10 ⁻⁷	6.7x10 ⁻⁴	3.5x10 ⁻²	0.51	1.9x10 ⁻⁵	1.9x10 ⁻²	1	15
atm x ft ³	4.6x10 ⁻¹¹	4.6x10 ⁻⁸	2.4x10 ⁻⁶	3.5x10 ⁻⁵	7.5x10 ⁻¹⁰	7.5x10 ⁻⁷	3.9x10 ⁻⁵	5.8x10 ⁻⁴	1.4x10 ⁻⁹	1.4x10 ⁻⁶	7.1x10 ⁻⁵	1.0x10 ⁻³	4.6x10 ⁻⁸	4.6x10 ⁻⁵	2.4x10 ⁻³	3.5x10 ⁻²	1.3x10 ⁻⁶	1.3x10 ⁻³	6.8x10 ⁻²	1
seconds	1	60	3.6x10 ³	8.6x10 ⁴	6.1x10 ⁵	2.6x10 ⁶	3.1x10 ⁷													
minutes	1.7x10 ⁻²	1	60	1.4x10 ³	1.0x10 ⁴	4.3x10 ⁴	5.2x10 ⁵													
hours	2.8x10 ⁻⁴	1.7x10 ⁻²	1	24	1.7x10 ²	7.2x10 ²	8.8x10 ³													
days	1.2x10 ⁻⁵	6.9x10 ⁻⁴	4.2x10 ⁻²	1	7	30	3.7x10 ²													
weeks	1.6x10 ⁻⁶	9.8x10 ⁻⁵	5.9x10 ⁻³	0.14	1	4.3	52													
months	3.8x10 ⁻⁷	2.3x10 ⁻⁵	1.4x10 ⁻³	3.3x10 ⁻²	0.23	1	12													
years	3.2x10 ⁻⁸	1.9x10 ⁻⁶	1.1x10 ⁻⁴	2.8x10 ⁻³	1.9x10 ⁻²	0.83	1													

To convert leakage rate units, find the starting pressure x volume units on the left hand side of the chart. Move horizontally on that line, to the column which is 1 for those units. Move vertically to the line which contains the desired new units. Multiply the old leakage rate by the new units to obtain a new pressure x volume.

To convert the time units, obtain the time conversion factors in the above described manner and divide the leak rate by the appropriate conversion factor.

Example: Convert 5 psi x ft³/month to atm x cc/sec

$$5 \text{ psi} \times \text{ft}^3/\text{month} \times 1.9 \times 10^3 \text{ atm} \times \text{cc}/\text{psi} \times \text{ft}^3 \times 1/2.6 \times 10^6 \text{ sec}/\text{month} = 3.7 \times 10^{-3} \text{ atm-cc}/\text{sec}$$

ORIGINAL PAGE IS
OF POOR QUALITY

ORIGINAL PA
OF POOR Q

1002

2052

REFERENCES - APPENDIX D

1. "Glossary of Terms Used in Vacuum Technology Committee on Standards", American Vacuum Society (1958).
2. M. Knudsen, Ann. Physik, 28, 75(1909); 35, 389(1911).
3. G. E. Normand, Ind. Eng. Chem., 40, 783 (1948).
4. S. Dushman, "Scientific Foundations of Vacuum Technique", Chapt. II, John Wiley and Sons, N.Y.C. (1962).
5. J. M. Poiseuille, Compt. Rend., 11, 1041 (1840); 12, 112 (1841); 15, 1161 (1842).
6. J. H. Perry, "Chemical Engineering Handbook", 3rd Ed., Sect. 5, McGraw-Hill N.Y.C. (1950).
7. J. C. Hunsaker, and B. G. Richtmire, "Engineering Applications of Fluid Mechanics", Chapt. VIII, McGraw-Hill N.Y.C. (1947).
8. S. Glasstone, "Textbook of Physical Chemistry", 2nd Ed., D. Van Nostrand Co. N.Y.C. (1946), p. 279.
9. E. S. Creutz and L. R. Zumwalt, J. App. Phys., 33, p. 2883 (1962).
10. G. Burrows, Trans. Inst. Chem. Engrs., 39, p. 55, (1961).
11. D. J. Santeler, "A Graphical Solution for the Analysis of Vacuum Systems Performance", Vacuum Symposium Transactions (1955), p. 31.
12. W. C. Edmister, Ind. Eng. Chem., 32, p. 373, (1940).
13. "International Critical Tables", 5, p. 79-84, (1929).
14. D. J. Santeler and T. W. Moller, "Fluid Flow Conversion in Leaks and Capillaries", Vacuum Symposium Transactions (1956), p. 29.
15. A. Guthrie and R. K. Wakerling, "Vacuum Equipment and Techniques", Chapt. 5, McGraw-Hill N.Y.C., (1949).
16. W. J. Moore, "Physical Chemistry", Chapt. 16, 2nd Ed., Prentice-Hall Inc. N.Y.C., (1955).
17. R. B. Nelson, Rev. Sci. Instr., 16, 55 (1945).

Appendix E

CRYOGENIC SEALING - R. B. Fleming

The sealing of cryogenic fluids has been considered a separate category in this study because in several respects, the problems associated with sealing cryogenic fluids differ greatly from those encountered at room temperatures and above. Furthermore, the sealing of cryogenic fluids is an important category in the general subject of dynamic sealing, as several of the presently-used rocket fuels and oxidizers are cryogenic fluids.

This Appendix is divided into the following sections:

1. Introduction
2. Problems Associated With Cryogenic Sealing
3. Present Practice
4. Experimental Work on Dynamic Sealing of Cryogenic Fluids
5. Experimental Work on Friction and Wear
6. Areas in Which Further Knowledge is Needed
7. References

1. Introduction

Oxygen, hydrogen, and fluorine are the cryogenic fluids of greatest current interest as fuels and oxidizers for rocket engines. Also, liquid nitrogen and liquid helium are of interest for providing refrigeration in electronic devices and for other purposes.

Of the various types of dynamic seals, the positive contact seal is generally selected for cryogenic fluids. (See Present Practice below). Therefore, this Appendix will be devoted primarily to the positive contact dynamic seal, in which a rotating sealing member slides in positive contact

with a stationary seal. This type of seal commonly takes the form of a face seal, in which the sliding surface is perpendicular to the axis of rotation.

2. Problems Associated With Cryogenic Sealing

There are two major problem areas in the sealing of cryogenic liquids. The first is the friction and wear problem, and the second is the problem associated with sealing a liquid near saturation.

a) Friction and Wear

Most seals for use at cryogenic temperatures are of the positive contact type, and thus involve the rubbing of two solid surfaces. The problem of friction and wear results first from the fact that at cryogenic temperatures all common liquid lubricants become solid and therefore unsuitable as lubricants. In addition, many commonly used solid lubricants, such as carbon, are not suitable in certain cryogenic fluids, because these fluids do not possess the necessary lubricating properties. For reasonably low friction and wear, carbon and several other solid seal materials depend on a thin surface layer of dissolved or adsorbed gases or liquids. (References 20, 21, 22). A carbon seal in the presence of water vapor or oxygen operates satisfactorily because this lubricating surface film is replaced as fast as it wears off. However, inert or reducing cryogenic fluids (such as nitrogen or hydrogen) do not possess this filming property and are consequently more difficult to seal with conventional seal materials.

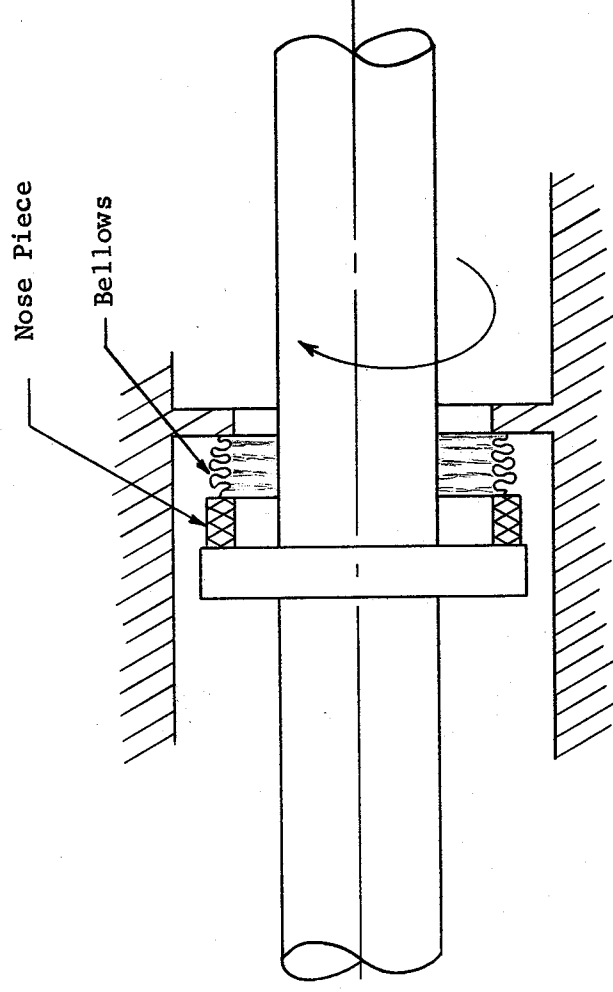
b) Sealing A Liquid Near Saturation

The second major problem involved in cryogenic sealing results from the fact that the fluid being sealed is close to its saturation temperature. Thus, any small addition of heat will either cause the fluid to boil or will produce an unstable liquid in which boiling will take place suddenly upon introduction of a nucleus for bubbles. It is this unstable condition which sometimes results in flashing of liquid to gas between the seal surfaces, which may cause the seal surfaces to separate periodically, with a consequent large increase in leak rates.

If the leak rate is low relative to the frictional heat generated between the seal surfaces, the liquid being sealed will vaporize either before entering the seal or within a short distance after entering the seal. The amount of heat transferred to the seal from warmer parts of the system also influences the evaporation rate of the liquid.

3. Present Practice

The most common type of dynamic seal for cryogenic fluids is the positive contact face seal. In this seal, the usual design is for a shoulder on the rotating shaft to slide against a nose piece of carbon-graphite composition which is held against the shoulder by means of a metal bellows. A sketch of this arrangement is shown on the next page.



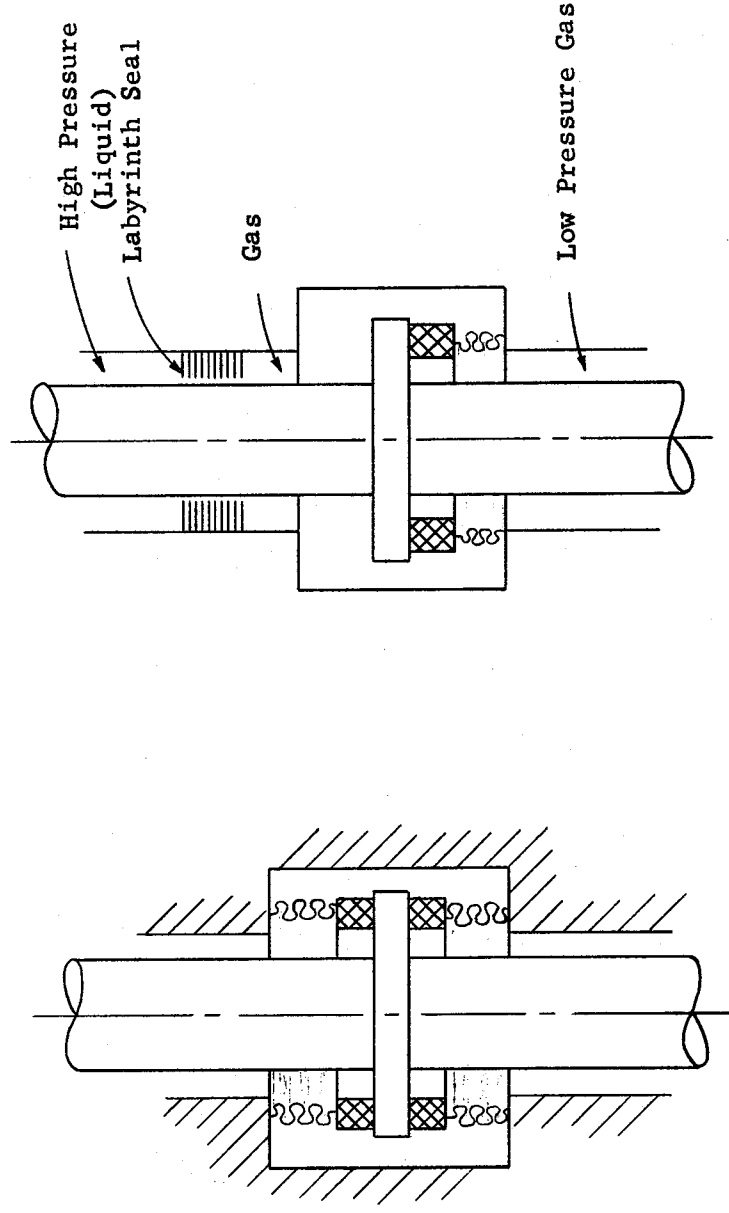
The metal bellows provides a "secondary seal" which maintains alignment of the sealing surfaces, compensates for wear of the seal materials, and provides a spring force to keep the seal surfaces in contact.

Carbon or graphite are generally considered satisfactory seal materials for oxygen, but they are not satisfactory for nitrogen, hydrogen, or helium. These inert or reducing fluids do not provide the necessary adsorbed film on the carbon surface for friction and wear reduction. For sealing these fluids, therefore, various impregnants must be added to the carbon to provide satisfactory lubricating properties. The impregnant used may vary depending upon the fluid to be sealed. A common impregnant for carbon seals is molybdenum disulfide. The exact compounding of most carbon seal materials is generally considered proprietary information of the carbon manufacturer. In addition to the carbon compounds, various polymers such as Teflon have been used as seal materials.

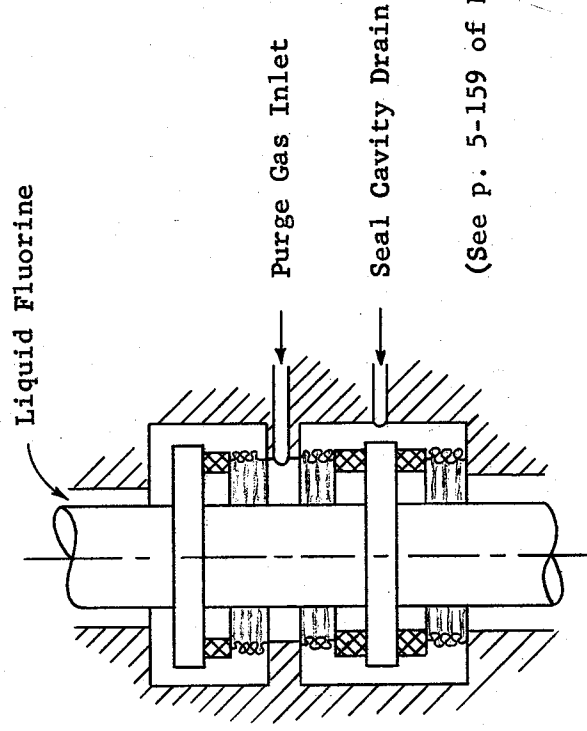
In addition to improving friction and wear capabilities of the carbon-graphite compositions, impregnants are also employed to reduce porosity of

the material so that static losses of fluid are reduced.

Because of the problem, mentioned in the last section, of liquid boiling violently between the seal surfaces, two or more seals are sometimes employed in series. With this arrangement boiling and complete vaporization of the liquid takes place within the first seal, so that the second seal operates in an atmosphere of gas only. The first seal may be a labyrinth type of seal (see Appendix C). Two possible arrangements are sketched below.



The sealing of fluorine liquid involves some unique problems. Because fluorine can react with carbon, even at fairly low temperatures, carbon seals are generally not used in fluorine systems, without the use of a bleed gas. One system which has been used to seal fluorine liquid is sketched on the next page.



(See p. 5-159 of Ref. 17)

Oxygen or an inert gas such as helium can be used as the purge or bleed gas. The purge gas is at a pressure higher than the fluorine with the result that leakage occurs from the purge gas into the fluorine system through one of the carbon seals. Therefore, the fluid being sealed is really the purge gas, not the fluorine. A system for sealing fluorine without the use of a purge gas would be desirable, but at present such a system is not known to exist.

4. Experimental Work on Dynamic Sealing of Cryogenic Fluids

Most of the work on dynamic sealing of cryogenic fluids has been done by firms engaged in liquid rocket engine work. In most of the effort these firms have applied, the problem of dynamic sealing has been a secondary problem in the design of pumps and turbines for cryogenic fluids. To our knowledge, no comprehensive work on seals for cryogenic fluids as such has been performed. Also, all investigations carried out thus far have been experimental, with very little analytical effort.

There are two government installations at which significant studies on dynamic sealing of cryogenic fluids are in effect. One of these is the Cryogenic Engineering Laboratory of the National Bureau of Standards, located at Boulder, Colorado. This program has recently commenced under USAF sponsorship. Their apparatus will be used to test bellows-loaded face seals. Two seals will be tested at once, with loading forces in opposite directions to eliminate the need for thrust bearings on the shaft.

Seals loading forces will be small - about 5.5 to 6 pounds. Maximum shaft speed will be 10,000 rpm, though it is felt that speeds of 40,000 to 60,000 rpm will be needed in the future. Liquid nitrogen and liquid hydrogen will be tested with pressures ranging up to 50 psi. It is expected that conventional type seals of various carbon compositions will be evaluated.

The other government installation engaged in this work to a significant extent, is the Lubrication Section at NASA Lewis Research Center, Cleveland, Ohio. This group has constructed two different sets of seal testing apparatus, one for cryogenic fuels and one for cryogenic oxidizers.

The Lewis dynamic seals apparatus for cryogenic oxidizers was designed for both liquid oxygen and liquid fluorine. Included in the device is a disposal system for waste fluorine gas. The designed maximum speed is 60,000 rpm. Provision has been made for measuring leak rates, torque, and wear.

The dynamic seals apparatus for cryogenic fuels at Lewis is designed for liquid nitrogen and liquid hydrogen.

The Lubrication Section of the Lewis Research Center has produced a considerable amount of experimental data on friction and wear characteristics of materials in cryogenic atmospheres. While not relating directly to

sealing problems, their work on friction and wear gives significant support to the study of the problem of sealing. References to their work, and the work of others, are given in the next section.

We are not presently aware of any significant effort having been applied to friction and wear in fluorine or to the dynamic sealing of liquid fluorine. It is known (Ref. 17) that fluorine reacts with carbon, even at fairly low temperatures. This may preclude the use of conventional carbon seals for sealing liquid fluorine (without the use of a bleed gas). It is known also, that all metals react to some extent with fluorine, and in fact, the metals which are customarily used in fluorine service form an adherent film of the metal fluoride which prevents further chemical reaction between the fluorine and metal (Ref. 17 and 18). It is not known whether or not this fluorine film possesses lubricating properties. The dynamic sealing of fluorine is considered a very difficult problem (Ref. 18).

5. Experimental Work on Friction and Wear

It was pointed out in the second section of this Appendix that friction and wear are major problems in the dynamic sealing of cryogenic fluids. For this reason, data which has been obtained in cryogenic friction and wear testing is expected to be pertinent to the problem of dynamic sealing.

In addition to cryogenic friction and wear tests, tests obtained in a high vacuum are likely to be useful. The reason for this is that in a very high vacuum, adsorbed surface layers of contaminants are prevented from forming rapidly enough to be effective as lubricants (Ref. 16). Under the usual atmospheric conditions, so-called "dry friction" is not really dry at all, because of the presence of adsorbed films of water and other

contaminants, which may act as lubricants. Ref. 16 points out that even at the low pressures in which most "dry" friction tests have been made (10^{-6} to 1 mm mercury pressure) the residual gases in a system are still sufficient to cover a clean surface with an adsorbed film in a short time.

Because of the absence of lubricating films in most cryogenic fluids, and also under high vacuum conditions, it is possible that the friction and wear characteristics of materials under high vacuum conditions are similar to the same characteristics in say, liquid nitrogen or hydrogen. For materials which do not depend strongly upon adsorbed films for lubrication, it is possible that testing in the atmosphere is sufficient to determine friction and wear characteristics.

A number of materials have been tested in cryogenic friction and wear, and in dry friction and wear experiments. The table beginning on page 118 is an abbreviated list of these materials. The materials are divided into the following categories, which are indicative of the type of dry lubrication.

1. Layer-latticed solid lubricants as surface films, powders, or solid compositions.
2. Other solid lubricants.
3. Surface treatments of materials.
4. Untreated metals and alloys.
5. Polymers.

No attempt is made here to evaluate these various materials as cryogenic sealing materials, because the correlation between friction and wear data and the performance of the material as a cryogenic seal is not known. However, it is expected that a material which performs poorly in a dry friction

and wear test is considered a necessary but not sufficient condition for satisfactory performance as a cryogenic contacting seal material. It is felt that many of the materials listed in the table would be good candidates for testing in a cryogenic seals experimental program.

6. Areas In Which Further Knowledge Is Needed

The subject of the positive contact dynamic seal operating in a cryogenic fluid is thus far relatively unexplored, both analytically and experimentally. The analytical approach is extremely complicated by the fact that so many phenomena must be considered. These phenomena include;

- (1) the fluid mechanics of flow between closely-spaced, moving boundaries,
- (2) heat transfer, (3) friction, (4) the effect of wear particles, (5) two-phase flow, if boiling is present, (6) the dynamics of the seal system, including the secondary seal (shaft run-out, axial vibrations, etc.), and (7) compatibility of materials (possible chemical or physical reactions with the fluid). These complexities have thus far discouraged significant attempts at analysis of the general problem.

It appears, then, that experimental data must be produced and compiled in order to guide the analytical effort. It would be valuable to know, for example, which of the above phenomena can be ignored in certain cases. At present, this knowledge is lacking because of the scarcity of experimental data. Our evaluation of the state of this art indicates that there has been no comprehensive experimental program on dynamic sealing of cryogenic fluids completed thus far. It is anticipated that some of the programs being conducted by governmental and industrial laboratories will begin producing the needed information in the near future.

In order to improve the techniques of dynamic sealing liquid fluorine, it would be desirable to have knowledge of the friction and wear or the sealing characteristics of various seal materials in a fluorine atmosphere.

SOLID LUBRICANTS FOR DRY FRICTION AND CRYOGENIC FRICTION TESTS

1. Layer-latticed solid lubricants, as surface films, powders, or solid compositions:

<u>Lubricant</u>	<u>References</u>	<u>Testing Conditions, Etc.</u>
MoS ₂	1, 2, 6, 13, 15, 19, 23	Vacuum, liq. N ₂
CdCl ₂	2	Normal atmosphere
CdI ₂	2, 10	Normal atmosphere, liq. N ₂
PbI ₂	2	Normal atmosphere
CoCl ₂	2	Normal atmosphere
AgSO ₄	2	Normal atmosphere
CuBr ₂	2	Normal atmosphere
WS ₂	2, 7	Normal atmosphere, vacuum
Graphite	2, 4, 8, 13, 19	Vacuum, liq. N ₂
BN	5, 7	Normal atmosphere, vacuum
Sintered aluminum oxide	5	Normal atmosphere

2. Other solid lubricants

<u>Lubricant</u>	<u>References</u>	<u>Testing Conditions, Etc.</u>
Zinc Stearate	2	Normal atmosphere
AgI	2	Normal atmosphere
Fe ₃ O ₄	2	Normal atmosphere
Mica	2, 19	Normal atmosphere, vacuum
Talc	2	Normal atmosphere
NiO	2	Normal atmosphere
CdO*	3	High temperature;
Sodium sulfate*	3	High temperature;
Cadmium sulfate*	3	High temperature
Carbon	5, 10, 13, 14, 23	Vacuum, Liq. N ₂ , Liq. H ₂ (with various impregnants)

* Mixture with graphite

<u>Lubricant</u>	<u>References</u>	<u>Testing Conditions, Etc.</u>
CaF ₂	6	Vacuum
Diamond	19	Vacuum
PbO	3	High temperature

3. Surface treatments of materials

<u>Material</u>	<u>References</u>	<u>Testing Conditions, Etc.</u>
Stainless steel with N ₂ , S, & Cr surface treatments	15	Liq. N ₂

4. Untreated metals and alloys

<u>Material</u>	<u>References</u>	<u>Testing Conditions, Etc.</u>
Silver	6, 13	Vacuum, Liq. N ₂
Tin	6	Vacuum
Gold	1, 6	Vacuum
Lead	6	Vacuum
Various steels	13	Liq. N ₂

5. Polymers

<u>Material</u>	<u>References</u>	<u>Testing Conditions, Etc.</u>
PTFE (polytetrafluoroethylene)	5, 9, 10, 12, 13, 15	Normal atmosphere, Liq. N ₂ , Liq. H ₂ (used with various impregnants)
PTFE, glass-fiber filled	9, 13	Liq. N ₂ , Liq. H ₂
PTFCE (polytrifluorochloroethylene)	15	Liq. N ₂
Nylon & MoS ₂	5	Normal atmosphere
Nylon & Graphite	10	Liq. N ₂ & Liq. H ₂
Laminated phenolics	13	Liq. N ₂
Melamine resin, glass fiber filled	13	Liq. N ₂
Resin bonded fabrics	5	Normal atmosphere (with various impregnants)
PTFE in carbon	23	Vacuum

7. REFERENCES FOR APPENDIX E

1. T. W. Flatley, H. E. Evans: "The Development of the Electric Field Meter for the Explorer VIII Satellite (1960)"; NASA Technical Note D-1044, Washington, D.C., April 1962
2. M. B. Peterson, R. L. Johnson: "Friction of Possible Solid Lubricants with Various Crystal Structures"; NACA Technical Note 3334, Dec. 1954
3. M. B. Peterson & R. L. Johnson: "Friction Studies of Graphite and Mixtures of Graphite with Several Metallic Oxides and Salts at Temperatures to 1000°F"; NACA Technical Note 3657, Feb. 1956
4. J. Spreadborough: "The Frictional Behaviour of Graphite"; Wear, Vol. 5 (1962), p. 18-30
5. F. F. Simpson: "A Comparison of Materials for Use as Unlubricated Journal Bearings"; Proc. Instn. Mech. Engrs, Vol. 175, No. 10, 1961
6. D. H. Buckley, M. Swikert, R. L. Johnson: "Friction, Wear & Evaporation Rates of Various Materials in Vacuum to 10⁻⁷ mm Hg"; ASLE Trans., Vol. 5, p. 8-23, (1962)
7. M. T. Lavik, G. E. Gross, G. W. Vaughn: "Investigation of the Mechanism of Tungsten Disulfide Lubrication in Vacuum"; Lubrication Engineering, Vol. 15, No. 6, (1959), p. 246-249; 264
8. R. H. Savage & D. L. Schaefer: "Vapor Lubrication of Graphite Sliding Contacts"; Journal of Applied Physics, Vol. 27, No. 2, p. 136-138, Feb. 1956
9. H. W. Scibbe, W. J. Anderson: "Evaluation of Ball-Bearing Performance in Liquid Hydrogen at DN Values to 1.6 Million"; ASLE Trans., Vol. 5, p. 220-232 (1962)
10. D. W. Wisander, R. L. Johnson: "Wear & Friction of Impregnated Carbon Seal Materials in Liquid Nitrogen and Hydrogen"; Advances in Cryogenic Engineering, Vol. 6 (Proc. of the 1960 Cryogenic Engineering Conference) Plenum Press, N. Y., 1961
11. D. W. Wisander, R. L. Johnson: "A Solid Film Lubricant Composition for Use at High Sliding Velocities in Liquid Nitrogen"; ASLE Trans., Vol. 3, No. 2, 1960, p. 225-231
12. D. W. Wisander, C. E. Maley, R. L. Johnson: "Wear and Friction of Filled Polytetrafluoroethylene Compositions in Liquid Nitrogen"; ASLE Trans., Vol. 2, No. 1, p. 58-66, (April 1959)

13. D. W. Wisander, W. F. Hady, R. L. Johnson: "Friction Studies of Various Materials in Liquid Nitrogen"; Advances in Cryogenic Engineering, Vol. 3 (Proc. of the 1957 Cryogenic Engineering Conference), Plenum Press, N. Y., p. 390-405, 1960. More detailed report (Same title) in NACA Technical Note 4211, Feb. 1958.
14. D. W. Wisander and R. L. Johnson: "Wear and Friction in Liquid Nitrogen and Hydrogen of the Materials Combination Carbon-Stainless Steel and Carbon-Carbon"; Paper presented at the 1960 Air Force-Navy-Industry-Propulsion Systems Lubricants Conference, San Antonio, Nov. 1960.
15. D. W. Wisander, R. L. Johnson: "Wear and Friction in Liquid Nitrogen with Austenitic Stainless Steel Having Various Surface Coatings"; Advances in Cryogenic Engineering, Vol. 4, (Proc. of the 1958 Cryogenic Engineering Conference), Plenum Press, N. Y., 1960, p. 71-83
16. L. E. St. Pierre and A. J. Haltner: "Ultrahigh Vacuum Techniques for the Investigation of Space Lubrication"; TIS No. 61-RL-2755C, General Electric Research Laboratory, Schenectady, N. Y., June 1961
17. P. S. Gakle, et. al.: "Design Handbook for Liquid Fluorine Ground Handling Equipment"; WADD Technical Report 60-159, Dec. 1960; Report No. AD 266719, Armed Services Tech. Info. Agency, Arlington, Va.
18. H. W. Schmidt and E. A. Rothenberg: "Some Problems in Using Fluorine in Rocket Systems"; Proc. of the Propellant Thermodynamics and Handling Conference, Special Report No. 12, Engrg. Experiment Station, Ohio State Univ. (1961)
19. R. H. Savage: "On the Friction & Wear of Graphite and Other Layer-Latticed Solids", General Electric Research Laboratory Reprint No. 2201, Schenectady, N. Y.
20. R. H. Savage; "Physically & Chemically Adsorbed Films in the Lubrication of Graphite Sliding Contacts", Annals of the New York Academy of Sciences Vol. 53, Art. 4, pp. 862-869
21. W. H. Austray, J. E. Diehl, E. I. Shobert II; "Simulated Altitude Carbon Brush Investigations", A.I.E.E. Paper No. CP 58-909
22. R. H. Savage; "Vapor Lubrication of Graphite Sliding Contacts", Journal of Applied Physics, Vol. 27, No. 2, pp. 136-138, Feb. 1956
23. B. R. Atkins, J. R. Bradshaw, and P. J. Mitchell; "New Carbon Materials for Mechanical Applications", Scientific Lubrication, Vol. 13, No. 7, p. 13-19 (July 1961)

Appendix F

TWO-PHASE PHENOMENA IN DYNAMIC FACE SEALS - L. H. Bernd

Dynamic seals feature relative rotation between a static part and moving part. Dynamic seals leak (usually outwards), and pending a radical breakthrough in sealing principles, it is possible only to minimize leakage, not prevent it. To do this, it is obviously necessary to understand the principles by which these devices work. In some cases, such as the labyrinth or "screw" seal, the principles have been extensively studied analytically, and reliance may be placed in the theory presently available. The face seal, however, which comes close to the requirement for zero leakage from a dynamic seal, is not as fully understood as these other types. Because of its known performance and desirability, it has been singled out for a particular study, since it is possible that even better sealing can be obtained from this device once its method of operation is explained.

A research program sponsored by industry at Battelle has established, among other things, the following aspects of the operation of the face seal: (1)

1. There exists an interfacial film in a dynamic face seal.
2. The film is not continuous but consists of discrete regions of vapor and fluid. That is, two phases, vapor and liquid, exist concurrently in the seal.

A. Conditions Causing 2-Phases in Liquids

Cryogenics

Heat influx and seal friction cause cryogenic liquids to boil.

We are concerned with liquid hydrogen, oxygen and fluorine. Liquid gases are stored in lightweight tanks under low pressure to minimize vehicle weight. The storage tanks are heavily insulated to cut down evaporation losses. These losses are in the order of 1 per cent per day. Liquid gases are therefore usually at, or very close to, boiling conditions.

Shafts or pumps furnish a conducting path by which heat can readily enter a cryogenic system. Liquid in contact with a shaft or seal will probably boil due to this heat influx alone. An additional heat source is the fluid friction between the faces of the shaft seals used in engine components. Should boundary lubrication exist, physical contact between faces makes for additional heat release.

Conventional Liquids

Reaching boiling in normal boiling point liquids is determined by the shear rate in the liquid, and liquid viscosity, vs. the cooling provided. Many of the fuels and oxidizers used in rocket engines are of low viscosity. Hence, even in spite of the high shear conditions that predominate (as a result of the high speeds used to reduce weight and bulk), boiling is probably not a typical condition. The significance is that raising the temperature helps cavitation to occur. Temperatures are estimated to cover a wide range.

Cavitation results when the pressure within a liquid is reduced to below the vapor pressure. Battelle Memorial Institute, in their current industry-supported seal program⁽¹⁾, have repeatedly photographed "cavitation" trails in the liquid film confined between the sealing surfaces of dynamic face seals. One of the seal faces was made of glass to permit direct observation. The British Hydromechanics Research Association has also photographed cavitation in seals under certain conditions⁽²⁾. The cavitation obtained by Battelle is generally in the form of long thin striations; i.e., apparently elongated voids separating thin channels of liquid. The void and liquid paths are concentric to the center of rotation, describe circular trails, and start at definite points. The British photograph trails of quite a different nature, consisting of many small bubbles. We have also apparently seen both types of cavitation in a brief preliminary investigation. Thus, it is necessary to consider two-phase effects even when not boiling.

Cavitation in Lubrication

Cavitation has been used to explain the load bearing capacity of thrust bearings. Lubrication-wise, a thrust bearing is similar to a face seal. Salama⁽³⁾ assumed a sinusoidally varying surface separated from a flat surface by a liquid. Alternate areas of positive and negative pressures result when the surfaces move parallel to one another. "Hills" produce positive pressures, "valleys" .. tension. The assumption was made that a liquid has no tensile strength, and that hence the liquid separates from the valleys. This permitted Salama to disregard tension areas, and estimate the load-bearing capacity as the sum of the positive pressure regions.

Salama's tests encompassed conditions to be found in typical dynamic face seals, and apparently justified his theory. Experiments were carried out

with relatively long surface undulations (1/16 to 1/2 in.), with amplitudes from 0.00005 to 0.0012 in. Seals are normally manufactured to a 10 to 20 micro-inch surface. Performance was compared with a 1.9 micro-inch surface considered to be "flat."

The 1.9 micro-inch "flat" surface seized at loads lower than the seizure loads obtained for most of the other surfaces. This agrees with common observations that "perfectly" finished seals do not lubricate well, and fail readily.

Quite a few investigators have assumed the existence of cavitation in seeking load-bearing mechanisms. For instance Nahavandi and Osterle,⁽⁴⁾ analyzed two cases: (2) vibration, that is a periodic change in the spacing between faces, and (b) a "gyroscopic motion" in which the geometric axis of the shaft precessed around the vertical axis on a conical surface. Neither of these physical models has been supported by the observations in the Battelle study.

Centrifugal and Centripetal Stresses

One way of producing two-phase cavitation trails of the type discovered by Battelle is by the application of centrifugally produced tensile stress. Also, certain types of viscoelastic liquids when sheared are known to produce a reverse action, or "centripetal" stress. This can also produce cavitation trails under certain conditions. Liquids that are normally Newtonian may become significantly non-Newtonian under the high shear existent in seals and exhibit viscoelastic effects. A general analysis of these fluid stresses is given in Appendix B, by Dr. G. M. Rentzepis.

B. Cavitation Trails in Seals

Possibility of Sealing Against Pressure:

As previously mentioned, Battelle repeatedly photographed "cavitation" trails in a transparent face seal. It seemed probable that this type of cavitation could be used to explain low leakage in a seal. In some cases, pressures as high as several hundred psi can conceivably be sealed in this way. The pressure sealed is a function of the number of trails, surface tension, wetting and wetting angle hysteresis.

The alternate dark and light bands seen in the seal, perpendicular to the direction of liquid leakage (ie, radial flow) are interpreted as being alternate bands of liquid and cavitation voids (Fig. 6a). A cavitation void may be gas or vapor. Fig. 6b is a cross-section through the cavitation voids assuming typical physical properties. The precise details of such a cross-section cannot be obtained from Battelle's work to date. This we must do now to some extent to justify further inquiry.

Within each void, pressure must be produced by surface tension acting at the liquid/void interface. This pressure P is:

$$P = \frac{2\sigma \cos \theta}{d \times 69,000} \quad (1)$$

Where:

P = Pressure, psi

σ = Surface tension, dynes/cm

d = Gap width, cm.

In Fig. 6b, the wetting angle θ is shown as being the same on each side of a void. If now, as in Fig. 6c, some flow has taken place, the wetting angles may change, resulting in a head opposed to the flow. This head is proportional to the number of voids in the cross-section. The advancing wetting angle (θ_A) becomes larger than the receding wetting angle (θ_R). This phenomenon is known as "hysteresis" of the wetting angles. The net head each void is capable of sustaining is then equal to:

$$P = \frac{2\sigma (\cos \theta_R - \cos \theta_A)}{d \times 69,000} \quad (2)$$

For this mechanism to work, it is necessary for θ to be large, and $(\theta_R - \theta_A)$ to be large. $(\theta_R - \theta_A)$ can be as large as 40° , or even more (ref. 5). However, if $\theta \rightarrow 0$, then $(\cos \theta_R - \cos \theta_A) \rightarrow 0$, and no head can be sustained.

Pressure supported in a capillary:

An easy way to demonstrate sealing capabilities would be to place alternate layers of gas and liquid in a capillary. Jamin⁽⁶⁾ states that he was able in this manner to support pressure heads of up to 4 atmospheres across a capillary. The pressure was held for as long as 5 days, presumably the duration of the test. The number of liquid/gas interfaces was not given. Mercury produced this effect, alcohol and oil did not. He also noted that the maximum head sustained was 54/200 of the head a single interface would sustain in a capillary.

Partington,⁽⁷⁾ commenting upon this effect, states, "A chain of air bubbles in a capillary tube, separated by short water columns, can sustain a finite pressure.....This effect is not shown when the apparatus is quite clean and is due to hysteresis of contact angles caused by a trace of grease." The number of cavitation trails noted in Battelles photographs range from 180 to 285 per inch. (In only a few instances did Battelle not find trails.) Taking a surface tension of 20 dynes per cm, assuming a seal face width of $1/4"$, and using Jamins ratio between capillary head and hysteresis, the total pressure that could be sustained across a seal face for a twenty microinch gap is 187 psi, illustrating that this mechanism may indeed be an explanation for face seal operation in the thin film region.

Wetting Angles:

The wetting angle θ varies from zero to approximately 145° , depending upon the material, its state of cleanliness, the surface roughness and porosity. Basically, a wetting angle is a measure of the adhesion between the liquid and the solid, and as such, varies over a wide range. If a wetting angle is less than 90° , it is decreased if the surface is porous; and if more than 90° , it is increased if the surface is porous. Clean, smooth, non-porous substances, generally do not exhibit any difference between an advancing angle and a receding angle. Table 3 lists some values of the wetting angle of water taken from the literature. Glass, silica and some metals are generally known to have $\theta \rightarrow 0$ when clean; waxes, paraffins and organics range from 60° to 140° . Recorded values vary widely.

The purpose of Table 3 is to illustrate some of these variations. In order to determine wetting angles, and wetting angle hysteresis; to see whether

cavitation voids can support pressure in typical seal components, a limited number of experiments were conducted. These are described in a later section of the report.

Surface tension:

Before continuing with the possible effects of these cavitation voids, let us examine the total head maintained by the meniscus in a capillary for different liquids. This will give an order of magnitude of the basic effect, upon which the wetting angle hysteresis acts as a secondary effect. Referring to Fig. 7, if the liquid wets the capillary surface well, as for water and clean glass ($\theta = 0$) the head maintained is then directly proportional to the surface tension, and universally proportional to the tube diameter.

Similarly, if a seal contained a liquid under pressure, and the ambient fluid were a gas, and if it were also possible to obtain the proper wetting angles and geometry at the gas/liquid interface to fully utilize the surface tension forces, then a seal could be constructed capable of maintaining a pressure head at low gap clearances. Seals have been designed using this criterion. (8) Table 4 lists various liquids and the pressure that could be sustained in a 20 micro-inch clearance gap. Twenty micro-inches is about the minimum gap size one might conceive of, considering normal surface finishes; gaps of 20 to 500 micro-inches are more likely to occur. (9)

Experiments:

Some wetting angle tests were conducted at ATL during this report period to see whether large enough values of the wetting angle (θ) could be obtained, combined with sufficient hysteresis ($\theta_R - \theta_A$) to justify investigating cavitation trails as a mechanism capable of sustaining a pressure head. For the few materials initially tested, the conclusion is: for some cases definitely yes, for others, not at all.

Water and kerosene were chosen as two test fluids because of their widely divergent properties. Water, for instance, is highly ionic, while kerosene is a hydro-carbon, coordinate bond liquid. Stellite/Graphitar seal members were prepared, and operated under face loads of 10 to 50 psi at very low velocities, to ensure that wear tracks would be obtained. Wear was needed, because a material whether in a contaminated "as received" or in a "cleaned condition"--is quite different in its surface properties than the virgin subsurface material. The equipment for wearing in the seal is shown in an overall view in Figure 1. Typical test specimens, with a faint wear track on each at an inner radius, are seen in

Figure 2. The Stellite-faced runner rotated against the stationary carbon-graphite seal face.

Following several hours of "wearing in" on this machine, the rotating and stationary parts were removed and placed in the equipment shown in Figure 3, for measurement of wetting angles. With the specimen submerged in test fluid in a transparent container, an air bubble was placed on it, and the image of the bubble-material region projected (inverted) on the screen at the rear. By rotating the table in either direction, velocity and direction of motion effects on the wetting angle could be observed.

Typical wetting angle behavior under different directions of motion are shown in Figures 4 and 5, which are taken from behind the screen, looking toward the light source, which may be seen at the left in these photos. The change in both advancing and receding angles, with the change in direction of motion, may be seen.

Numerical results from these tests are listed in Tables 5 and 6. Conclusions of significance can be drawn from this information, although further tests are desirable.

Stellite and water had the highest hysteresis and largest wetting angle, not because of the properties of Stellite, but because the original lapping process left an oily film on the surface. No hysteresis whatsoever was obtained with the kerosene. The change in the surface properties can be traced by noting the different wetting angles as the tests progressed. Kerosene exhibited no hysteresis.

An example of the potential use of data of this type, the pressure that a Stellite-water combination could sustain (for a 20 micro-inch gap, 180 cavitation trails per inch, 1/4 in. seal width) is:

$$\begin{aligned}\theta_R &= 45 & \theta_A &= 90^\circ \\ P &= 41.7 \times \frac{180}{4} & (\cos \theta_R - \cos \theta_A) &= \underline{1320 \text{ psi.}}\end{aligned}$$

C. Cavitation

If cavitation phenomena exist in seals, the first question is "Are the effects significant?" If shown to be of major importance in sealing, and/or explaining load bearing, then of equal concern is the question, "What is the cause of cavitation, and under what specific conditions is cavitation produced?"

This is very important, since a very good case can be built up to show that cavitation is influenced by many variables; that the incidence of cavitation

probably varies widely. What at first thought might be considered identical seals may perform quite differently in different locations.

Although cavitation is generally assumed to occur when the vapor pressure is greater or equal to the pressure head on a fluid, this is not always true. Wide variations do occur. As an extreme, consider the maximum tensions that have been measured under laboratory conditions.

Tensile Stress--Briggs⁽¹⁰⁾ obtained 250 atmospheres when applying centrifugal force to a column of distilled water. In other liquids ranging from mercury to CCl₄ and C₆H₆, tensile stresses from 425 to 130 atmospheres were reached.

Boiling point--Harvey⁽¹²⁾ raised the boiling point of water from 212°F to 392°F. This is equivalent to 14-1/2 atmospheres internal pressure created by the vapor pressure. Briggs⁽¹³⁾ raised the boiling point to achieve 50 atmospheres. Others⁽¹⁴⁾ have tried different fluids, ranging from ethyl alcohol at 154 atmospheres to 43 for liquid sulfur dioxide.

Supersaturation with dissolved gas⁽¹⁵⁾--Heating a liquid drives out dissolved gas to initiate cavitation of a gaseous type. At least 100 atmospheres supersaturation has been reached with nitrogen dissolved in water.

Realizing only a small fraction of these values would prevent cavitation from taking place. In fact, moderate tensile stress values are frequently obtained in liquids. Pure, "laboratory-clean" liquids are not necessarily a requirement.

Cavitation (and boiling) are affected by the following variables:

1. Adhesion of liquid to solid, also internal cohesion of the liquid, to measure maximum tensile stress capabilities.
2. Gas on a surface or in pores to nucleate cavitation.
3. Solid contaminants acting via (1) or (2) to cause cavitation, or gas nuclei (small bubbles) present in the liquid.
4. Previous history--Applying pressure to the liquid tends to dissolve gas so that higher tensions are realized. For instance, only 100 psi applied for a few minutes can produce a definite, but moderate increase in tension.

At the conclusion of this report section, it should be pointed out that the preceding discussion is not intended to present a complete, fully developed

theory. Its purpose is rather to show the various influences on what may become a significant new theory in dynamic fluid sealing, and is subject to changes as further thought is applied to this important problem.

D. Conclusions

Two-phase fluid conditions frequently exist in face seals. By "two-phase" is meant the concurrent existence of both liquid and gas. Two-phase phenomena are significantly different than the "single-phase" flow that takes place when only liquid is present. Hence, two-phase phenomena are appraised as a major area requiring investigation before it will be possible to put the design of face seals on a satisfactory, rational basis for rocket engine use. It is even anticipated that two-phase effects can, in certain cases, be exploited to improve seal performance.

Leakage flow, and the load bearing capacity of seal faces can be expected to be strongly influenced by two-phase conditions, because of the difference in fluid properties. For instance, a two phase fluid is compressible. Shear/viscosity relations and flow stability conditions are modified. The fluid may become non-homogeneous, and possess different properties in different places. Flow/pressure drop relations may change. If the second phase (usually vapor or gas) is finely divided within the liquid, or small clearances exist, surface properties enter, and surface tension plays a role.

It appears quite probable that seal performance is affected differently, depending upon the origin and form of the second phase. The second phase can be produced by boiling and/or cavitation.

B. References

1. Hamilton, D.B., "Summary of Mid-year Meeting of the Rotary Shaft Seal Research Group," Battelle Memorial Institute, Columbus 1, Ohio, June 28, 1962.
2. Austin, Fisher, Nau, Sutehall, "General Review of Recent Seal Research at B.H.R.A.," British Hydromechanics Research Institute, April 1962.
3. Salama, "The Effect of "Macro-roughness on the Performance of Parallel Thrust Bearings," Institution of Mechanical Engineers, Proceedings, Vol. 163, 1950, p. 149-161.
4. Nahavandi and Osterle, "The Effect of Vibration on the Load-carrying Capacity of Parallel Surface Thrust Bearings, ASME Paper 60-LUBS-3.
5. Adam, "The Physics and Chemistry of Surfaces," Oxford, 1938, p. 181.
6. Jamin, "Equilibrium and Movement of Liquids in Porous Substances," Compt. Rendus, Vol. 50, 1860, p. 172, 311, 385.
7. Parington, "An Advanced Treatise on Physical Chemistry, " Vol. II, Properties of Liquids, Longmans, Green and Company, 1955.
8. Brkch, "Mechanical Seals--Theory and Criteria for their Design," Product Engineering, Vol. 21, 1950, p. 85-89.
9. Denny, "Some Measurements of Fluid Pressures Between Plane Parallel Thrust Surfaces with Special Reference to Radial-face Seals," Wear, Vol. 4, No. 1, 1961, p. 64-83.
10. Briggs, "Limiting Negative Pressure of Water," J. of Appl. Physics, Vol. 21, July, 1950, pp. 721-2.
11. Harmann, "Physico-Chemical Effects of Pressure," Academic Press, 1957, p. 216.
12. Harvey, Barnes, McElroy, Whiteley, Pease, "Removal of Gas Nuclei from Liquids and Surfaces," J. Amer. Chemical Society, Vol. 67, June '45.
13. Briggs, "Maximum Superheating of Water as a Measure of Negative Pressure," J. Applied Physics, Vol. 26, Aug. '55, p. 1001-3.
14. Kendrick, Gilbert, Wismer, "The Superheating of Liquids," J. of Physical Chemistry, 1924, Vol. 28, pt. 2, p. 1297-1307.
15. Kendrick, Wismer, Wyatt, "Supersaturation of Gases in Liquids," J. of Physical Chemistry, Vol. 28, 1924, p. 1308-1315.

Formula	Mol. Wt.	Boiling and Freezing Points °F	Spec. Gravity	Viscosity cp.	Flash Pt. °F	Spec. Heat	Heat of Vaporization	Heat of Surface Tension
							BTU/lb.	Dynes/cm
<u>MONO PROPELLANTS</u>								
Hydrazine	34	236.3 34.7	1.0045 25°C	.90 25°C	126	.737	54.0	26.5
UDMH	60	146 -71.0	.786 25°C	.509 25°C	5	.653	251	24.0
Hydrogen peroxide (100%)	34	302.4	1.44 25°C	1.156 25°C		.628	652.9	80.4
<u>FUELS</u>								
Hydrogen (liquid)	2	-423.0	.07 -439°F	.013 -439		1.45	197	1.91
RP-1 Hydrocarbon (High boiling pt. kerosene)		350-525 -40	.81 68°F		110			.086
<u>OXIDIZERS</u>								
Nitrogen Tetroxide N ₂ O ₄		70.1 -11.8	1.45 20°C	.416 20°C			178.2	26.5
Fluorine (liquid) F ₂	38	-363 -306	1.505 -363	.257 83.2°K				12.3
Chlorine Trifluoride CF ₃	92	53.2 -107.1	1.809 25°C	.412 25°C		.302	128	22.7
Oxygen (liquid) O ₂	32	-297.45 -361.9	1.142 -183°C	.190			91.26	13.23
WATER	18	212 32	1.00	1.14		1.00	970.3	72

Table 1- General Properties of Liquids

Table 2

Viscosity and Heat Transfer
Properties of Liquids

	<u>μ Centi- poise</u>	<u>Sp. Gr.</u>	<u>Boiling point OF</u>	<u>K</u>	<u>$\frac{\mu}{K}$</u>
Hydrazine	.90	1.00	236		
UDMH	.51	.786	146	.12	4.25
H ₂ O ₂	1.156	1.44	302		
H ₂ liquid	.013	107	-423	.0693	1.87
RP-1 (kerosene like)	1	.81	350/525	.086	1.16
Diborane					
N ₂ O ₄	.416	1.45	70.1		
F ₂ liquid	.257	1.51	-363		
ClF ₃	.412	1.8	53.2		
O ₂ liquid	.19	1.14	-297.5	.0867	2.19
Water	1.14	1.0	212	.343	3.32

Table 3

WETTING ANGLES OF DIFFERENT SOLIDS AGAINST WATER

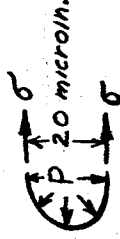
	<u>Min. Angle</u>	<u>Max. Angle</u>
Paraffin	105-110 [±] 6	
	99-110	
Carnauba wax	107	
Shellac	107	
Polystyrene	91	
Fluoro-ethylene compounds (Teflon)	90-105	
Barium stearate	88-90	
Ceylon graphite	87.8	
Talc	86	
Glyptal resin	61	
Methyl methacrylate	50° advancing	
Glass	0	30-80
Gold		68 [±] 4
Platinum	0	63 [±] 4
Chromium	0	
Stainless Steel	7-10	60-94
Aluminum	0	

Table 4

SURFACE TENSION--PRESSURE DEVELOPED AT A LIQUID/GAS INTERFACE

$$P = \frac{2\sigma}{d \times 69000}$$

Where: σ = dynes/cm
 P = psi
 d = cm



Liquid metals (Na, Li, K)	Surface Tension dynes/cm	Pressure P - psi
H ₂ O ₂	425/430	246/255
H ₂ O	80.4	46.6
Nitrogen tetroxide (N ₂ O ₄)	72.0	41.7
Hydrazine (N ₂ H ₄)	26.5	
Chlorine trifluoride	22.7	
RP-1 (High boiling point kerosene)	20/30	15.4/17.4
Oxygen	13.2	7.6
Fluorine	12.3	7.1
Hydrogen	1.91	1.1

Table 5

Wetting Angle Tests

Lubricant-Water

Stellite on graphitar 80; stellite lapped with diamond dust and oil, graphitar as machined

	<u>Advancing</u>		<u>Receding</u>	
<u>Stellite</u>	Static Motion		Static Motion	
Original surface	75	100	75	45
Before test	95	101	83	45/60
After test				
Wear track				
After 2 hrs.		33/67		15/33
End of } No carbon deposit Test } Carbon deposit	93	106	75	51
	59	75/90	21	14/16
<u>Graphitar</u>				
Original surface	20	20	20	20
Wear track				
After 2 hrs.		23/90		11
End of test	59	90	34	34

Table 6

Wetting Angle Tests

Lubricant - kerosene

Stellite on graphitar 80; stellite lapped with diamond dust and oil, graphitar as machined.

	<u>Advancing</u> static	<u>Receding</u> static
Before test		
Stellite	20	20
Graphitar	30	30
After 5 hrs. - graphitar	15	15
After 15 hrs.		
Stellite - original surface	8	9
wear track	7	8
Graphitar - original surface	20	20
wear track	9	8
End of test		
Stellite	10°	10°
Graphitar	5	5

Graphitar started at 30°, and went to 5°
Stellite started at 20°, and went to approximately 10°

ORIGINAL PAGE
BLACK AND WHITE PHOTOGRAPH

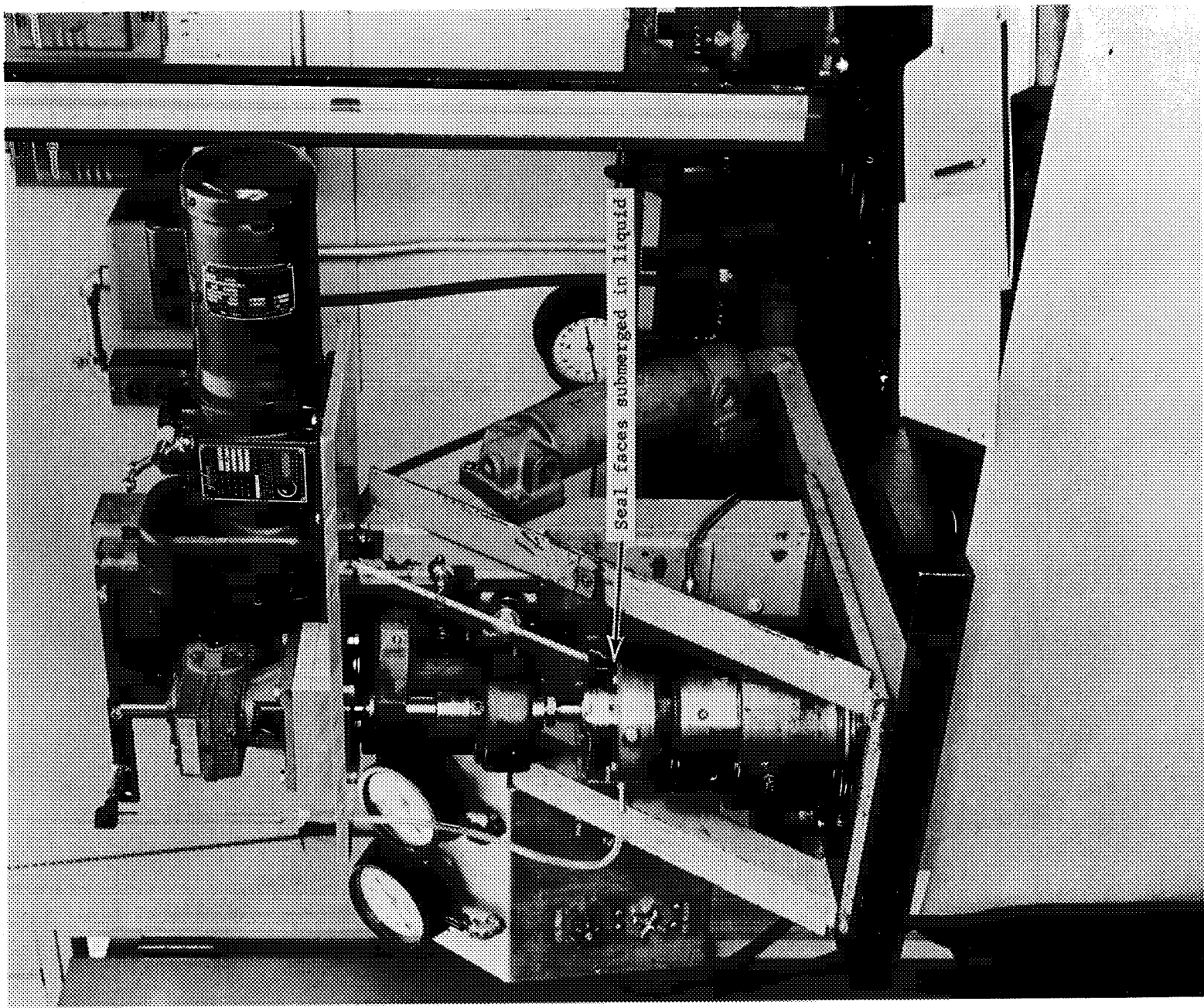


Fig. 1 Wetting Angle Experiment--Seal Tester--Wearing in Surfaces

ORIGINAL PAGE
BLACK AND WHITE PHOTOGRAPH

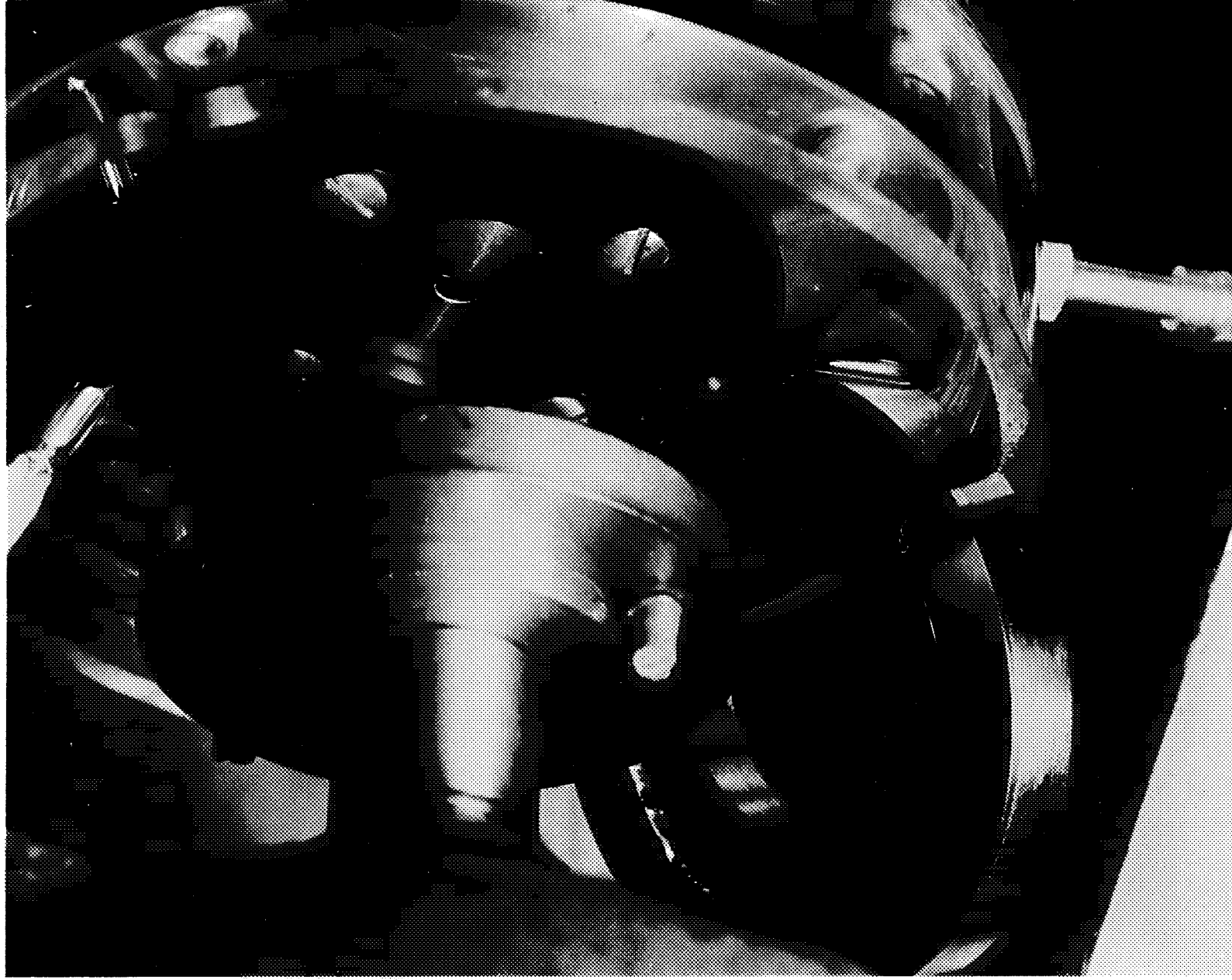


Fig. 2 Seal Tester Close-up--Showing Wear Track on Stellite and Graphitor Surfaces

ORIGINAL PAGE
BLACK AND WHITE PHOTOGRAPH

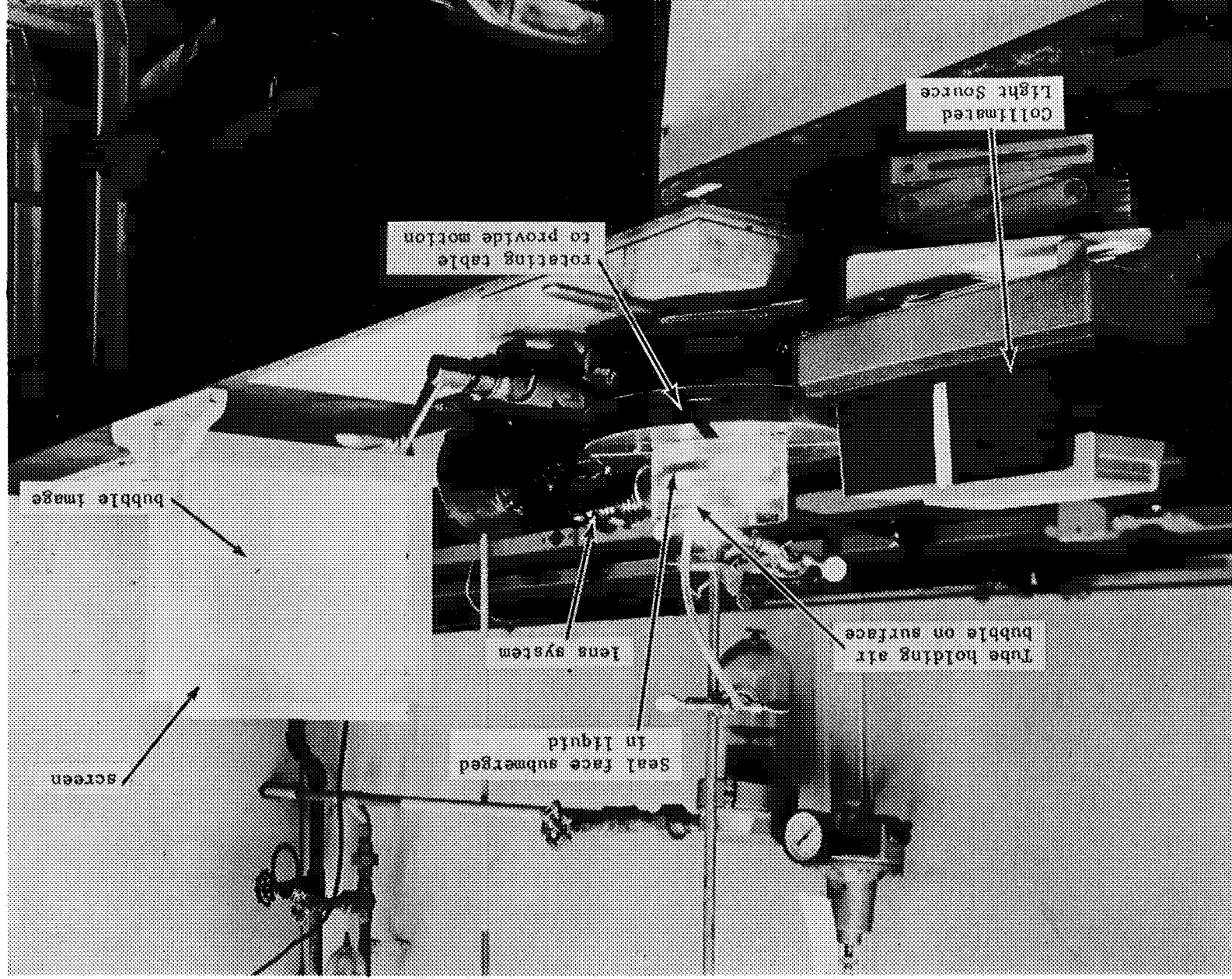


Fig. 3 Measurement of Wetting Angle

ORIGINAL PAGE
BLACK AND WHITE PHOTOGRAPH

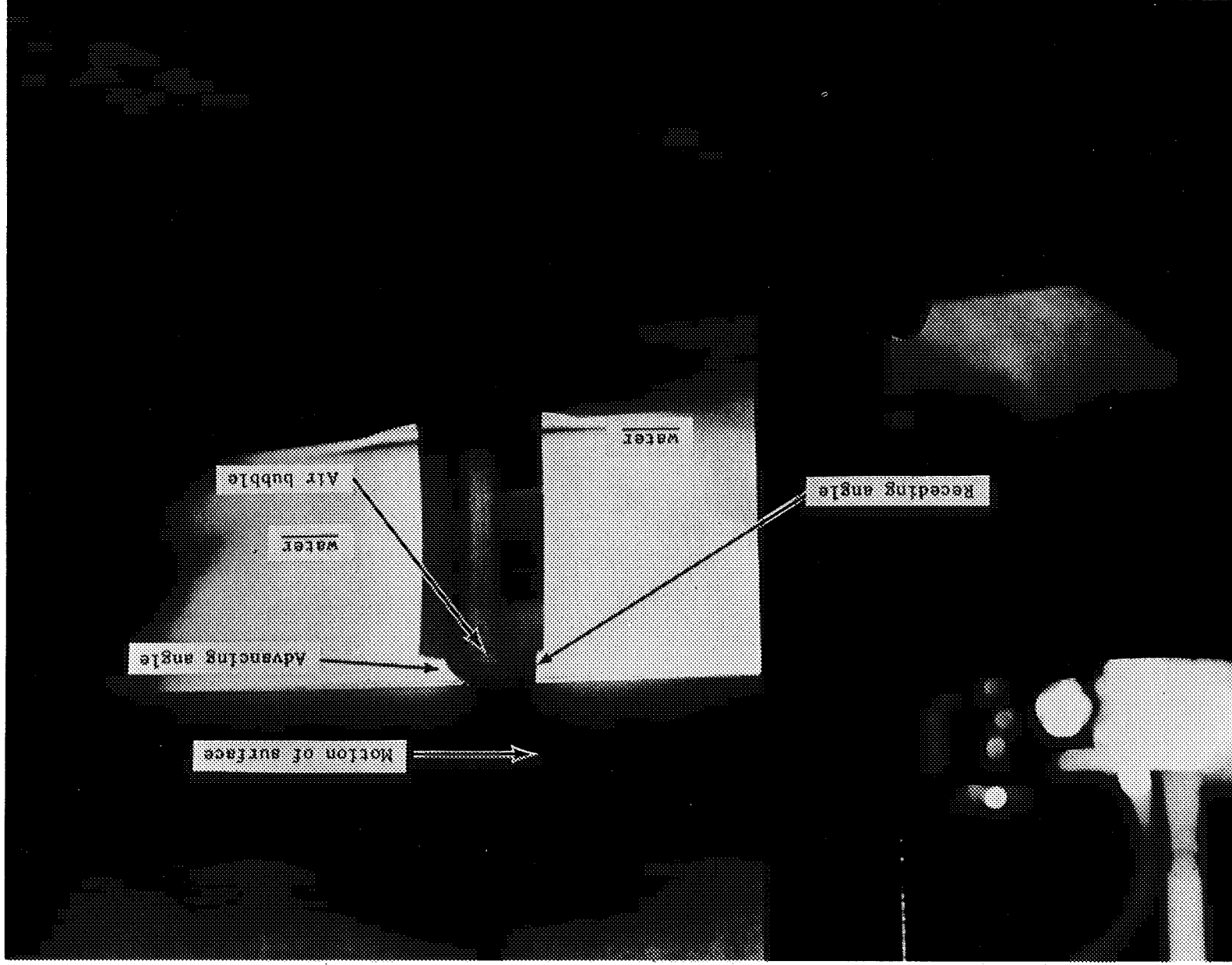
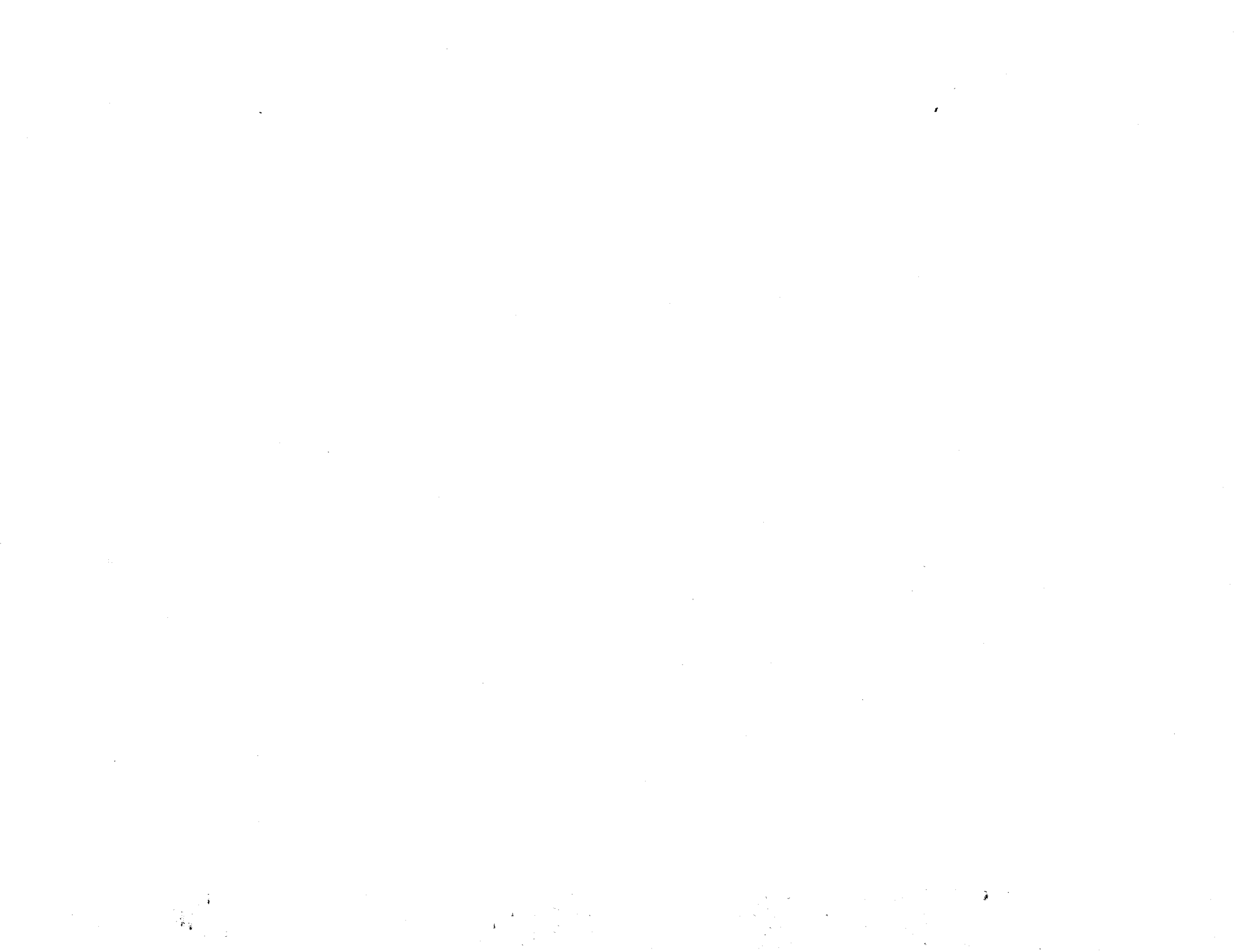


Fig. 4 Advancing vs. Receding Wetting Angles--Water on Lapped Metal



ORIGINAL PAGE
BLACK AND WHITE PHOTOGRAPH

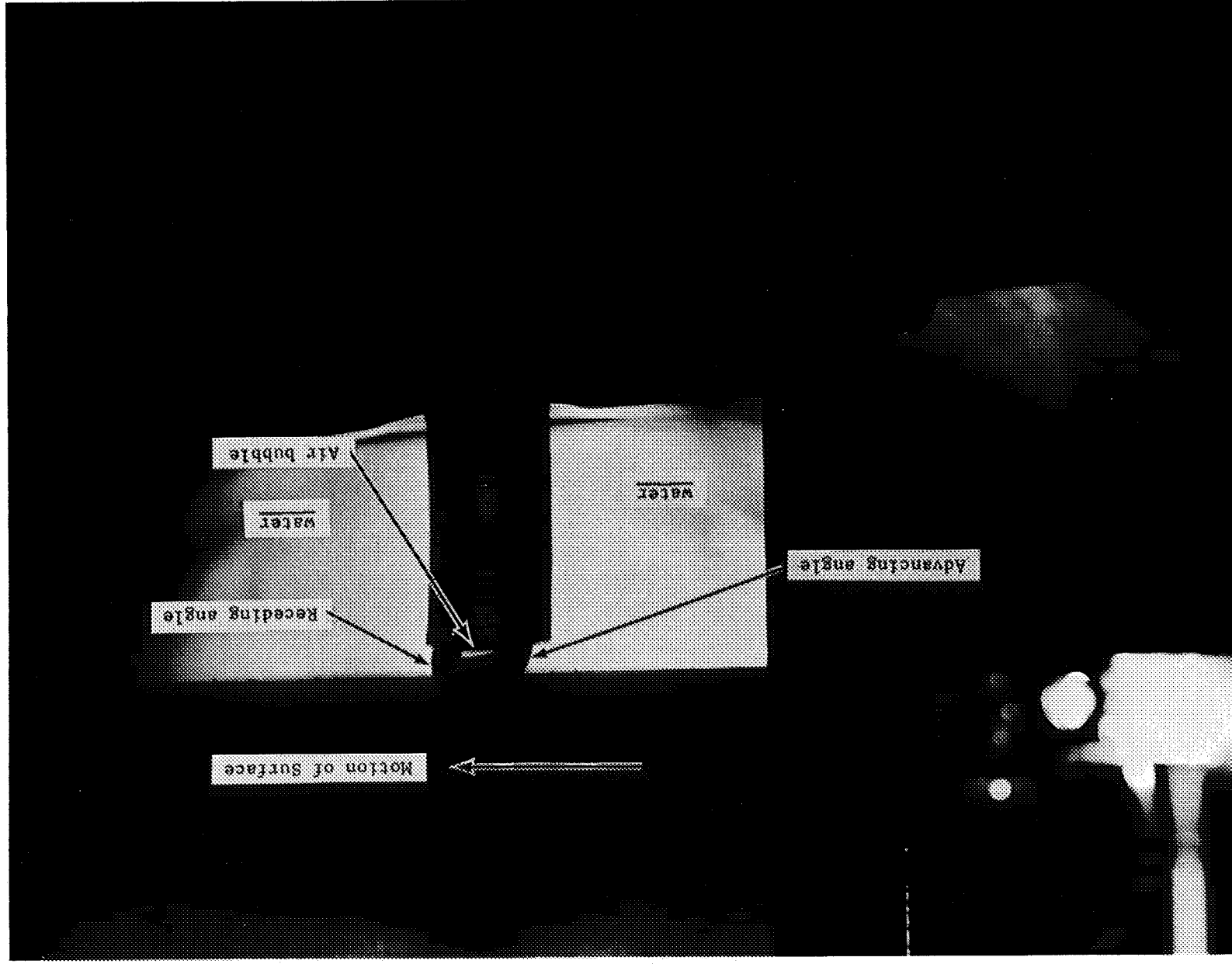
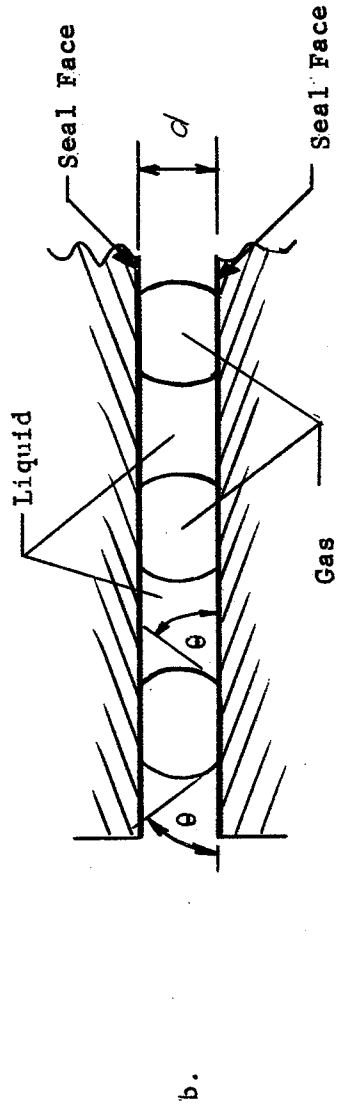
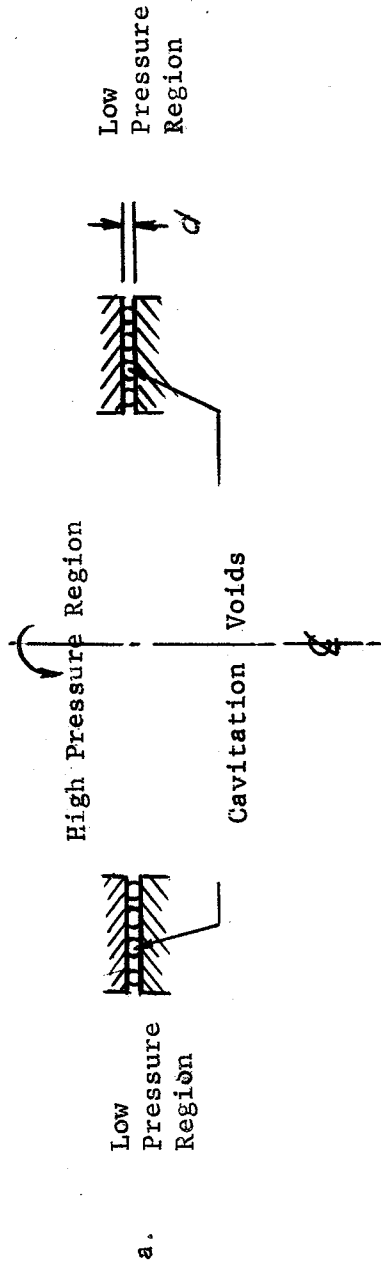


Fig. 5
Advancing vs. Receding Wetting Angles--Same as previous figure, but direction of motion reversed.



θ = Wetting Angle

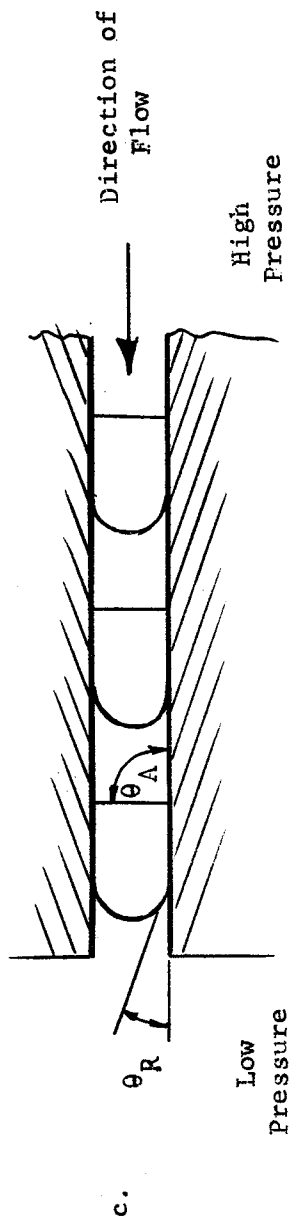
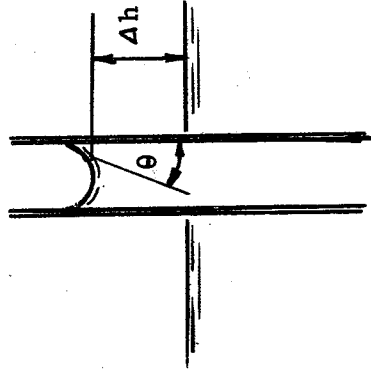
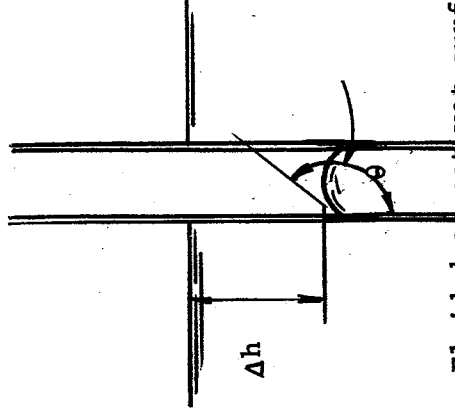


Fig. 6 Cavitation Voids in Seal Films



Fluid Wets
Surface
 $\theta < 90^\circ$



Fluid does not wet surface
 $\theta > 90^\circ$

Fig. 7

Liquid Head in a Capillary

Appendix G

SEAL MATERIAL STUDY - R. E. Lee, Jr.

Introduction

The primary function of a seal is to prevent or control migration of gases or liquids across a joint or opening in a vessel or assembly. Sealing primarily falls into two classes: Static, where there is no relative motion between joined parts, and Dynamic, where some form of motion occurs between "rigid" members of an assembly. In dynamic sealing there are two predominate types; e.g. positive contact where there is rubbing contact between the rotating and stationary members, and controlled clearance where there is normally no rubbing contact between seal components, and limited but controlled leakage rates are permissible.

Seal Material Considerations

To establish applicable design criteria for rocket seal material selection, a complete awareness of rocket sealing requirements is first necessary. Table G-1 presents a general outline of rocket engine seal functional requirements. This illustrates the various environmental and operational requirements which must be met by seal materials in both static and dynamic rocket seal applications. A better understanding of material properties as related to static and dynamic sealing operation is next in order. The predominant seal material properties are shown in Table G-2 along with an indication of general magnitude of their relative importance as related to static and dynamic rocket seals.

Unfortunately, there is no single material that can meet the wide range of rocket seal requirements. Realizing this, a compromise between material type, design, and operating parameters is necessary. Table G-3 consists of a compilation of some of the more important controllable and uncontrollable variables which will strongly influence the ultimate choice of specific materials

for rocket engine seals. The uncontrollable variables are generally fixed requirements and have to be met, whereas the controllable variables are somewhat flexible and can be beneficially used towards optimizing rocket seal performance.

Classes of materials under consideration to meet the stringent requirements imposed by rocket seal operation are shown in Table G-4. Considerable future work however is needed to determine the applicability of such materials for rocket seal use.

State of the Art

From the rapid technological advancement associated with present rocket propulsion systems and newer concepts arise numerous problem areas, some of which in themselves can be classified as new technologies. Seal materials and propellants for such systems fall well into the category of new technology, and from the limited information evidenced to date will have to be developed as such. True, some of the knowledge associated with conventional fluid sealing can, and will be applied to rocket seals. However, one is immediately made aware of the radical differences between the two sealing systems. Such a comparison is shown in Table G-5 for dynamic and static contact sealing, where seal material and fluid requirements are compared for conventional and propellant sealing.

Table G-5

CONVENTIONAL SEALING REQUIREMENTS VS. PROPELLANT SEALING FOR CONTACT SEALS

CONVENTIONAL SEALING

1. Low leakage is often acceptable
2. Reasonable material wear is acceptable in many instances because of ease of seal material replacement and/or 1 above.
3. Most sealing fluids are not damaged when leakage occurs, are not toxic or reactive in nature
4. The liquids being sealed often provide a load carrying film between contacting seal surfaces resulting in negligible wear.

PROPELLANT SEALING

- Leakage is critical
- Wear is critical because of stringent leakage requirements, and inability for material replacement.
- Many of the propellants are highly reactive, thermally unstable and toxic in nature.
- The liquid propellants in general are poor (like water) in their ability to provide a load carrying fluid film between their sliding surfaces. A comparison of the viscosity of various propellants with water and oil can be seen in TABLE G-6.

CONVENTIONAL SEALING

5. Selection of seal material is generally not critical when hydrodynamic operating conditions prevail, but is more so when boundary operating conditions prevail.

6. In general, most of the seal materials and fluids associated with conventional sealing are not prone to react together.

7. For extremely high loads where severe metal to metal contact is encountered, active chemical materials such as chlorine, sulfur and lead compounds are often added to the fluid for the purpose of reducing wear and/or surface damage. These additives react chemically to form a low-shear surface layer.

Having discussed the material-propellant needs from the broader operational viewpoint one may summarize these pertinent requirements:

- A. A Contact seal material must possess an extremely low wear rate, and preferably low friction.
- B. Compatibility between seal material, coating and additive is essential.
 - A mismatch could result in:
 1. Seal material going into solution (Solubility tendencies)
 2. Alteration of seal material properties
 3. Chemical Reaction (Corrosion)
 4. Detonable mixture causing explosion
- C. The mechanical and physical properties of the seal material must of course meet sealing design requirements. These pertinent material properties, along with controllable and uncontrollable variables were discussed previously.

PROPELLANT SEALING

The low viscosities of the propellants indicate that one would expect boundary seal operating conditions most of the time, depending upon load and velocity. The wear factor is extremely important when boundary conditions prevail.

The very character of the propellant makes the choice of seal material (irregardless of how compatible the materials are from the standpoint of friction and wear) extremely critical. Violent reactions have been known to occur.

Chemical additives, like the seal materials per se will have to be carefully selected because of the high reactivity of many of the propellants. Inertness to the propellant is probably mandatory.

It might be well at this point to re-emphasize the critical nature of (B) above. For example, it is known that fluorinated hydrocarbons from detonable mixtures with chlorine trifluoride, and titanium has been reported as being sensitive to impact, causing a spontaneous explosion in liquid fluorine. There is, unfortunately, no reliable analytical means at present for predicting fuel-material compatibility, so that we must continue to rely on experimental data as the basis of selection.

Friction and Wear

From our study of this subject thus far, it can be said that the state of the knowledge of seal materials operating in rocket propellant atmospheres is poor. Most of the seal friction and wear studies to date have been conducted in conventional fluids like oil, water, air, and some others of lesser extent in gases like helium and nitrogen. Limited efforts on material-propellant friction and wear studies have been conducted by Rocketdyne (Ref. G-1). Some of the more successful materials and their respective lubricating propellants are tabulated in Table G-7.

Efforts which may be applied to the problem of filling the void in seal material-propellant technology become apparent. Current recommendations for advances in this field are as follows:

1. Correlate present available seal test data with propellant-material requirements. The type of data more representative of propellant-seal material operating conditions would evolve from such investigations as past studies made in water (low viscosity), dry sliding studies, and gas environments such as Helium, Nitrogen, and Hydrogen. Examples of the latter can be seen in Tables G-8 and G-9.
2. Draw upon the knowledge accumulated in the structural materials-propellant compatibility studies for the consideration of potential

dynamic, and particularly static seal materials.

3. Devise a program based on conducting seal material tests in the various propellants.

New Concepts

In addition to the basic study discussed above, new concepts should be considered and explored to the extent they merit. Some concepts of potential value are as follows:

1. Resilient Composite Material

This is a recent development in which a metal-fiber skeleton is impregnated with a softer pliable material. The former provides elasticity, and the latter provides plasticity. An example is a stainless steel or molybdenum skeleton impregnated with tin or silver.

2. Free Energy Relationships

Consideration should be given to the possibility of using free-energy relationships between propellant or gas, and seal materials, for the purpose of judging the probability of an existing chemical reaction between the lubricant (fuel or gas) and the seal substrate. In effect, one would be utilizing thermodynamic material properties to predict chemical reactivity. While it is realized that other variables will enter into the already complex situation, it is hoped that a trend might be effected. Subsequently, it would be determined if the chemisorbed film where limited chemical reactivity can exist, would prove to be a beneficial film from the standpoint of improving lubrication for positive contact seals. Some work has already been initiated in this area on rolling contact bearings by other researchers.

3. Lubrication Additives for Propellants

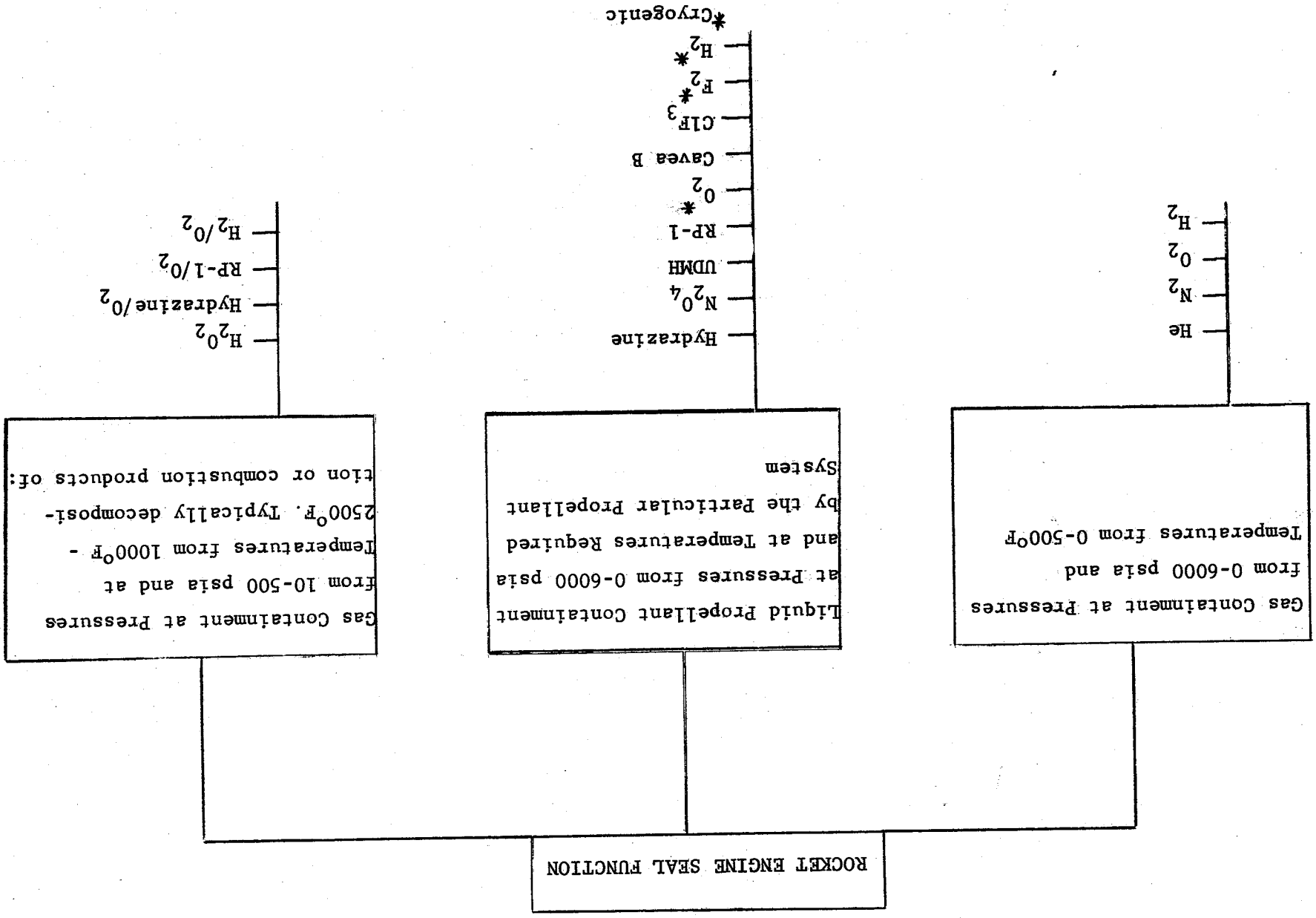
A brief review of potential additives that might prove suitable as lubricants in the presence of fuels and oxidizers should be made. Complete inertness

of the lubricant with the propellant would appear to be the major prerequisite. Work of this nature was conducted at ATL (Ref. G-4) on normal propyl nitrate (NPN). Several additives proved to be effective in improving the lubricating characteristics of NPN for bearing purposes.

REFERENCES:

- G-1. Propellant Lubrication Properties Investigation, M.F. Butner, Rocketdyne, WADD-TR-61-77, June, 1961.
- G-2. Development of Seals for Rocket Engine Turbopumps, J.E. Wolfe, R. E. Connelly, ASLE Preprint No. 58LC-5, Oct. 1958.
- G-3. High-Speed Rotating Shaft Seal for a Helium-Cooled Reactor Application, W. A. Glaeser, F. Orcutt, Battelle Memorial Institute, May, 1960.
- G-4. Effects of Additives on the Lubrication Characteristics of Normal Propyl Nitrate, R. E. Lee, Jr., May 1955, On File at Advanced Technology Laboratory, G.E. Company.

Table G-1



MATERIAL PROPERTIES EFFECTING ROCKET SEAL PERFORMANCE

Table G-2

PROPERTY	STATIC		DYNAMIC	
	Controlled	Clearance	Controlled	Positive Contact
Dimensional Stability	2	1	1	1
Compressive Strength	1	2	1	1
Impact Strength	1	3	1	1
Thermal Shock Resistance	2	2	2	2
Hardness	2	3	1	1
Modulus of Elasticity	1	3	2	2
Thermal Conductivity	1	1	2	2
Permeability	1	2	1	1
Coefficient of Thermal Expansion	1	1	2	2
Wear Resistance	3	3	1	1
Corrosion Resistance	1	1	1	1
Homogeneity	1	2	1	1

LEGEND

- 1 Highly Effective
- 2 Effective
- 3 Little to no Effect

CONTROLABLE AND UNCONTROLABLE VARIABLES EFFECTING SEAL MATERIAL SPECIFICATION

Table G-3

Controlable Variables (Seal Design Parameters)	Uncontrolable Variables (Operating Conditions)
Configuration	Temperature a. Cryogenic b. To 2000 F
Compatibility (friction and wear)	Containment Pressure
a. Solubility b. Oxidation	Ambient Pressure
Surface Finish a. Direction of contours b. Class of finish	Fluid
Impermeability a. To gases b. To liquids	Vibration Spectrum
Load	Radiation
Velocity	Space Availability
	Life requirements

Table G-4
 CLASSES OF POTENTIAL ROCKET ENGINE SEAL
 MATERIALS PRESENTLY UNDER CONSIDERATION

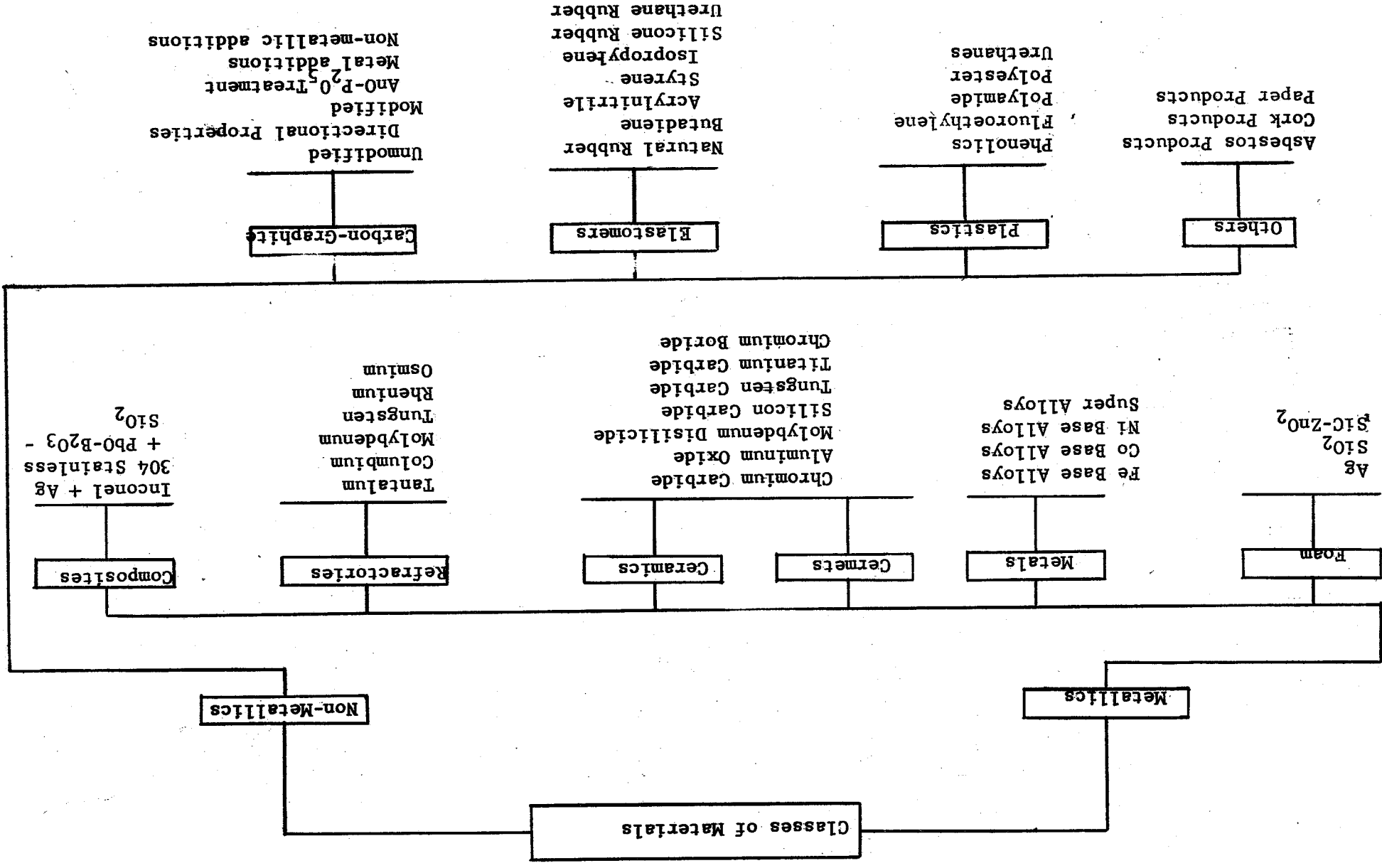


Table G-6

COMPARISON OF ABSOLUTE VISCOSITIES FOR VARIOUS FLUIDS

<u>FLUID</u>	<u>FORMULA</u>	<u>ABSOLUTE VISCOSITY (Centipoise)</u>
<u>WATER</u>	H ₂ O	1.00 at 70°F
<u>OIL SAE 10</u>	Light Petroleum Oil	70 at 70°F
<u>MONO PROPELLANTS</u>		
Hydrazine	N ₂ H ₄	0.90 at 77°F
UDMH	(CH ₃) ₂ NNH ₂	0.509 at 77°F
Hydrogen Peroxide	H ₂ O ₂	1.156 at 77°F
<u>FUELS</u>		
Hydrogen (Liquid)	H ₂	0.013 at -439°F
RP-1 Hydrocarbon	----	1.17 at 100°F
<u>OXIDIZERS</u>		
Nitrogen Tetroxide	N ₂ O ₄	0.342 at 100°F
Fluorine (Liquid)	F ₂	0.257 at -374°F
Chlorine Trifluoride	CF ₃	0.412 at 77°F
Oxygen	O ₂	0.15 at -280°F

Table G-7

FRICTION AND WEAR TESTS (Ref. G-1)

Essentially six materials were run under sliding conditions in various propellants for the purpose of determining their friction and wear behavior. The more successful material combinations are listed under the respective propellant in which they were tested. The test specimens consisted of a 3/8 inch diameter rider loaded against a rotating disc. Loads were Hertzian in nature and sliding velocities from 1500 fpm to 9750 fpm. Further testing details and material limitations can be found in Reference G-1.

PROPELLANT

MATERIAL COMBINATION

RP-1

Nitralloy 135 M vs. 9310
 440C vs. 440C
 Nitralloy 135 M vs. Nitralloy 135 M
 9310 vs. 440C or 52100
 Glass supported Teflon vs. 52100
 Carbon (U.S. Grade 2) vs. 52100
 Phenolic linen (LLB grade) vs. 52100

Ethylene Diamine

Glass supported Teflon vs. 52100

Unsymmetrical
 Dimethylhydrazine

440C vs. 440C
 Glass supported Teflon vs. 52100

Hydrazine

Berylco 25 vs. 440C
 440C vs. 440C
 Carbon (US Grade 2) vs. 52100

Liquid Hydrogen

Glass Supported Teflon vs. 52100
 440C vs. 440C

Liquid Oxygen

440C vs. 440C
 Glass supported Teflon vs. 52100

Liquid Tetroxide

Carbon (US Grade 2) vs. 52100
 440C vs. 440C

Inhibited Red Fuming
 Nitric Acid

440C vs. 440C
 Glass-supported Teflon vs. 52100

Table G-8

FACE TYPE SEAL MATERIALS EVALUATION (Ref. G-2)

Speed = 8000 ft/min Load = 200 psi, Test Fluid = Liquid N₂

Materials Nose Piece	Mating Ring	Wear, in.		Test Time min.	Comments
		Nose	Ring		
Carbon	Nitralloy	0.006	0.0002	5	Low leakage
Carbon	Chrome Plate	0.005	0.0001	5	Low leakage
Bronze	Nitralloy	0.001	0.0005	3	Severe scoring of bronze and excessive leakage
PTFCE	Nitralloy	0.042	NMW ⁺	1	Seal failure
PTFE	Nitralloy	0.018	NMW	0.5	Seal failure
Carbon	Titanium- carbide composition	NMW	NMW	5	Low leakage
Aluminum (hard anodized)	Chrome plate	---	---	10 sec	Complete failure chrome ring galled anodized case worn through

+ No Measureable Wear

HIGH SPEED ROTATING SHAFT SEAL STUDIES (Ref. G-3)

Environment = Helium Gas
 Specimen Configuration = Ring Seal
 Mean Face Load = 6.6 psi

Table G-9

Material Combination Rotor/Stator	Speed (rpm)	Wear Factor	Environment Temp. (°F)	Coeff. of Friction	Helium Leakage (lb/hr)	Bulk Stator Temp. °R	Comments
Flame-plated Cr ₂ C ₃	11,600	Negligible	273	0.12	0.001	150	Water Cooled, (Spray) 6-1/2 hrs. run.
Metal Salt Impregnated Carbon Graphite	17,000	0.3	270	0.20	0.005	150	
"	20,200		230	0.20	0.005	135	
"	11,600	Negligible	227	0.20	0.007	272	Dry Run 2-1/2 hrs.
"	17,600	0.8	267	0.29	0.008	317	
"	20,400		290	0.35	0.008	345	
"	11,000	Negligible	280	0.15	0.0035	185	Spray cooled with polyalkylene glycol 3 hr. run
"	18,000	Negligible	235	0.18	0.0065	200	
"	20,400		230	0.20	0.0070	165	



5 FEB 66 25740